Improving a 1D coastline model for mega nourishments

Incorporating cross-shore profile redistrubution in ShorelineS for the Bacton Sandscaping study case

Master Thesis by Job Wiezer

TU Delft Delft University of Technology

Royal HaskoningDHV
Enhancing Society Together

DELFT UNIVERSITY OF TECHNOLOGY

MSc Thesis

Improving a 1D coastline model for mega nourishments

Job Wiezer
4718216

Master: Hydraulic Engineering
Specialty: Coastal Engineering

Delft University of Technology
Faculty of Civil Engineering and Geosciences

September 30, 2024

Supervision by:

Friso Dam	Royal HaskoningDHV
Ruben Borsje	Royal HaskoningDHV
Matthieu de Schipper	Delft University of Technology
Alessandro Antonini	Delft University of Technology
Ad Reniers	Delft University of Technology

Preface

This master thesis is the product of research executed in collaboration with Royal HaskoningDHV and the Delft University of Technology. With it, I conclude my degree of Master of Science in Hydraulic Engineering.

Mega nourishments are a relatively recent innovation in coastal protection, with only a handful of these large-scale projects completed worldwide. The proven effectiveness of these existing structures has spurred interest in constructing more in the future. To ensure the optimal design and performance of future mega nourishments, it is crucial to gain a deeper understanding of their behavior and evolution. This research aims to contribute to this knowledge base, given the significant potential of mega nourishments as a sustainable coastal defense strategy.

What motivated me in my research, were the large potential and innovative character of mega nourishments. I have found it special to be able to contribute to something like that. Completing my degree after such a long time was a significant personal goal. I'm immensely proud of this achievement. While the thesis writing process was challenging at times, I'm grateful for the unwavering support of some exceptional individuals.

A special thanks to Friso Dam and Ruben Borsje who were my supervisors from RHDHV. They were an invaluable support throughout this process. Their input and feedback during our meetings were incredibly helpful, and I could always go to them with questions or to get a different perspective. I'd also like to give special thanks to my other RHDHV colleagues for creating such a friendly and enjoyable work environment. Also, I'd like to thank Matthieu de Schipper, Alessandro Antonini and Ad Reniers who were my committee for giving me guidance and feedback during this project. Their knowledge and input helped me to find the right direction during this journey. Despite the busy and important agendas, you provided me with valuable feedback during the collective progress meetings and individual moments of contact. And finally, I would like to thank my parents, sister and girlfriend, whose love and encouragement have been the guiding stars in my academic journey. Thank you for reading my report and helping me make it even better.

Job Wiezer
Rotterdam, September 30, 2024

Summary

This thesis investigates how to improve the predictive capabilities of the one-dimensional (1D) coastline model, ShorelineS. The main challenge explored in this research is the exclusion of cross-shore sediment redistribution in 1D models like ShorelineS, which affects the model's ability to predict coastal evolution accurately, especially in the case of Bacton.

The Bacton Sandscaping project was initiated to address the significant coastal erosion threatening the Bacton Gas Terminal, which is critical to the UK's energy supply. Traditional hard engineering solutions were ruled out due to their potential to increase erosion in adjacent areas. Instead, a soft engineering approach was chosen, inspired by the Dutch "Zandmotor" (Sand Engine). This involves placing a large volume of sand along the coastline, which is naturally redistributed by waves and currents to provide long-term coastal protection.

While the Bacton Sandscaping project has proven successful, limitations were identified in the design and modeling process, particularly in accurately predicting how the coastline would evolve. The ShorelineS model, used in this thesis to simulate the coastline evolution, only considers longshore sediment transport and assumes that the cross-shore profile (the slope of the beach) is in equilibrium. However, in the case of Bacton, the cross-shore profile was not in equilibrium after construction and redistribution played a significant role in how the shoreline evolved. Its exclusion from the model leads to inaccuracies. Therefore the main research question addressed in this thesis is:

How can the predictive capability of a one-dimensional coastline model of the shoreline evolution of mega nourishment be improved by incorporating cross-shore profile redistribution?

Two supporting questions are posed:

1. How well does ShorelineS predict the coastline evolution of the Bacton Sandscaping project in its current form?
2. How can cross-shore profile redistribution be incorporated into ShorelineS? and does this improve its predictive capability on the coastline evolution of a mega nourishment?

The research begins with an assessment of ShorelineS in its current form, evaluating its performance using data from the Bacton Sandscaping project. The current ShorelineS performance is evaluated by comparing modeled and measured positions in MSL (Mean Sea Level) contour using absolute, relative distances, and planform area. Additionally, the model-predicted coastline change is analyzed and compared with the volume-based change. Next, cross-shore redistribution is integrated into ShorelineS by defining a redistribution factor (R-factor) based on measured and modeled coastline changes. The modeled coastline change is calculated using volume balance, and the measured coastline change is determined at a specific level. The redistribution of sediment within the profile is a time-dependent process and two relationships are tested, linear and exponential relationships. Finally, the modeled coastline positions are adjusted to account for redistribution by applying the R-factor to the average modeled coastline change and calculating the additional coastline change. The adjusted model is then evaluated using the same metrics as the original model.

The assessment of ShorelineS in its current form shows that the model underestimates the erosion of the terminal section and overestimates sediment feeding to the villages. This leads to a continuous increase in both relative and absolute distance between modeled and measured MSL contours, indicating worsening predictions over time. The model's imposed conservation of planform area contributes to this error, as the modeled planform area remains

relatively constant while the measured area decreases. Analyses show that ShorelineS generally performs poorly in predicting shoreline changes, with no clear relationship between average wave power and shoreline changes and little agreement between modeled and volume-calculated shoreline change. These findings suggest that the 1D coastline model ShorelineS is not well-suited for predicting the coastline evolution of a mega nourishment.

The results show that incorporating the R-factor slightly enhances the model's performance for the terminal section, but conversely, it deteriorates the performance for the village section. This is due to the model's imposed conservation of sediment. Applying the R-factor only to the terminal section slightly improves the overall model performance, but the effect is minimal. The R-factor's impact is limited by the small average modeled coastline change and the model's conservation of sediment. In response to these findings, a new approach is tested. This approach differs from earlier approach as the adjusted coastline is reintroduced back into ShorelineS and the R-factor is only applied to the terminal section. The improvement this makes is little, but it does indicate that there is potential in including cross-shore redistribution to enhance the performance of 1D coastline models.

The general findings highlight the significant influence of cross-shore redistribution on coastline change, as observed in the Bacton monitoring data and supported by previous research on other mega nourishments. It is found that the R-factor, while improving predictions slightly, does not fully address the limitations of ShorelineS, suggesting that other factors may contribute to its inaccuracies. The limitations of the study include the model's inherent volume conservation, the use of the CERC2 transport equation, and the limited frequency of coastline updates. Additionally, the R-factor's sensitivity to small values and the assumption of a multiplicative relationship are identified as potential limitations. Future research directions include improving model calibration, testing different transport equations, incorporating more frequent coastline updates, exploring alternative approaches for cross-shore redistribution, conducting further research on cross-shore redistribution itself, and conducting a sensitivity study on its impact on mega nourishment evolution.

The R-factor introduced in this research aimed to address the limitations of ShorelineS in predicting coastline evolution, particularly the underestimation of erosion in the terminal section due to the exclusion of cross-shore redistribution. By multiplying the modeled coastline change by the R-factor, the model could account for the additional coastline change caused by sediment redistribution within the profile. While the R-factor did show some improvement in the predictions, it was not enough to fully overcome the limitations of ShorelineS. The model's inherent tendency to conserve sediment over the nourished area significantly impacted its accuracy. This means that ShorelineS often overestimated the retention of sediment and underestimated erosion, leading to discrepancies between the model's predictions and the actual coastline evolution.

Contents

List of Figures

List of Tables

1 Introduction

1.1 Bacton's solution to coastal erosion

Numerous factors, including sea level rise, sand mining, and subsidence, contribute to the erosion of soft and sandy coastlines worldwide. This coastal degradation is particularly worrisome given that a significant portion of the global population resides in coastal regions, where beaches and dunes serve as crucial barriers against many waters. North Norfolk's soft cliff coast, situated on the west coast of the UK, exemplifies this issue. Research by Hobbs et al. [12] reveals that between 1880 and 1967, the North Norfolk coast eroded at a rate ranging from 0.30 to 0.75 meters per year. This relentless erosion not only exposes the hinterland to increased risks of coastal flooding but also amplifies the impact of rising sea levels, further increasing the threat to coastal communities. Consequently, storm surge events in 2007, 2013, and 2017 resulted in severe flooding of coastal roads and properties due to wave overtopping [12]. In response to this pressing issue of coastal erosion, the Kelling to Lowestoft Ness Shoreline Management Plan (SMP) was established to provide a blueprint for coastal management for the next 100 years. This comprehensive management plan delineates four primary policies for each coastal segment [1].

1. Hold the existing defense line
2. Advance the existing defense line
3. Managed realignment
4. No active intervention

Most of these policies speak for themselves, but the policy of Managed realignment requires more attention. This policy is selected when protecting the coastline is deemed unsustainable and unaffordable in the long term. Such is the case for Walcott, a small village along the North Norfolk coast. Protecting the coastline in its current position is too expensive, which means that in the future, this village will have to let go of its coastline defenses, allowing the coastline to erode freely into a more natural shape. It also means that the villagers have to accept that communities will have to adapt or move away.

Stretching along the North Norfolk coast is the Bacton gas terminal, which is responsible for the supply of one-third of the UK's national gas demand. During the storm events in 2007 and 2013, the minimum margin between the cliff edge and terminal boundary fence was halved to 10m [12]. This prompts serious concerns about the buried infrastructure in the cliff and underneath the beach. Subsequently, the storm events underscored the necessity for action. Due to the economic value of the terminal and the related cost of moving the infrastructure, an SMP policy of 'Holding the existing defense line' was selected for the gas terminal. Provided that it would not increase the erosion further along the coast in the neighboring villages of Bacton and Walcott. For these villages, the SMP states that until the lifetime end of the current sea defense, which was about 5-15 years in 2015, the defense could be maintained, but after that, the coastline should be allowed to retreat to a more natural defense line under a Managed realignment policy [8]. However, due to a lack of policy and funding around coastal adaptation, the 300 households and businesses are not yet in a position to relocate or otherwise adapt to coastal change [12].

Because of this requirement of not increasing erosion in the neighboring villages, all hard solutions such as seawalls, rock revetment, and breakwaters are ruled out, as these solutions

would increase erosion on adjacent coasts. Besides, a hard defense would not deliver enough benefits to justify investing in such a solution. Hybrid solutions were also considered and found to be too expensive. Eventually, RHDHV landed on a soft solution named the Bacton Sandscaping Scheme, which was inspired by the Dutch so-called 'Zandmotor'. The concept of this 'Zandmotor' or sand engine in English, is that the coast is nourished with a substantial amount of sediment, which is then naturally redistributed along the coast through waves and currents. Therefore, consequently feeding the adjacent coast with sediment. This was found to be the most beneficial solution as it would help protect the terminal as well as Bacton and Walcott, and it would not increase erosion on the adjacent coastline. Plus, it would also offer great potential for additional benefits such as recreation and tourism.

In 2019, the construction was finished, and after some time, it was concluded that the Bacton Sandscaping works to protect its hinterland. During this period large storms have occurred and no wave overtopping was measured [8]. In an interview with the BBC a community member indicated that he feels a lot safer now [23]. This success of the scheme gives confidence that these types of solutions work and it raises the question if a sand engine is not widely applicable to other coastal areas in the UK.

1.2 Problem in the Sandscaping design sequence

Even though the success of the Sandscaping schemes is apparent, there are still challenges to be addressed, namely in the design sequence. In October 2014, Royal HaskoningDHV was appointed by Shell, one of the Bacton terminal companies (BTC), to assist with the identification of coast protection measures that would meet the wider objectives of the companies [25].

1. To implement coast protection as soon as possible
2. To stop erosion to the cliff in front of the BTC for at least the next 50 years
3. To prevent an increase in erosion to the cliffs adjacent to the terminal
4. To ensure a minimum cover of material of 1.2 m over the pipeline for at least the next 50 years
5. To have no significant adverse impact as a result of the work

These objectives boil down to two key features. Namely, during the lifetime of the terminal structures a minimum profile should be guaranteed so the pipelines are covered with at least 1.2 m material and protected against a storm that occurs once every 10,000 years [12]. Next, the sand engine should be able to feed the adjacent coast with enough sediment during its entire lifetime, without running out of sand itself. For the design, the team of Royal HaskoningDHV executed an iterative process approach with three parallel stages: technical analysis (including modeling), environmental studies, and contractor engagement. In this process, iterations were done on shape, volume, grain size and configuration. For the technical assessment a so-called conceptual model was built, which combined the one-dimensional LITLINE model with a two-dimensional area model [8]. Here, the LITLINE model was the so-called central design engine. This one-dimensional model only includes longshore sediment transport and is very well suited to simulate the coastline evolution on large temporal and spatial scale. However, it does not include cross-shore sediment transport and since RHDHV was under the assumption that a lot of sediment would be lost offshore they included the cross-shore sediment transport from the 2D area model as sink and sources in the LITLINE model to account for these possible

offshore losses.

The two-dimensional area model was based on the open-source TELEMAC-MASCARET modeling system. However, as with most two-dimensional area models, it does not capture the ongoing and gradual process of beach recovery under normal conditions, making it difficult to produce good results if the simulation is done over a long time period. Another well-known drawback of 2D area models is that they require a lot of computational effort. On the contrary, a 1D coastline model, like LITLINE, does not take a lot of computational effort and is well suited for large space and temporal scales. However, 1D coastline models do not incorporate the cross-shore evolution of coastlines as these models are only one-dimensional and focus on the alongshore transport of sediment. 1D models assume that the cross-shore profile is close to equilibrium, which justifies the absence of cross-shore sediment transport. Most nourished profiles, however, are constructed under a steeper slope than natural and, therefore, will undergo redistribution of sediment within the profile. In other words, on average, sediment will move from higher up on the profile downward to flatten the profile. This phenomenon is called cross-shore redistribution and will increase the reduction in coastline width and beach or planform area. In addition to the expected erosion due to longshore processes. More on how this works can be found in the next paragraph 1.3. In the case of the Dutch Sand engine, this phenomenon has a relatively small effect due to its large scale and the relative importance of longshore processes. Therefore, 1D coastline models perform well in predicting its coastline evolution. On the contrary, the engineers of RHDHV found that in the case of Bacton Sandscaping, which is of a much smaller scale, this effect does play a role. From analysis of the monitoring, it became clear that cross-shore redistribution has an important effect on coastline evolution. Despite the effort to add cross-shore sediment transport as sinks and sources into the LITLINE model, the results were still not accurate.

1.3 Cross-shore redistribution

The previous section already touched upon the subject of cross-shore redistribution and how it affects the evolution of the Bacton Sandscaping Scheme. To support understanding the aim of this research, this section shortly addresses the phenomenon of cross-shore redistribution and why it is important in the Bacton study case.

To understand this, one must first look at what is an equilibrium profile and Bruun was one of the first to introduce the theory of a dynamic equilibrium beach profile [9]. Based on his analysis of the Danish and California coasts Bruun proposed an empirical equation for the equilibrium beach profile. Later on, Dean supported this equation by reasoning that for a certain grain size, nature strives towards uniform energy dissipation per unit volume across the surf zone [14]. The reasoning behind this was that there are 'constructive' and 'destructive' forces present that will move sediment on- or offshore, respectively. Automatically this will mean that if there is a balance in the forces there will be no movement of the sediment particle, meaning the particle is in equilibrium. Think of a grain particle with a certain size and weight and on this particle acts gravitational forces. The grain is stable as long as the forces acting on the grain balance the gravitational forces. Now think of a profile that is constructed under a steeper slope than natural, altering the energy dissipation of the wave. On a steeper slope, the dissipation will take place at a shorter distance than on a more gradual slope, so more energy will dissipate on a certain area. Therefore, the 'destructive' forces are not balanced, which will cause grains to be stirred up and moved downslope. If this same wave condition is maintained for long enough the profile will be reshaped into an equilibrium profile. Beaches with smaller grains will be less steep than beaches with coarse grains, as these smaller grains will require

less energy to get moving and the dissipation of energy will have to be more gradual. The process of reshaping the beach under wave forces is called profile equilibration and during this process grains get redistributed within the profile.

It is expected that over a certain period the profile will have moved towards an equilibrium. As a result, there will be a balance between constructive and destructive forces, and the evolution of the coastline will be primarily influenced by longshore sediment transport. Therefore, profile equilibration is a time-dependent process, but the exact nature of this relationship remains unclear. As well as the time it will take for the profile to reach equilibrium.

Since a natural beach profile is often very gradual it is almost impossible to construct a nourishment profile under the same slope. As the machines used for nourishment are not very precise and construction would become very expensive. Therefore nourishment profiles are almost always steeper than natural and thus will undergo profile equilibration. During this, it will become increasingly more gradual. The consequence of this is that it goes hand in hand with shoreline retreat, as sediment higher up on the profile gets transported downward, below water level, to flatten the profile. This retreat is on top of the shoreline retreat caused by longshore sediment transport. This redistribution of sediment is not included in a 1D coastline model because these models assume the cross-shore profile to be in equilibrium and, therefore, assume a linear relationship between volume loss due to longshore transport gradients and coastline retreat. This affects the amount of shoreline regression predicted by a 1D coastline model. In the case of the 'Zandmotor', this effect is not as prominent because the scale of this project is so massive that this effect is negligibly small. In contrast, this effect can not be neglected in the case of Bacton, whose scale is much smaller compared to that of the 'Zandmotor'.

1.4 Research question and objectives

The sections above discuss how RHDHV experienced limitations in the predictive capabilities of shoreline evolution of a 2D area model and a 1D coastline model, as neither was capable of producing solid output. For the 1D coastline model, this problem is thought to be caused by the exclusion of cross-shore sediment redistribution in the model. Therefore the main research question is:

How can the predictive capability of a one-dimensional coastline model of the shoreline evolution of mega nourishment be improved by incorporating cross-shore profile redistribution?

A mega nourishment is defined as a very large concentrated nourishment that feeds adjacent coasts in an alongshore direction through physical forcing conditions. The Bacton Sandscaping design will be used as a case study to explore this. An example of a 1D coastline model is ShorelineS created by Deltares Delft. Since this model is already available for the study case of the Bacton Sandscaping, it will be selected to answer the research question.

The research question is answered via the following supporting questions:

1. How well does ShorelineS predict the shoreline evolution of the Bacton Sandscaping project in its current form?
2. How can cross-shore profile redistribution be incorporated into ShorelineS? and does this improve its predictive capability on the shoreline evolution of a mega nourishment?

The research aims to enhance the predictive capability of a 1D coastline model for mega nourishments by incorporating cross-shore redistribution. Chapter 2 will discuss what cross-shore redistribution is and examine the general approach of 1D shoreline models and the underlying physical principles they use. The next Chapter, Chapter 3, will introduce the case study of the Bacton Sandscaping. This will be followed by a Chapter (CH 4) describing the methodology of how cross-shore redistribution is incorporated into ShorelineS and how the performance of the current ShorelineS and the adjusted ShorelineS will be assessed. Subsequently, this report will address the results of this research in Chapter 5. Followed by a discussion (CH 6) of the results and finally a conclusion of the findings in Chapter 7.

2 Literature review

This chapter aims to review relevant literature used in this thesis and, by doing so, touches upon some definitions of the coastal area (2.1). Paragraph 2.3 provides more theory on the equilibrium beach profile and profile equilibration. The penultimate paragraph covers analytical methods for predicting nourishment evolution (2.4). Finally, it discusses how the 1D model ShorelineS predicts coastline evolution (2.5).

2.1 Coastline breakdown

This paragraph introduces relevant coastline definitions. The coastal zone is defined as the area where the land meets water and it can be divided into four subzones 1:

1. Coast: The coast is the first zone and stretches from an inland boundary that marks the boundary of the hinterland to the coastline. This location of the coastline marks the location of maximum storm reach.
2. Shore: The second zone is the shore or beach zone, which extends from the coastline until the line of MLW (Mean Low Water). Then again a subdivision was made in the foreshore and backshore. The division of these zones lies at the limit of wave uprush during high tide or, in other words, the shoreline. Dividing the 'wet' beach and the 'dry' beach.
3. Shoreface: The next zone is the shoreface. This zone has its offshore limit where the influence of wave action on sediment transport on average is negligible in comparison to other influences.
4. Continental shelf: The final zone is the continental shelf that extends to the self-break.

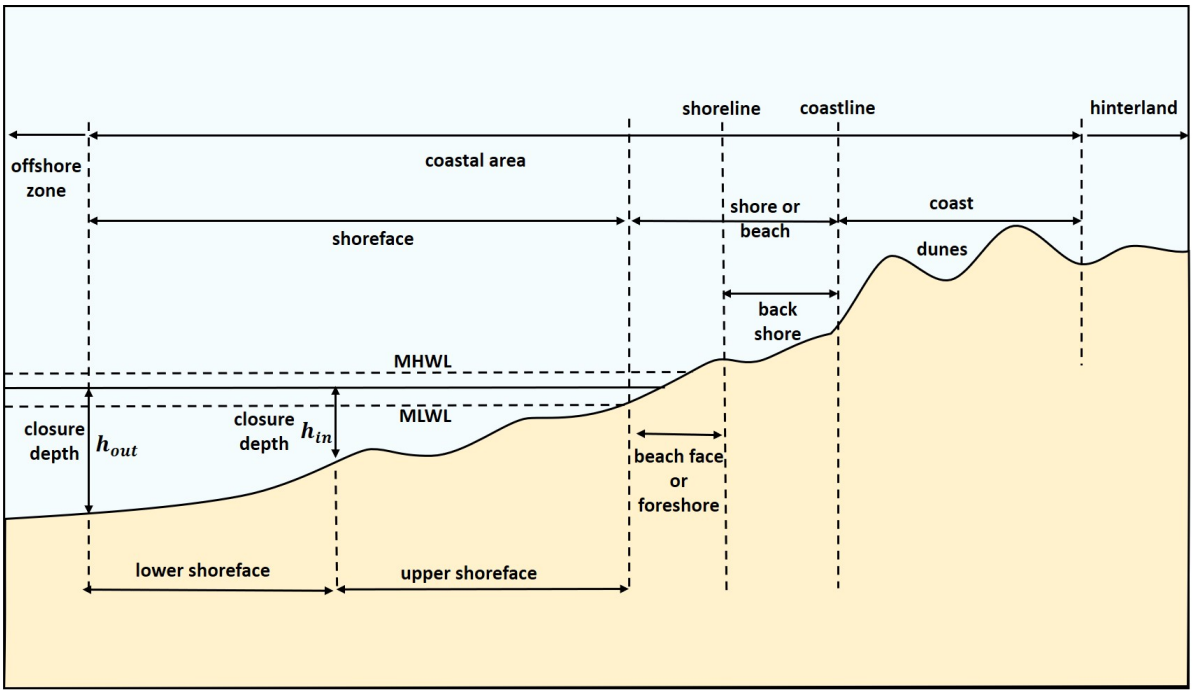

Figure 1: Definition coastal zones from Shore protection manual [17].

Figure 1 also shows two important water depths. The first is the inner closure depth h_{in}, defined by Hallermeier as the seaward limit of the zone actively affected by waves on a yearly

basis [18]. Beyond this depth, seabed surveys show minimal sand level change due to seasonal wave climates. Hallermeier suggested calculating this depth using the wave height exceeded only 12 hours per year. The second depth is the outer or lower closure depth h_{out}, which represents the depth below which waves typically do not interact with the seabed under average conditions. Therefore one can assume that sedimentation or erosion is negligibly small beyond this depth of closure point and thus no sediment flux from or to the coastal shelf.

2.2 Beach nourishments

This paragraph aims to establish a clear definition of beach nourishment. A beach nourishment involves adding a significant amount of sand to a beach, typically done in areas experiencing erosion that threatens the safety of the hinterland. Over time, beach nourishment projects have grown in scale, evolving from localized efforts that strengthen weak spots to large-scale interventions impacting entire coastlines. A recent development is the "mega nourishment" a massive, localized sand placement that significantly alters the adjacent coastline. Mega nourishments create large perturbations in the alongshore coast. Over time the natural system will try to restore balance by smearing out this perturbation via longshore and cross-shore sediment transport. In this manner, a mega nourishment is also beneficial for neighboring coasts.

2.3 Beach profile equilibration

The problem statement, paragraph 1.2, already discussed profile redistribution and equilibrium profile. The purpose of this paragraph is to further delve into the theory behind these phenomena.

Bruun was one of the first to introduce the theory of a dynamic equilibrium beach profile [9]. This theory states that if a beach with a specific grain size is exposed to a constant forcing condition, it will develop a profile shape that is constant in time. Based on his analysis of the Danish and California coasts Bruun proposed an empirical equation for the equilibrium beach profile.

$$h = A(x')^m \tag{1}$$

where:

- m is exponent equal to $2/3$
- A is a shape factor
- x' is cross-shore distance
- h is water depth

Later on, Dean supported this equation by reasoning that for a certain grain size, nature strives towards uniform energy dissipation per unit volume across the surf zone [14]. Building upon the concept of depth of closure and his equilibrium profile research, Dean proposed that the profile shape is solely determined by the sediment fall velocity.

$$A = 0.067w^{0.44} \tag{2}$$

$$w = 14D_{50}^{1.1} \tag{3}$$

Consequently, he reasoned that for similar grain sizes, the profile form would remain constant during sediment gains or losses. In such scenarios, the entire profile would simply translate horizontally according to the below equation. This translation is displayed in figure 2. In this formula, h_* is closure depth and B is berm height both in meters. The depth of closure assumed here is the inner depth defined by Hallermeier [18]. Where h_e and T_e are nearshore significant wave height and period.

$$\Delta y_0 = \frac{V}{h_* + B} \tag{4}$$

$$h_* = 2.28H_e - 68.5(\frac{H_e^2}{gT_e^2}) \tag{5}$$

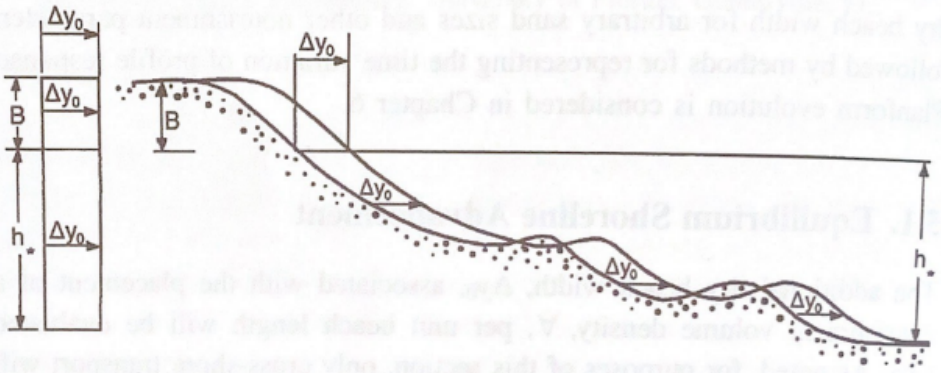

Figure 2: Profile translation associated with volume change of compatible sand, from [15].

As already discussed in the introduction 1, when a beach is nourished, it is generally constructed on a steeper slope than natural. Therefore, over time, the waves will reshape and equilibrate the profile. The time the equilibration process takes is important for investors since wide beaches give a higher level of protection against waves and provide more area for recreation. Due to seasonality and variability in forces like storm forces, the prediction of this process and its time scale is very difficult, and no known cross-shore models have successfully simulated it. However, Dean stated that for compatible sediments, the divergence of proportional volume and planform area with time is an indication of the equilibration over

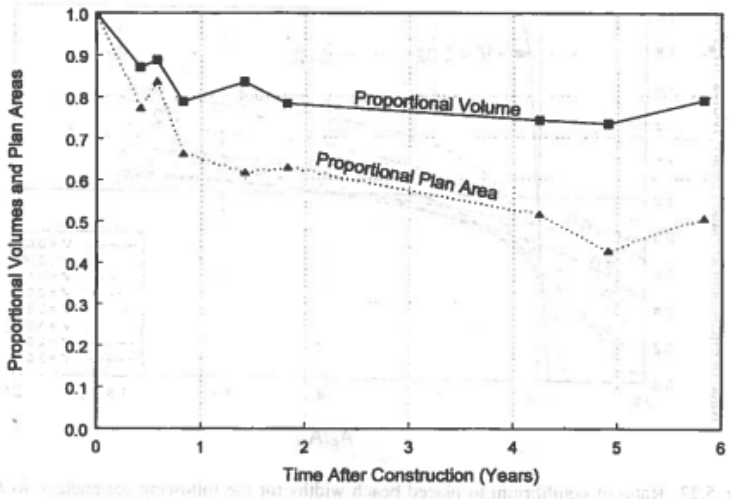

Figure 3: Proportional volumes and planform area remaining Manateen Country project, from [15].

time. This is visualized in figure 3. The ratio of proportional volume and total planform area is R, and for time going to infinity, the profile will reach equilibrium and therefore $R_{EQ} = h_* + B$.

$$R(t) = \frac{V_T(t)}{PA_T(t)} \tag{6}$$

$$R(t) = R_{EQ} + (R(0) - R_{EQ})e^{-K't} \tag{7}$$

In this equation, V_T and PA_T represent proportional volume and planform, respectively, and $R(0)$ is the equilibration factor for t=0. $(K')^{-1}$ is the 'folding time' and represents the time for which 63% of the equilibration has taken place. The problem with this equation by Dean is its assumption of uniform sediment size and fall velocity across the entire profile. As in real life, there will be a range of different grain sizes present on the profile. Therefore the equilibration process will happen differently and the profile can not be described with one constant A factor. Not only in the profile but also the fill will contain a range of grain sizes.

2.4 Analytical nourishment evolution models

This paragraph aims to examine existing analytical methods for predicting nourishment evolution. The application of analytical nourishment evolution models is proven to be very useful for engineering applications, as they offer a clear picture of how physical forces (waves, tides, etc.) influence shoreline morphology, providing both qualitative and quantitative understanding. Analytical models are built on fundamental physical principles and simplified representations of beach dynamics. This simplicity offers a key benefit. Compared to complex numerical models, analytical models reveal the underlying mechanisms of shoreline change more transparently. Additionally, they provide a rapid estimation tool for assessing the impact of potential shoreline modifications. However, it's crucial to recognize that analytical models rely on assumptions and simplifications. When interpreting results, it is essential to consider these limitations to avoid drawing inaccurate conclusions. First, the theory of the analytical model will be addressed in 2.4.1, followed by different directions to solving this model in 2.4.2.

2.4.1 Theory

A one-line model is aimed to predict medium to long-term variation of the coastline. The first one-line model proposed was by Pelnard-Considere [24]. As mentioned in paragraph 2.3, this model assumes that the cross-shore profile is in equilibrium and, therefore, the entire profile translates landward or seaward depending on the longshore sediment flux. A conservation of mass can be established for this sediment flux along the coast and a cross-sectional area of the beach. See the sketch in figure 4.

$$\frac{\delta Q}{\delta x} + \frac{\delta V}{\delta t} = 0 \tag{8}$$

Where Q is the longshore sediment transport rate, x is the alongshore location, V is the volume of sand per unit beach length, and t is time. A general expression of the longshore sediment transport is:

$$Q = Q_0 sin(2\alpha_b) \tag{9}$$

Where Q_0 is the amplitude of the longshore sediment transport and α_b is the incident wave angle with respect to the local coastline.

$$\alpha_b = \alpha_0 - tan^{-1}(\frac{\delta y}{\delta x}) \tag{10}$$

α_0 represents the angular orientation of breaking wave crests when measured in relation to a line drawn parallel to the coastline. Linearisation of equation 9 and application of Taylor series to the first order leads to:

$$Q = Q_0(2\alpha_b - 2\frac{\delta y}{\delta x}) \tag{11}$$

Both Q_0 and α_b are independent of space and time. Therefore, a diffusion equation can be derived. In this equation, G is a diffusion coefficient.

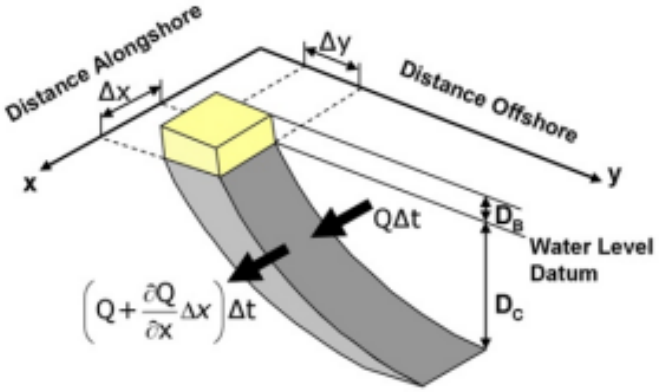

Figure 4: Sketch of shoreline change based on the gradient in longshore sediment transport, from [19].

$$\frac{\delta y}{\delta t} = G\frac{\delta^2 y}{\delta x^2} \tag{12}$$

$$G = \frac{2Q}{h_*} \tag{13}$$

2.4.2 Longshore sediment transport

What follows from the above is that according to Pelnard-Considère the evolution of nourishment in time can be described with a simple diffusion equation including a diffusion coefficient that is dependent on the longshore sediment transport rate. One well-known and still widely applied equation of longshore sediment transport is the one constructed by the Coastal Engineering Research Center (CERC). This formula gives the bulk longshore sediment transport due to action of waves approaching the coast. Hence, only the effect of wave-generated current is taken into account. The CERC equation in the most general form reads:

$$Q = \frac{K}{\rho g(s-1)(1-p)}(Enc)_b cos(\phi_b) sin(\phi_b) \tag{14}$$

where:

- K is a transport coefficient [-]
- ρ is the density of the water [kg/m^3]
- s is the relative density of the sediment [-]
- p is porosity [-]
- g gravitational accelaration [m^2/s]
- E is wave energy [J/m^2]
- n ratio between wave group and phase velocity [-]
- c wave phase velocity [m/s]

- ϕ wave angle of incidence [-]
- b subscript referring to the conditions at the breaker zone

Dean [15] discusses four different solutions for the Pelnard-Considère diffusion equation in combination with CERC, according to different boundaries: 1) nourishment on the full length of the barrier island 2) nourishment on the central point of the barrier island 3) nourishment extending from one end of a long barrier island 4) nourishment starting near one end of a long barrier island, as shown in figure 5.

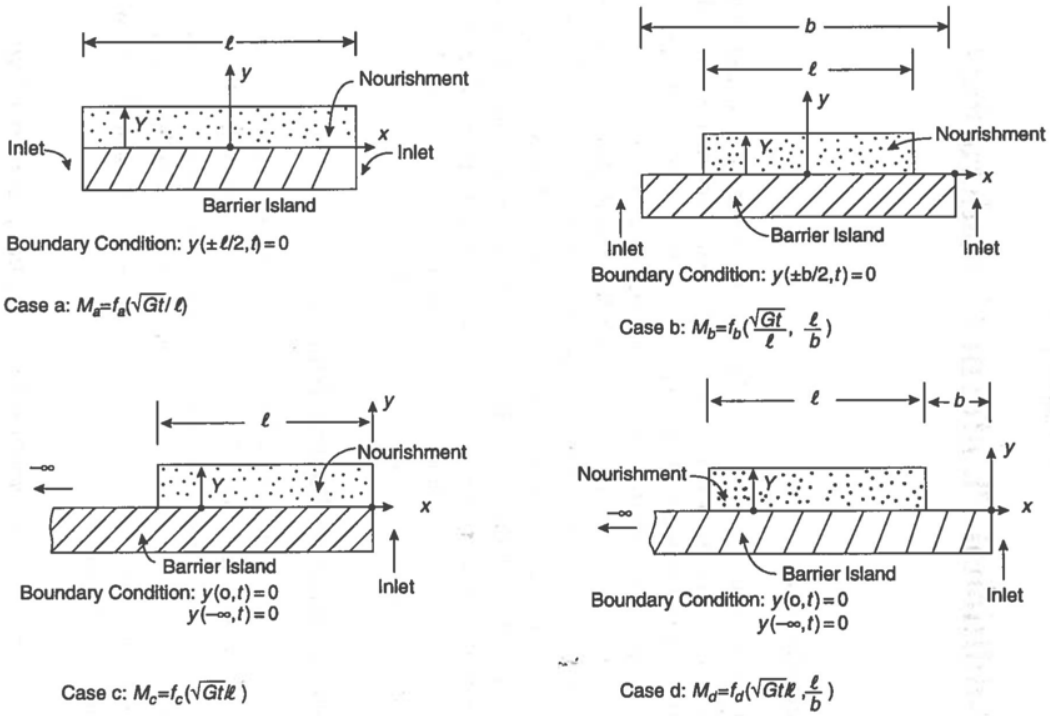

Figure 5: Four different cases with solutions for Pelnard-Considère equation, from [15].

Another commonly used longshore sediment transport equation is conceived by Kamphuis [20]. He researched alongshore sediment transport rate based on a three-dimensional model experiment. Kamphuis measured deep-water wave conditions, wave height through the surf zone, wave-breaking angles, longshore current velocity distribution, and bed and suspended sediment load simultaneously, all to come up with an expression that links sediment transport rates with wave steepness, beach slope, grain size and breaking angle. Kamphuis mentions that alongshore sediment transport is a function of a combination of wave, fluid, sediment and beach profile parameters like wave height period and angle, water depth, fluid and sediment density, fluid viscosity, gravitational acceleration, space coordinates, and many more. Herein Kamphuis differs from the CERC formula as it includes the influence of the beach shape and sediment characteristics. Because of this large number of parameters whose effects are interrelated, Kamphuis suggests simplifying the analysis by making use of the dimensional properties of various parameters.

$$Q = f(H, T, \alpha, d, \rho, \mu, g, x, y, z, t, \rho_s, D, m) \tag{15}$$

$$\pi_Q = \Phi(\frac{H}{gT^2}, \alpha, \frac{H}{d}, \frac{H\frac{H}{T}}{\frac{\mu}{\rho}}, \frac{x}{gT^2}, \frac{y}{gT^2}, \frac{z}{d}, \frac{t}{T}, \frac{\rho_s}{\rho}, \frac{H}{D}, m) \tag{16}$$

By making a series of assumptions certain terms can be eliminated from the equation, resulting in the following.

$$\frac{Q}{(\frac{\rho H^3}{T})} = (\frac{H}{L_0})^p m_b^q (\frac{H}{D_{50}})^r sin^s(2\alpha_b) \tag{17}$$

Where q, p, r, and s are exponents, which Kamphuis determined using successive approximation. In this successive approximation, the exponent with the highest influence gets determined first, subsequently the second most important exponent, and eventually the interaction between the first two. The measure of goodness of the fit used is the standard error of estimate.

$$S_{y/x} = \sqrt{\frac{(\log Q_c - \log Q_m)^2}{k^{-2}}} \tag{18}$$

Where Q_c and Q_m are the calculated and measured values of Q respectively, and k is the number of data points. According to sensitivity analysis done by Kamphuis on a situation of irregular waves, the exponents could vary over the following ranges without greatly affecting the results.

$$1.15 < p < 1.30; \quad 0.6 < q < 0.85; \quad 0.15 < r < 0.30; \quad 0.55 < s < 0.6 \tag{19}$$

A new predictive formula for the total longshore sediment transport (LST) rate is presented by Bayram [4]. He based this new formula on the energetics concept similar to Inmann and Bagnold's model [3]. Inmann and Bagnold hypothesized that the fluid acts as a machine expending energy at a certain efficiency to offset the work done in transporting sediment. Bayram begins by stating that most existing LST formulas focus solely on wave-induced currents, neglecting the influence of other factors like winds and tides, which is an important addition to his formula. In the derivation of his equation, Bayram mentions that suspended sediment is the dominant mode of transport. Breaking waves are required to stir up the sediment in suspension to obtain a certain concentration in the water column, Whereas any type of current can transport the sediment. The total amount of work (W) needed to keep the sediment in suspension is given by the product of the concentration and the submerged weight of the particles with the fall velocity.

$$W = \int_0^{x_b} \int_{-h(x)}^{0} c(x,z)(\rho_s - \rho) g w_s \, dz \, dx \tag{20}$$

Where x is the cross-shore coordinate originating at the shoreline and taken positive seaward, z is the vertical coordinate originating at the still-water level, and h is water depth. Only a portion (ϵ) of the wave energy flux (F) is used to stir up sediment, therefore $W = \epsilon F$. Subsequently, the product of the suspended concentration and the longshore current velocity gives the longshore sediment transport rate.

$$Q_{lst} = \int_0^{x_b} \int_{-h(x)}^{0} c(x,z)V(x,z)\,dz\,dx \tag{21}$$

In addition, assuming a constant or representative current velocity and replacing the integral with the fraction of the incoming wave energy that is used for keeping the sediment in suspension yields equation 22. In this equation $\overline{V}$ is the mean flow velocity and a is the porosity. The transport coefficient ϵ can be derived from field and or laboratory data or theoretical considerations.

$$Q_{lst} = \frac{\epsilon}{(\rho_s - \rho)(1-a)gw_s} F\overline{V} \tag{22}$$

All these three longshore sediment transport equations, together with the diffusion equation of Pelnard-Considère, can be used to solve the coastline evolution analytically. Solving these equations analytically takes a lot of effort and that is why people came up with 1D-coastline models.

2.5 1D coastline models ShorelineS

This paragraph will discuss the functioning of ShorelineS. One-dimensional coastline models make it easier to investigate the long-term evolution of the coastline. These models focus on large temporal and spatial scales, which is why they are particularly useful for mega nourishment, as they are very large and meant to have an impact even after many years. Because it is so suitable for large time and space scales, some assumptions have been made for processes happening on smaller time and space scales. One important assumption is that of the equilibrium profile discussed in paragraph 2.3. And for the computation of shoreline changes a 1D coastline model generally uses bulk longshore sediment transport, like the one mentioned earlier in subparagraph 2.4.2.

Generally, 1D coastline models are based on the principle of conservation of sediment. The coastline is represented by grid cells or points, and for each grid cell or point, the longshore sediment transport is calculated by the model for each timestep. A gradient in longshore transport between cells will mean a shift of coastline at that location.

2.5.1 Introducing ShorelineS

This thesis focuses on the 1D coastline model ShorelineS since this model is already available for the study case of the Bacton Sandscaping. ShorelineS is a new coastline model, developed by J.A. Roelvink (Deltares/Unesco-IHE/TU Delft) and B.J.A. Huisman. In ShorelineS, the coastline is described as a string of grid points that can expand or shrink freely, depending on the change of volume. A visualization of this is given in figure 6. These points represent the movement of the active coastal profile and simulate the coastline contour. The conservation equation used in ShorelineS for updating the coastline

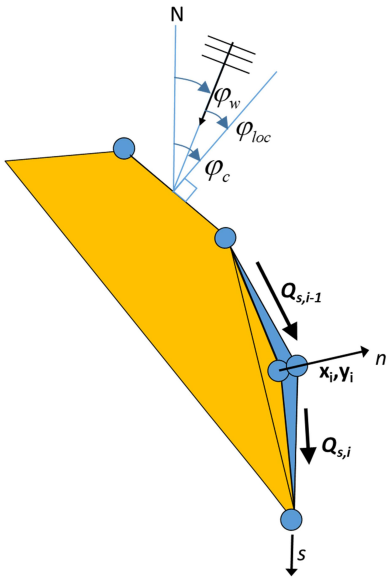

Figure 6: Coastline schematization used in ShorelineS, from [13].

is:

$$\frac{\delta n}{\delta t} = -\frac{1}{D_s}\frac{\delta Q_s}{\delta s} - \frac{RSLR}{tan(\beta)} + \frac{1}{D_s}\sum q_i \qquad (23)$$

Where:

- n is the cross-shore coordinate
- s is the longshore coordinate
- t is time
- D_s is the active profile height
- Q_s is the longshore sediment transport
- $tan(\beta)$ is the average profile slope
- $RSLR$ is Relative Sea Level Rise
- q_i are other source or sink terms

In line with other 1D coastline models, ShorelineS also assumes the cross-shore profile to be in equilibrium, justifying the absence of cross-shore sediment transport. Hence, coastline changes are driven by wave-driven longshore transport. Longshore transport equations available in shorelineS are listed in table 1.

Longshore transport equation	Formula
CERC1	$Q_s = bH_{s0}^{5/2}2sin(\phi_{loc})$
CERC2	$Q_s = K_2 H_{s0}^{12/5} T^{1/5} cos^{6/5}(\phi_{loc}) sin(\phi_{loc})$
CERC3	$Q_s = bH_{sb}^{5/2}2sin(\phi_{loc})$
Kamphuis	$Q_s = 2.23 H_{sb}^2 T^{1.5} m_b^{0.75} D_{50}^{-0.25} sin^{0.6}(2\phi_{loc})$
Mil-Homens	$Q_s = \frac{1}{(\rho_s-\rho)(1-p)} 0.149 H_{sb}^{2.75} T_p^{0.89} m_b^{0.86} D_{50}^{-0.69} sin^{0.5}(2\phi_b)$
van Rijn	$Q_s = \frac{1}{(\rho_s-\rho)(1-p)} 0.006 K_{swell} \rho_s H_{sb}^{2.6} (tan(\beta)^{0.4} D_{50}^{-0.6} V_{total}$

Table 1: ShorelineS Longshore transport equation, from [26].

ShorelineS introduces two calibration coefficients for CERC1 and CERC2, b and K_2 respectively. These are computed as:

$$b = \frac{k\rho\sqrt{g/k}}{16(\rho_s - \rho)(1-p)} \qquad (24)$$

$$K_2 = (\frac{g\gamma}{2\pi})^{1/5} K_1; \quad K_1\ 0.4 \qquad (25)$$

Where:

- k is the wave number
- K_1 is the default calibration coefficient according to the Shore Protection Manual [17].

Most of the equations are defined in terms of the breaking wave angle, indicated with the subscript b. Only the CERC1 and CERC2 make use of the offshore wave angle. CERC1 is the simplest formula and is great for giving a broad idea of what happens. While CERC2 is a direct derivation from the official CERC equation. ShorelineS makes use of two equations that have not been discussed yet, which will be briefly introduced.

Mil-Homens
In his study, Mil-Homens [22] evaluates the predictive capability of three of the most commonly used longshore sediment transport formulas, CERC, Kamphuis and Bayram. For this he used the largest data set available. In his study Mil-Homens tried to improve the calibration coefficient in the three formulas. He employed a least-square algorithm which resulted in an improvement of the predictive capability.

Van Rijn
The above equations are only suitable for sandy beaches with relatively smaller grains and in addition, some equations are only valid for larger grains like the one from Soulsby and Damgaard [28]. Van Rijn [29] acknowledges this gap of knowledge and tries to invent a formula that is applicable to both sandy, gravel, and shingle beaches. In this equation of van Rijn, he introduces two new parameters K_{swell} and V_{total}. The first parameter is the swell factor. The influence of wave period is more significant for swell waves than for wind waves and to account for this the swell factor is introduced.

$$K_{swell} = 0.015\rho_{swell} + (1 - 0.01\rho_{swell}) \tag{26}$$

Here ρ_{swell} is the percentage of swell waves, ranging from 1, where there are no swell waves to 1.5 where there are only swell waves. If the amount of swell wave increases the amount of sediment transport also increases. The second parameter is there to account for additional currents, like tide or wind-driven currents.

$$V_{total} = V_{wave} + 0.01p_1V_1 + 0.01p_2V_2 \tag{27}$$

With V_1 and V_2 the representative velocity due to tide and wind in positive and negative direction, respectively. p_1 and p_2 are the percentages in time where it is positive and negative. The wave-induced longshore current is given in the following formula.

$$V_{wave} = 0.3(gH_{sb})^{0.5}sin(2\phi_{loc}) \tag{28}$$

2.5.2 Numerical implementation

The aim of this subparagraph is to address the numerical implementation of ShorelineS. ShorelineS schematizes the coastline by two column vectors x_{cm} and y_{cm} and these coordinates may be in any Cartesian system. Each set of coordinates represents one point along the coastline, see figure 6. During the simulation, ShorelineS uses a trick to prevent grid sizes from becoming too small or too big. When the simulation continues, and the grid size expands, a new grind point is introduced when the grid size exceeds twice the initial prescribed grid size. The opposite will happen if the grid size becomes half of the original. Then, a grid point will be removed. To avoid large variations in the grid size a smoothing factor is applied, see equation 29. In this equation, f is the smoothing factor.

$$s_{i,smooth} = f_{s,i-1} + (1-2f)_{s,i} + f_{s,i+1} \tag{29}$$

In ShorelineS the offshore wave climate can be specified in three ways [13]:

- By means of wave direction and a spreading sector. A uniform distribution is assumed between the mean wave direction and plus or minus half the spreading sector. For time step a random wave direction will be chosen from this sector.
- By means of a wave climate considering a number of wave conditions. A condition will be chosen randomly for every timestep.
- By means of a time series of wave conditions.

For the transformation of deep water wave angle to nearshore or local wave angle, ShorelineS uses Snell's law of refraction, and for the transformation from the nearshore to the breaker line it uses the equations of van Rijn [29]. The refraction from deep water to the toe of the dynamic profile can be done based on the assumption of parallel offshore depth contours or using a 2D refraction model to provide alongshore-varying wave conditions.

2.5.3 Coastline evolution

In this paragraph it is explained how ShorelineS handles coastline evolution. In figure 6, one can see that the local direction of the coastline is determined by the two adjacent points. Between each coastline point the longshore sediment transport is calculated, and if there is a gradient from point to point, it will either build out or shrink accordingly. The mass-conservation equation 23 is solved using a staggered forward time-central space explicit scheme.

$$\Delta n_i^j = -\frac{1}{D_c}\frac{2(Q_{s,i}^j - Q_{s,i-1}^j)}{L_i}\Delta t \tag{30}$$

In this scheme j is the time step index and Δt the size of the time step, i indicate the point index and L_i is the length of the considered grid element computed as follows: $L_i = \sqrt{(x_{i+1}-x_{i-1})^2 + (y_{i+1}-y_{i-1})^2}$. Again, x and y here are Cartesian coordinates. In the case of normal displacement, the change in coastline position is:

$$\begin{aligned} \Delta x_i^j &= -n_i^j(y_{i+1} - y_{i-1})/L_i \\ \Delta y_i^j &= -n_i^j(x_{i+1} - x_{i-1})/L_i \\ x_i^{j+1} &= x_i^j + \Delta x_i^j \\ y_i^{j+1} &= y_i^j + \Delta y_i^j \end{aligned} \tag{31}$$

Since an explicit scheme is used the time step is limited for stability according to the following criteria: $\frac{\epsilon \Delta t}{\Delta s^2} < \frac{1}{2}$. Here, ϵ, the diffusivity, is related to the maximum gradient of sediment transport concerning the wave angle relative to the coast. Which can be approximated by: $\epsilon_{max} = 2Q_{max}/D_c$. Here, Q_{max} is the maximum transport rate in the model. From this, it follows that the limit for the time step is:

$$\Delta t < \frac{D_c \Delta s^2}{4Q_{max}} \tag{32}$$

2.5.4 High-angle wave instability

This subparagraph discusses how ShorelineS deals with high-angle incident waves. High-angle incident waves, waves with a higher angle than the maximum transport angle, will enhance small perturbations leading to instabilities like spit formation. To overcome this problem, a special treatment is selected in ShorelineS [2]. In cases where the local angle exceeds the maximum transport angle on one side and is less than the maximum transport angle at the updrift side, the transport at the downdrift point is set to the maximum transport, or the angle is set to the maximum transport angle.

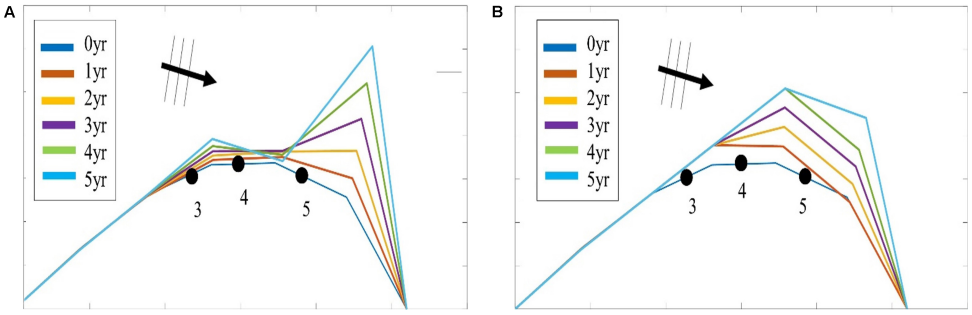

Figure 7: A comparison of coastline evolution using a high-angle unstable central scheme (left) and ShorelineS' upwind scheme (right), from [13].

This chapter has provided a review of the key literature underpinning this thesis. It starts with some essential terminology, followed by more theory of equilibrium beach profiles and profile equilibration. Afterward, it discusses the existing analytical method of predicting the nourishment evolution of Pelnard-Considère and introduces key longshore sediment transport equations that can be used to solve this equation. Finally, it introduces ShorelineS, the 1D coastline model used in this research. Presenting how ShorelineS handles the evolution of a coastline based on longshore sediment transport.

3 Study case: The Bacton Sandscaping Scheme

This chapter introduces the Bacton Sandscaping Scheme, which will be used as a study case throughout this thesis. First, the location and design will be discussed (3.1 and 3.2), followed by an overview of available data and wave conditions (3.3 and 3.4). Furthermore, this chapter delves into the observed behavior of the Bacton Sandscaping over time, looking into the changes in volume (3.5), planform area (3.6), and cross-shore profile (3.7). The general findings from this analysis are given in 3.8.

3.1 The Bacton site

This paragraph introduces the Bacton site. The Bacton Gas terminal is located to the north of the village of Bacton within the district of North Norfolk. A location plan is provided in figure 8. The terminal is surrounded by fields and to the south of the so-called Seagulls field lies Castaway Holiday Park, a caravan park. A total of 15 pipelines extend from offshore, passing beneath the beach to reach the terminal via vertical shafts constructed inland behind the cliff. These cliffs are made of soft deposits and have a long history of erosion. Analysis of historic cliff profiles shows that, on average, there has been a loss of volume of approximately $5,000m^3$ per year, and these cliffs have likely been eroding at this present rate for about the last 5,000 years. Applying the same analytical methods to historical beach profiles indicates an average volume loss of around $18,000m^3$. Current longshore transport is estimated at $300,000m^3$ per year [25]. Several attempts have been made to stem coastal erosion. For example, running along the entire length of the terminal frontage lies timber breastwork from Mundesley to Castaway Holiday Park. Seaward of these breastworks lie groynes, spaced 180 m apart and having a length of 90 m. More efforts have been made, like an artificial sand berm and rock armoring, but non were deemed to be very effective.

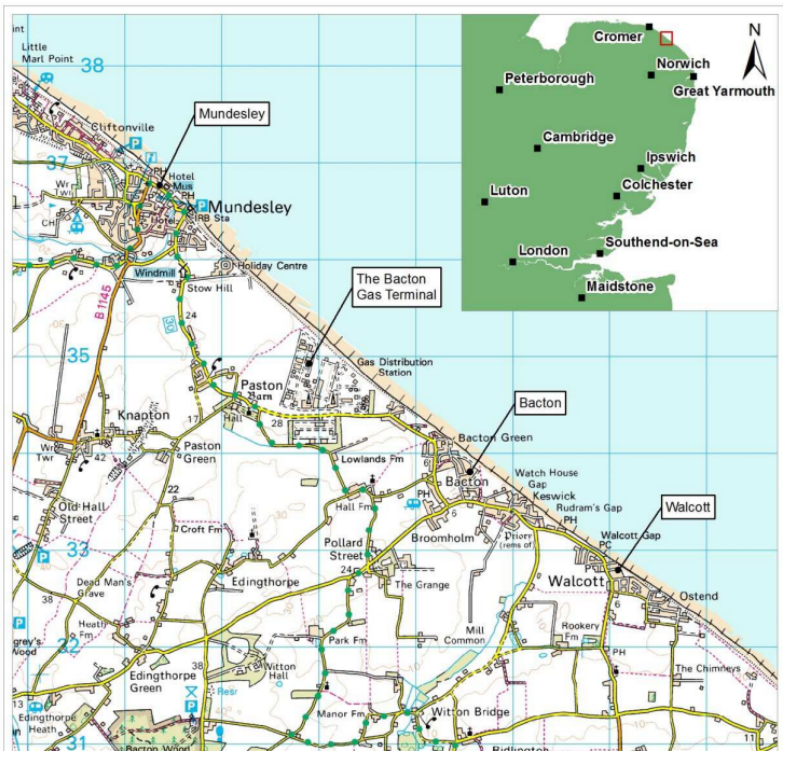

Figure 8: Location Bacton Sandscaping, from [25].

3.2 Final design Bacton Sandscaping

In this paragraph, the final design of the Bacton Sandscaping Scheme is discussed. The final design comprises two distinct elements. The first aims to deliver the necessary protection for the Bacton Gas terminal, while the second provides supplementary protection for the villages of Bacton, Walcott, and Ostend. The design documents talk about chainages, and those come from the LITLINE model and indicate longshore distance. In total, there are 4000 chainages with a distance of 50 m from each other.

ELEMENT 1 - TERMINAL

This first element extends from the northern end of the terminal at chainage 9100, where it ties into the existing beach, down to chainage 10800 at the northern end of the Castaways Holiday Park. The total volume of sediment for this element is approximately 1 million m^3. This element is characterized by a berm crest at +7m AOD and a berm width between 5 and 80 meters, whilst maintaining the minimum protection profile of a 20-meter-wide berm at +7m AOD directly in front of the terminal. In a seaward direction, the scheme slopes down towards the existing sea bed firstly at a 1 in 5 slope (top 1 meter) and then a 1 in 15 slope until it meets the existing seabed [11]. A cross-section of the scheme is given in figure 9a and this cross-section is located around the middle of the terminal.

ELEMENT 2 - VILLAGES

This element extends from chainage 10800 at Castaways Holiday Park down to the end of the scheme at chainage 14100 at Ostend. The total volume of sediment for this element is approximately 0.5 million m3. This element is characterized by a berm crest at +5m AOD at the start of the seawall at the southern end of the Castaways Holiday Park, sloping down to +4m AOD just to the south of Mill Lane, Bacton, and then continuing at +4m AOD for the remainder of the length. Until Walcott, where it begins to slope down to +3.0m AOD and later ties into the existing beach level at chainage 14400. The width of the crest is between 5 and 27 meters. In a seaward direction, the scheme slopes down towards the existing seabed firstly at a 1 in 5 slope (top 1 meter) and then a 1 in 15 slope until it meets the existing seabed [11]. Figure 9b displays a design cross-section located at the villages.

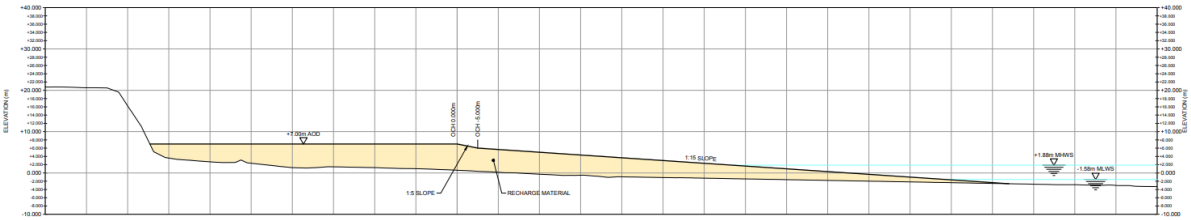

(a) Terminal

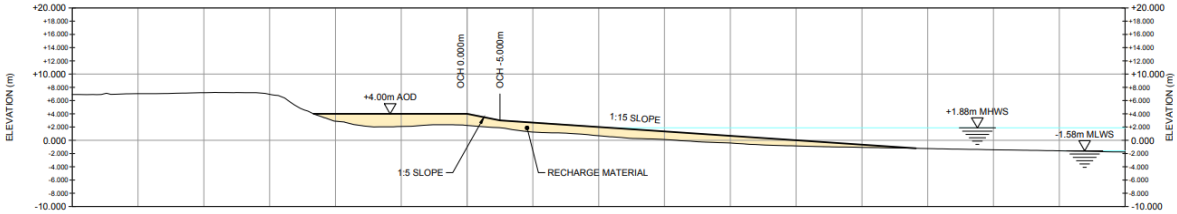

(b) Villages

Figure 9: Design cross-section terminal section (above) and village section (below), from [11].

In total, this is a volume of approximately 1.5 million m^3. The sediment was extracted from

an existing licensed aggregate extraction and it matched the grading of the native sediment currently present on the beach. This placement will protect the terminal coast for around 21 years, according to the modeling.

3.3 Data overview

The data utilized for analyzing the behavior of the Bacton Sandscaping scheme is examined in this paragraph. The data is derived from two primary sources. Initially, the post-construction survey (T0) was conducted by the contractor immediately after construction was completed. Additionally, surveys (T1-T7) are conducted by Shore Monitoring & Research, from now on referred to as Shore, who were tasked with conducting periodic assessments. The post-construction survey done by the contractor has some limitations as the period over which the survey was conducted spans approximately two weeks, and sediment has time to move from place to place within these weeks. On top of that, the extent of the survey is limited. Generally, it only extends until -2.5 to -3.0 m AOD. Therefore, it is combined with the pre-construction survey to make it complete. However, this also introduces some errors, as works might have influenced areas below -2.5 m AOD, and in certain sections these two surveys do not connect. The surveys done by Shore combined LiDAR topography and single-beam jet ski surveys at transects space 100 m in an alongshore direction. This survey results in a 2.0m x 2.0m DTM's (Digital Terrain Model). The accuracy of this measurement is of the order 5-10cm.

To characterize nearshore wave conditions two methods are applied both utilizing ERA5 data as input. For the first 5 periods (T0-T5) the wave data was introduced to MIKE21 Spectral Wave model. This model generated hourly wave data at a depth of -10m AOD. For the last two periods between surveys, the ERA5 wave data is transformed to nearshore using SWAN instead of MIKE21 to a depth of -12m AOD. More information about this is given later on in Chapter 4. This makes it possible to assess the coastal response to prevailing wave conditions.

The post-construction measurement and the first five Shore measurements were made available at the beginning of this thesis research. The first six measurements (T0-T5) have been fully documented by RHDHV. These rapports will be used for the analysis of the Bacton Sandscaping. Later, Shore measurements T6 and T7 became available, and where possible, these measurements were included in the analysis. However, this was not possible for all the analyses, and therefore, these analyses do not cover the full range of measurements. Ultimately, a total of eight measurements were conducted, spanning a period of 26-08-2019 to 02-05-2023. Due to COVID-19, the period between measurements was not constant and varied from interval. The conclusion date and interval of all measurements are listed in table 4.

3.4 Hydrodynamic conditions

This paragraph delves into the hydrodynamic conditions that prevailed during the time of interest. Conditions discussed include water levels and wave characteristics. Table 2 displays all the different tidal levels and extreme water levels with different occurrence frequencies. This table is produced by HR Wallingford on behalf of RHDHV [11]. The tidal abbreviations stand for the following:

- LAT: Lowest Astronomical Tide
- MLWS: Mean Low Water Spring

- MLWN: Mean Low Water Neaps
- MSL: Mean Sea Level
- MHWN: Mean High Water Neaps
- MHWS: Mean High Water Spring
- HAT: Highest Astronomical Tide

Tide (m AOD)		Water level (m AOD)		Future water level (m AOD)	
LAT	-2.55	1/1 year	2.86	1/1 years	3.28
MLWS	-1.58	1/ 10 years	3.28	1/10 years	3.70
MLWN	-0.75	1/50 years	3.64	1/50 years	4.06
MSL	0.11	1/100 years	3.79	1/100 years	4.21
MHWN	1.05	1/200 years	3.96	1/200 years	4.38
MHWS	1.88	1/1,000 years	4.39	1/1,000 years	4.81
HAT	2.71	1/10,000 years	5.08	1/10,000 years	5.50

Table 2: Water level and tide at Bacton (base year of 2009), from [11].

The table 2 presents two columns of water levels: one reflecting current conditions and the other projecting future water levels for 2065 to accommodate sea level rise, derived from the Environment Agency's coastal flood boundary conditions for the UK mainland and Islands (2011) [10]. Specifically for Bacton, RHDHV has considered a sea level rise of 0.42 meters, based on scenarios published in the UK Climate Projections 2009 [10].

A beach sediment sampling campaign and laboratory analysis were undertaken as part of the detailed design phase. The results of this are provided in table 3. The Bacton shoreface median grain size mainly varies from 0.25-0.39mm.

Morphological feature	Median particle size (mm)		% Sand				
	Minimum	Maximum	very fine	fine	medium	coarse	very coarse
Bacton dunes	0.2	0.3	0-1	30-61	38-67	0-3	0
Bacton upper beach face	0.3	0.4	0-1	18-32	53-63	6-22	0-4
Bacton lower beach face	0.25	0.65	0	14-51	29-40	8-30	5-36
Bacton shoreface	0.25	0.35	0-1	22-54	32-56	5-19	2-7
Walcott shoreface	0.25	0.25	0	24-31	51-58	13-15	4-6

Table 3: Particle size summary from sampling campaign , from [11].

A total of eight measurements were collected, spanning seven distinct measurement periods. Table 4 summarizes the average significant wave height, period, and direction relative to the coast for each measurement period. For a detailed time series of the hydrodynamic conditions during each individual period and the combined dataset, refer to Appendix A. Additionally, Appendix A includes wave roses illustrating the wave climate between survey periods.

Period	Shore surveys	Timespan	Hs (m)	Tp (s)	Dir (deg)	Hs,max (m)	Tmax (s)
period 0	T0 - 26 Aug 2019 T1 - 19 Oct 2019	54 days	0.62	6.23	40.78	2.41	18.2
Period 1	T1 - 19 Oct 2019 T2 - 21 Feb 2020	125 days	0.69	7.10	39.76	3.21	20.0
Period 2	T2 - 21 Feb 2020 T3 - 30 Oct 2020	252 days	0.66	6.61	34.86	5.01	28.6
Period 3	T3 - 30 Oct 2020 T4 - 9 Juni 2021	222 days	0.72	7.11	38.66	3.29	28.6
Period 4	T4 - 9 Juni 2021 T5 - 17 Sep 2021	100 days	0.60	5.84	37.09	2.25	25.0
Period 5	T5 - 17 Sep 2021 T6 - 12 Oct 2022	390 days	0.66	6.88	32.81	3.36	25.0
Period 6	T6 - 12 Oct 2022 T7 - 02 May 2023	202 days	0.67	7.40	42.38	3.09	20.0
Total	T0 - 26 Aug 2019 T7 - 02 May 2023	1345 days	0.67	6.86	36.89	5.01	28.6

Table 4: Summary of wave conditions during every measurement period.

Period 1:
The first period was a relatively short period, with a low maximum significant wave height if compared to other periods. The angle of incidence of the wave is relatively high in comparison to the average of the entire period. The spread, however, in all these values is not very large. The period covers the end of summer and the first weeks of fall.

Period 2:
Between October 2019 and February 2020, the wave climate is bimodal, with waves primarily coming from two directions, east and north-northeast (NNE). The somewhat higher waves originate from the NNE direction, and these waves generally have a larger period. Extreme conditions are therefore likely to be caused by storms further up the North Sea, resulting in swell waves coming in at the North Norfolk coast. This period covers a time when it is winter.

Period 3:
The second period runs from February 2020 to November 2020, covering spring, summer and fall seasons. During this period the dominant wave direction was North-Northeast. Again, the extreme waves with larger wave periods are expected to be caused by storms in the North Sea. It was expected to see some summer recovery after the winter period between T2 and T3, but the influence of two significant storm events on 28/08/2020 and 25/09/2020 nullified this.

Period 4 & 5:
Both the third (winter and spring) and fourth periods exhibit a predominant NNE wave direction. While the fourth period, occurring in summer, displays a similar wave direction, it is characterized by generally lower wave heights.

Period 6:
This period encompasses the largest time span, with little more than over a year. As expected the average wave height and period are almost equal to that of the entire measured period, but interestingly, the angle with respect to the coast is low in comparison to the other periods.

Period 7:

The final period covers the winter months, and therefore, it is thought to be characterized by relatively high significant wave height. However, this does not show up in the data. During this period, the waves have a generally high angle of incidence to the coast and a relatively large wave period.

3.5 Nourishment volume change

This paragraph discusses to what extent sand has been transported along the coast, and what kind of volumetric changes took place within the surveys. To calculate the volume changes between measurements, RHDHV subtracted the older survey from the newer survey to determine the change elevation. Subsequently, this elevation change is multiplied by the resolution of the survey (2x2 m) to obtain a volume change. The total volume change is calculated by summating all these 2x2 m cells. The cross-shore boundaries for this analysis were taken to be the cliff toe/apron and -8m AOD. This -8m AOD boundary was selected cause it was thought that beyond this point minimal bed level changes occurred. To understand how the shoreface readjusts over time the cross-shore profile is divided into the following sections, see table 5.

<table>
<tr><th></th><th>Reference level</th><th>Coastal zone</th></tr>
<tr><td rowspan="2">MHWS</td><td rowspan="2">+1.88m AOD</td><td>Subaerial beach</td></tr>
<tr><td rowspan="2">Higher intertidal zone</td></tr>
<tr><td rowspan="2">MSL</td><td rowspan="2">+0.11m AOD</td></tr>
<tr><td rowspan="3">Lower intertidal zone</td></tr>
<tr><td>MLWS</td><td>-1.58m AOD</td></tr>
<tr><td rowspan="2">LAT</td><td rowspan="2">-2.55m AOD</td></tr>
<tr><td rowspan="3">Shoreface</td></tr>
<tr><td>-5m AOD</td><td>-5m AOD</td></tr>
<tr><td rowspan="2">-8m AOD</td><td rowspan="2">-8m AOD</td></tr>
<tr><td>Nearshore zone</td></tr>
</table>

Table 5: Definition beach zones.

Period 0 & 1: As previously mentioned, during this period, the wave climate exhibits a bimodal pattern, with waves predominantly originating from two directions: East and North-Northeast. However, the high energy waves originate from NNE. Therefore sediment is expected to move southward. Interestingly, to see is that higher up in the profile volume is lost while from the lower intertidal zone and further downwards, the areas experience a net increase in volume. This means that after construction the profile is readjusting to a more natural profile shape. As expected since the constructed profile lies far from equilibrium. The terminal has a net loss of volume within this period while the village frontage has a net gain of volume, indicating the feeding capability of the terminal frontage. Overall the entire nourishment gains in volume over this period, which was not expected. It is thought that this increase can be explained by the change in coastline orientation from west to east that creates a reduction of sediment transport capacity between updrift and downdrift, but this can not be proven.

Aug19 - Feb 20	Terminal [m^3]	Villages [m^3]	Combined [m^3]
Sub-Aerial beach	-145,000	-51,000	-201,000
Intertidal zone	-15,000	-52,000	-67,000
Upper intertidal	-31,000	-67,000	-98,000
Lower intertidal	+16,000	+16,000	+32,000
Shoreface	+104,000	+217,000	+321,000
Net	-56,000	+114,000	+54,000

Table 6: Volume change between Aug 19 - Oct 20, from [7].

Period 2: During this 9-month period, the dominant wave direction was NNE. At the end of this period, two storm events took place which largely influenced the November 2020 survey. When comparing the volume changes of table 6 and table 7, it can be seen that within this second period, the erosion is significantly larger than during the previous period. This is unexpected, as summer typically brings calmer conditions that normally lead to beach growth. It can be explained by the storm events on 28/08/2020 and 25/09/2020. Additionally, the second period spans three months longer than the first. Similar to the first period, a redistribution of sediment within the profile is observed. Throughout this period a subtidal bar forms, as sediment is transported from higher up the profile toward the offshore area. During this period both the terminal frontage as well as the village frontage experienced a net loss of sediment and overall the sandscaping lost 171,000 m^3, resulting in a total loss of 120,000 m^3 from construction.

Feb 20 - Nov 20	Terminal [m^3]	Villages [m^3]	Combined [m^3]
Sub-Aerial beach	-71,000	-83,000	-154,000
Intertidal zone	-269,000	-437,000	-707,000
Upper intertidal	-53,000	-10,000	-64,000
Lower intertidal	-216,000	-428,000	-644,000
Shoreface	+196,000	+494,000	+690,000
Net	-145,000	-26,000	-171,000

Table 7: Volume change between Feb20 - Nov20, from [7].

Period 3: The third period covers a winter and spring season, during which the dominant wave direction is NNE and the climate is unimodal instead of bimodal. Again, the same trend of redistribution of the sediment within the shore profile can be seen, with sediment eroding from higher up in the profile and depositing on the shoreface. The total loss of volume throughout this period of the terminal and village front combined is 118,000 m^3 and of the same order magnitude as the previous period. The majority of this sediment originates from the terminal, with a slight volume increase observed at the villages, suggesting a potential feeding capacity of the terminal frontage towards the downdrift.

Nov 20 - Jun 21	Terminal [m^3]	Villages [m^3]	Combined [m^3]
Sub-Aerial beach	-62,000	-2,000	-64,000
Intertidal zone	-64,000	-27,000	-91,000
Upper intertidal	-13,000	+3,000	-10,000
Lower intertidal	-51,000	-30,000	-81,000
Shoreface	+5,000	+31,000	+36,000
Net	-120,000	+2,000	-118,000

Table 8: Volume change between Nov 20 - Jun 21, from [6].

Period 4: During the fourth period the dominant wave direction was again NNE with a maximum significant wave height of 2.25m and a corresponding wave period of 7.1 seconds. Similar to the previous period, there is a net sediment loss in the area, and for the first time since the completion the shoreface has lost sediment. This could be explained by the shoreward movement of the subtidal bar, which is indicated by the increase of volume in the lower intertidal area. This behavior is expected during summertime with periods of low energy waves and is also seen in measurement data as shown below in figure 10. This transect is located at the village frontage.

Figure 10: Onshore bar migration

Jun 21 - Sep 21	Terminal [m^3]	Villages [m^3]	Combined [m^3]
Sub-Aerial beach	-10,000	-21,000	-31,000
Intertidal zone	-21,000	+19,000	-2,000
Upper intertidal	-18,000	-6,000	-24,00
Lower intertidal	-3,000	+25,000	+22,000
Shoreface	-17,000	-20,000	-37,000
Net	-48,000	-22,000	-70,000

Table 9: Volume changes between Jun 21- Sep 21, from [6].

Over the entire period (T0-T5), it can be observed that the nourishment lost 301,000 m^3 of the initially placed 1.8M m^3. In other words, approximately 17% of the initially placed material in the project area eroded over a brief span of two years. Due to either offshore and or alongshore transport. The village frontage gained a net volume of 68,000 m^3, most of this deposited between the first two measurements. The terminal frontage, on the other hand, lost a volume of 369,000 m^3. From the tables, it becomes evident that a large part of sediment gets redistributed within the profile. The sub-aerial beach and intertidal zones lost about half a million and a million cubic meters, respectively, while the shoreface gained a million.

Aug 19 - Sep 21	Termianl [m^3]	Villages [m^3]	Combined [m^3]
Sub-Aerial beach	-288,000	-157,000	-445,000
Intertidal zone	-369,000	-497,000	-866,000
Upper intertidal	-115,000	-80,000	-195,000
Lower intertidal	-254,000	-417,000	-671,000
Shoreface	+288,000	+722,000	+1,010,000
Net	-369,000	+68,000	-301,000

Table 10: Total volume change Aug 19- Sep 21, from [6].

3.6 Contour movement

This paragraph aims to review the contour movement of the Bacton area over time. Therefore, contour lines of different elevations were plotted relative to the cliff line/apron to study the change in the nourishment's planform area. This approach allows for tracking contour movement over time, providing crucial information about their behavior. The specific contours of interest are detailed in table 5. The alongshore distance in the plots is shown in chainages in meters. The terminal frontage extends from chainage 9100 to 10800, followed by the village frontage, which continues to chainage 14100. In the figures, these locations are depicted by the dashed vertical gray lines. These two frontages will be examined separately.

Period 0: The analysis done by RHDHV on the contour movement in the first couple of periods did not extend beyond the -8m AOD contour as RHDHV did not deem this necessary since they did not expect activities beyond this point. Later on, they came back on this decision as they did see activity beyond -5m AOD and expanded their analysis to the depth of -8m AOD. During the first period the -5m AOD contour seems to maintain its position during these months. Both the contours LAT, MLWS and to a lesser extent MSL, shift seaward, while MHWS moves landward. Showing that the cross-shore profile moves to a more natural state. The villages section and the terminal section show similar behavior during this period.

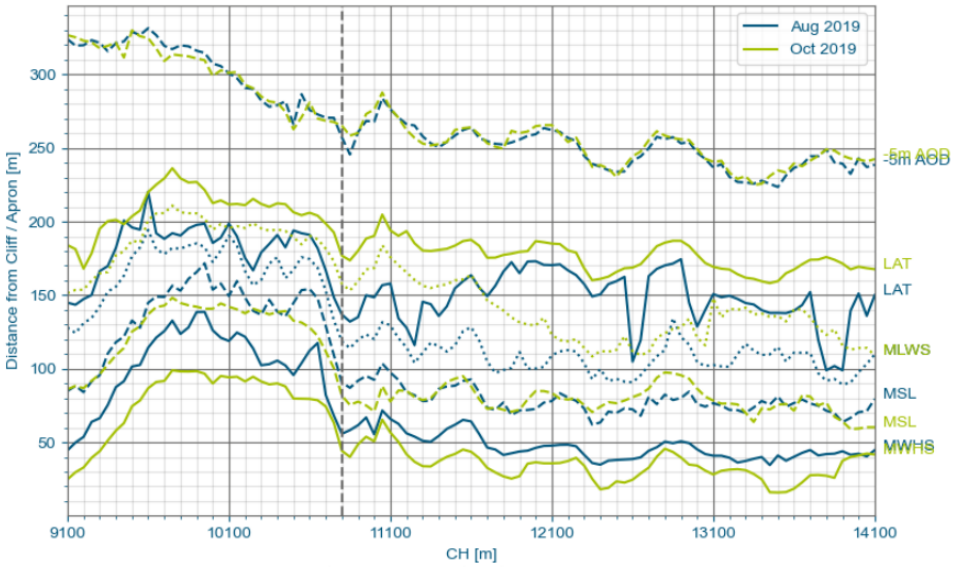

Figure 11: Contour movement Aug 19 - Oct 19, from [5].

Period 1: In front of the terminal, the two contours of MLWS and MSL do not seem to move that much, but the contours of MHWS (the figure displays MWHS, and this is a mistake) and LAT do show movement. The MHWS contour in February 2020 has propagated shore-

ward, meaning that the shoreline has retreated. On the contrary, the LAT contour has moved seaward. The combination of these two indicates sediment redistribution within the profile, with sediment lying higher up on the profile moved downwards. In front of the villages, all the contours show movement. The MWHS contour moves seaward, while MSL and MLWS move shoreward causing the shoreface profile to steepen in this region. Similar to the terminal the LAT contour shifts seaward, indicating accretion in this area.

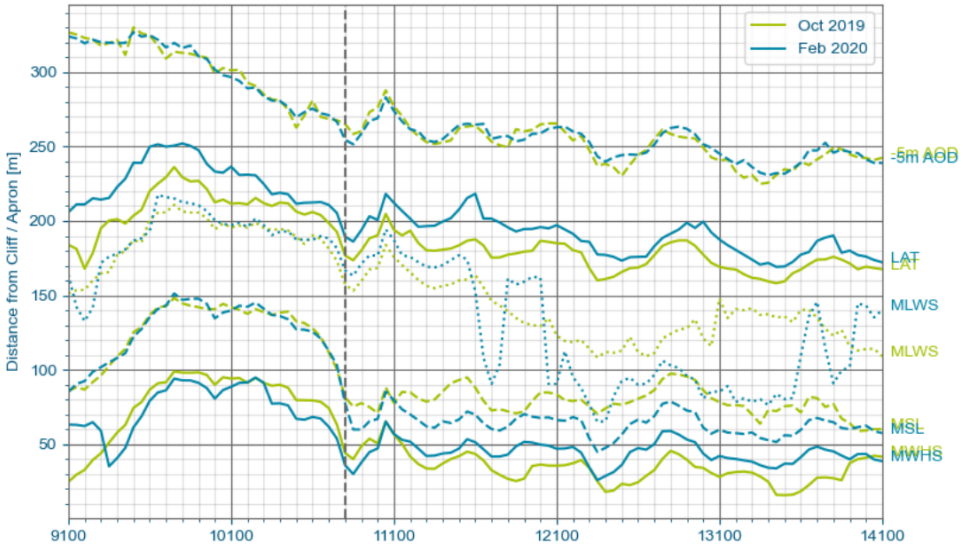

Figure 12: Contour movement Oct 19 - Feb 20, from [5].

Period 2: Immediately one notices a shift in the position of the -5m AOD contour from figure 13 and therefore justifying the inclusion of the -8m AOD contour. Almost all the contours have moved shoreward, except the -5m AOD contour. This contour moved seaward and in combination with the onshore movement of the LAT contour it indicates the formation of a subtidal bar. At the terminal, the MHWS and MSL move shorewards. Therefore the coastline retreats further during this period. The width between these two contours along the entire nourishment does not change, thus not altering the beach slope. Both the MLWS and LAT contours have moved landward quite significantly and the widths between MSL-MLWS and MLWS-LAT are rather uniform, suggesting a relatively uniform profile shape for both frontages. This could be caused by the severe storm events that took place during this period. At the terminal and especially at the transition between the two frontages the slope between MSL and MLWS has steepened.

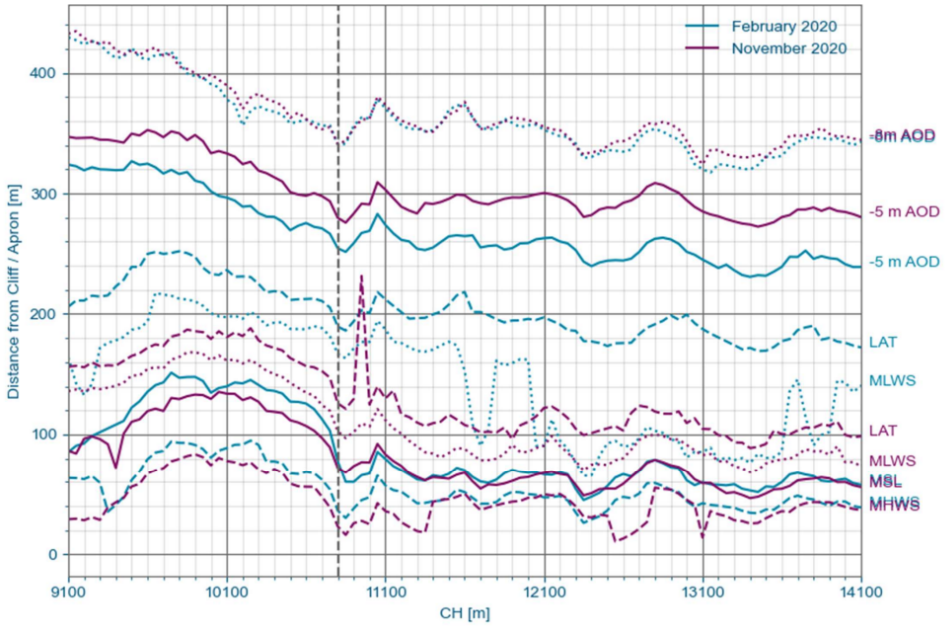

Figure 13: Contour movement Feb 20 - Nov 20, from [7].

Period 3-4: Between June 21 and September 21 no significant changes took place. This fourth period is relatively short compared to the others, and the energy of the waves was low during the summer season. Beach levels in front of the seawall have generally increased slightly along the villages, but the shape of the intertidal zone remains largely unchanged. Along the terminal, it can be observed that the contours LAT, MLWS, MSL, and MHWS shift landward slightly. These first two contours' movement hints at the onshore movement of the subtidal bar, which was already seen in paragraph 4.3.

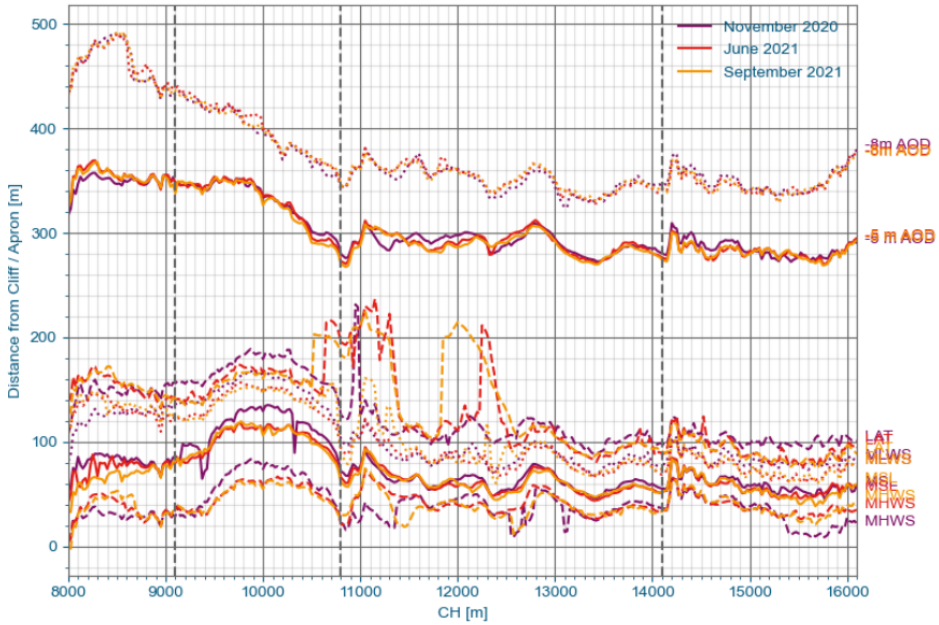

Figure 14: Contour movement Nov 20 - Sep 21, from [6].

Period 5: The plots will look a little different from this moment onwards, as the data for these periods came later and the analysis was done separately. In the figure red indicates measurement T5 and blue indicates measurement T6. It has become a little difficult to see

what happened between these two measurements especially the shift in contours LAT and MLWS. The shift covers a time of a little more than a year. What is interesting is that within this year, the lower two contours roughly maintain their positions, and so does the MSL contour.

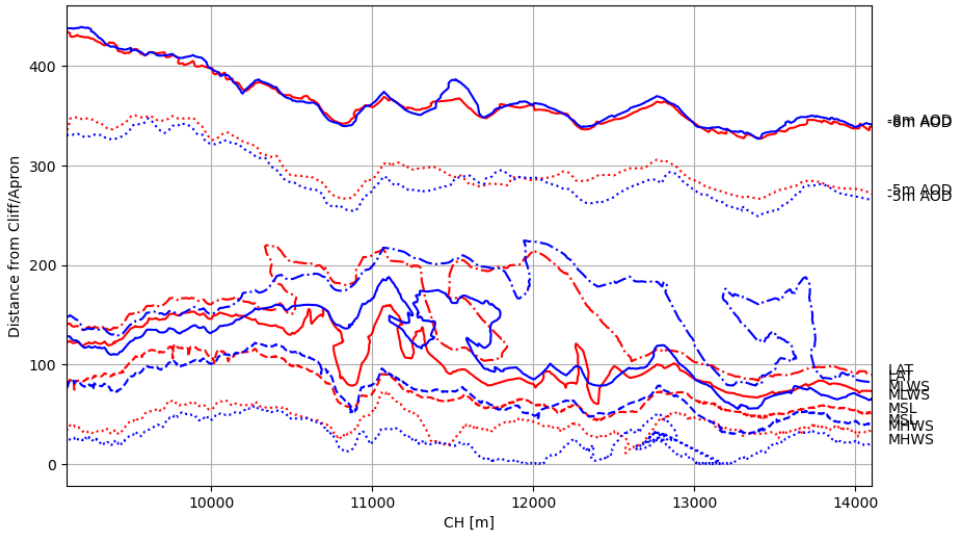

Figure 15: Contour movement Sep 21 - Oct 22.

Period 6: Similar to the plot of period 5, T6 is indicated with blue and T7 with green. Likewise, to period T5-T6, the lower contours pretty much remain in the same place. Noticeable from this plot is the chunk taken out of the beach or MSL contour. This also translates back to the loss of planform area observed in table 3.6.

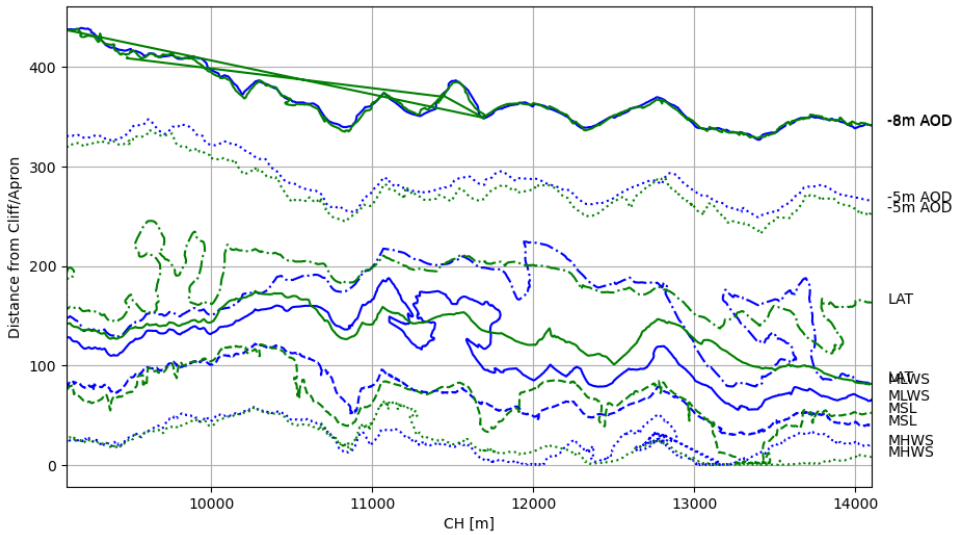

Figure 16: Contour movement Oct 22 - May 23.

Since the scheme's construction, the development has been dominated by the ongoing erosion of the sacrificial body at the terminal and the formation of a subtidal bar. The profile at the terminal has adjusted towards a natural beach profile, which has resulted in a large erosional zone in front of the terminal. The same can be observed for the village frontage but less profound.

All these plots together show a decrease in the beach area over time. An analysis was done

to quantify how much surface area the beach has lost. Regarding this, the MSL contour was subtracted from the cliff toe/apron line, thus assuming that the width of the beach is the distance from the cliff toe/apron to the MSL. The planform area is then calculated relatively easily by integrating this distance over the length of the nourishment. The two sections, terminal and villages, were separately inspected and the results of the calculation are shown in table 11. All the areas in the table are presented in m^2. One can see that most of the planform area was lost in the period between T0 and T2, but interestingly, the nourishment overall gained volume during this time. Therefore, the loss in planform area is not caused by loss of volume. This is due to the redistribution of sediment within the profile. One can argue that there is some sort of up-and-down trend in the decline of the planform area, the first period lot of activity the second period somewhat less and then the third period again a bit more active and so on. The reason for this can be that the first and third contain the winter season, during which the beaches generally tend to become smaller and less steep. Whereas during summer, beaches tend to become wider with steeper slopes. Contrary to the period between T0-T2, the decline of planform area in the following periods is much less. Even during the period T2-T3, which is known to be the period with the largest erosion, the decline in the planform area is not half as much as in the first period. Therefore it seems like the profile has moved toward a natural beach profile.

Remarkable from this analysis is that between the last two measurements, the decline in planform area is quite high in comparison to the preceding periods, especially in front of the terminal. This prompted a closer examination of volume changes during this timeframe. This volume change is calculated in a different way than before, namely 100 transects are drawn each with a spacing of 50 meters and for both measurements, these transects are subtracted from each other and multiplied by the spacing. The results from these calculations are that the terminal loses $25,366m^3$ and the villages $25,148m^3$, therefore in total the nourishment lost $50,515m^3$. However, this still does not explain the relatively large loss of planform area, since no particularly large volume was lost during this time if compared to other periods. Nonetheless, the calculation of volume change is done differently and therefore one should be careful in interpreting them.

Survey	Terminal	Diff	Daily diff	Village	Diff	Daily diff	Combined	Total diff	Daily diff
T0	229,491	-	-	255,298	-	-	484,789	-	-
T1	213,221	-16,270	-307.0	256,419	1,121	21.2	458,640	-15,149	-285.8
T2	213,958	737	5.9	208,224	-48,195	-388.7	422,182	-47,458	-382.7
T3	187,475	-26,483	-105.5	205,657	-2,567	-10.2	393,132	-29,050	-115.7
T4	172,139	-15,336	-69.4	198,649	-7,008	-31.7	370,788	-22,344	-101.1
T5	172,635	496	5.0	197,588	-1,061	-10.7	370,223	-565	-5.7
T6	167,368	-5,267	-13.5	188,362	-9,226	-23.7	355,730	-14,493	-37.3
T7	152,222	-15,146	-75.4	181,825	-6,537	-32.5	334,047	-21,683	-107.9
Total		-77,269			-73,473			-150,742	

Table 11: Change in planform area.

3.7 Cross-shore adaptation

From the paragraphs 3.5 and 3.6, it became clear that a lot of activity happens on the cross-shore. To further examine this, in this paragraph, some transects are inspected to see how individual profiles readjust over time. Transects that are of interest in this analysis are CH9100, CH9950, CH10800, CH12450, and CH14100. CH9100 is the point where the terminal frontage starts, CH10800 is at the end of the terminal frontage and 9950 is right in the middle. The same holds for CH12450, which is in the middle of the village frontage.

In all the transects it becomes clear that a sandbar appears between Shore surveys 2 and 3. Later on one can also see it moving back landwards. The first plot 17a shows that the beach gains volume in the first period, which subsequently disappears. This gain is probably due to the diffusion of the terminal frontage. Over time this profile lost most of its volume between 1470m and 1600m and gained between 1600m and 1750m. The second plot 17b, the one in the middle of the terminal frontage, shows a lot of activity. Immediately after construction, the formation of a scarp can be observed. Almost all contours (MHWS, MSL, MLWS and LAT) move landward over the entire survey period, except the -5m AOD contour. Interestingly, the -8m AOD contour in this profile also moves offshore, but only from November 20, which means that there is activity beyond this point. The shift is very slight but present. The volume lost left of the 1600m line in this profile does not equal the gained right of this line, indicating an overall volume loss consistent with findings from previous paragraphs. Transect 10800 very nicely shows the onshore bar migration between November 20 and September 21. The fourth profile, located in the villages, shows very little shift in the MHWS contour seaward, indicating a gain of beach area. Again, the -8m AOD contour shows a slight shift offshore, showing activity beyond this point.

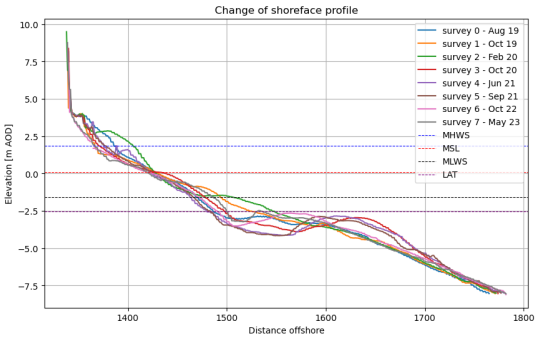

(a) transect 9100

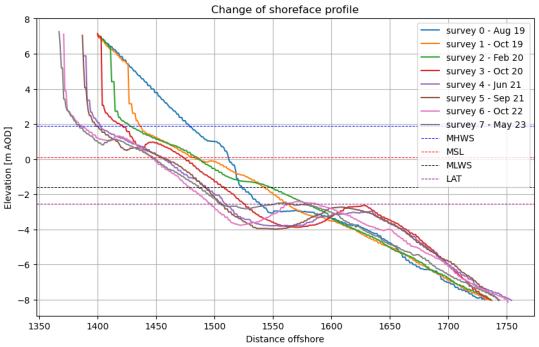

(b) transect 9950

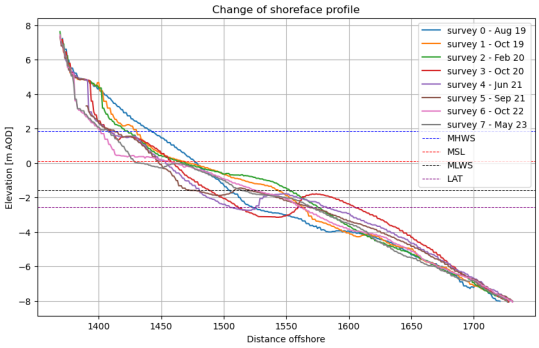

(c) transect 10800

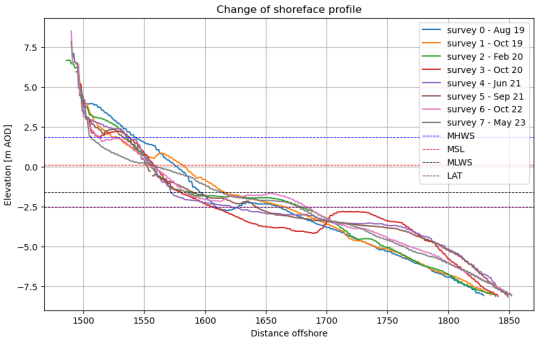

(d) transect 12450

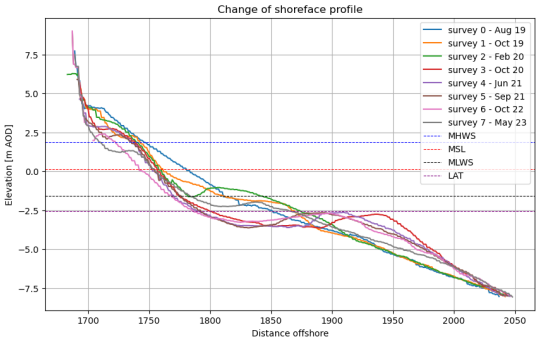

(a) transect 14100

Figure 18: Cross-shore profile adjustment for 5 transects (CH9100, CH9950, CH10800, CH12450 and CH14100).

3.8 General observations

Since the completion of the scheme until the last Shore measurement, the nourishment has lost approximately 20% of its original volume and about 30% of its planform area. All this volume was lost in about three and a half years. This erosion was not uniform over the nourishment. Looking at both sections individually, one can see that most of this volume was lost from the terminal section, whereas the villages actually gained a little. This development suggests that the terminal section is feeding the villages as was intended. The sedimentation is not uniform over the depth either. In table 10, it becomes clear that the sub-areal and intertidal zones lose volume while the lower shoreface gains sediment. This indicates that within the profile, redistribution of sediment takes place, consequently flattening the shoreface. The same phenomenon can be observed in the plots of the contours and cross-shore profiles. In the plots of the cross-shore profiles, one clearly sees the development of the subtidal bar and in the later stage the onshore movement of it. Therefore, it can be concluded that over time the profile has adjusted to a more natural profile.

4 Methodology

This chapter outlines the methodology for addressing the subquestions and, consequently, the research question. It demonstrates the anticipated form of the results. First, it explains how the current performance of ShorelineS in predicting coastline evolution is evaluated (4.1). Second, it describes how cross-shore redistribution will be included in ShorelineS (4.2) and finally, how the performance of this adjusted ShorelineS model is tested (4.3).

4.1 Current ShorelineS performance

This paragraph discusses how the predictive capability of the current ShorelineS model is evaluated. It is done by comparing Shore Monitoring and Research measurements with the ShorelineS model results.

First, the model setup is elaborated on, clarifying the required input for ShorelineS like the initial and boundary conditions (4.1.1). This is followed by an explanation of how the performance of ShorelineS is compared to the measurements of Shore Monitoring and Research (4.1.2).

4.1.1 ShorelineS model setup

ShorelineS was used for this analysis, as this was already available from RHDHV. The model was acquired from Max Leummens from RHDHV under its existing conditions. Max calibrated the model as part of a TKI program. The calibration consisted of comparing modeled coastline changes with and without nourishment. The goodness of the model was based on the location and magnitude of the peaks and troughs in coastline change. This is a different than normal. Normally, one would calibrate the model based on measured data, but because this is scarce, it was chosen to do it this way.

Initial conditions

ShorelineS requires a couple of input parameters, the first of which is an initial coastline. This can be acquired from the post-construction measurement by extracting the coastline contour from the data using QGIS. The initial coastline is visualized in figure 19 as the black line. ShorelineS assumes the given coastline to be around mean sea level so the contour extracted from the post-construction measurement is the +0.11m AOD MSL contour, see table 2. The boundaries of the domain automatically lie on the borders of the initial coastline. The post-construction measurement was concluded on 26 August 2019. This is also the starting point of the simulation or T_0.

Boundary conditions

Also, a set of boundary conditions need to be defined, one for every boundary. For this, ShorelineS has four options: a closed boundary, a fixed coastline position, a fixed coastline orientation, and a periodic boundary. The latter means that at the boundary, the transport at the start is averaged with that at the end of the grid. A closed boundary can mean zero transport at the edges of the domain, but it can also be a predefined constant flux. In the case of a fixed coastline position, the coastline at the edges of the domain will maintain its position and there is no sedimentation or erosion in this boundary cell. In contrast, this is not the case with a fixed coastline orientation. Here, the boundary cells can translate, but the orientation or the angle will remain constant. For the simulations, a constant coastline orientation is selected for

both boundaries.

Foreshore orientation

ShorelineS also requires the orientation of the foreshore. This area is defined as the region just outside of the longshore current and does not react instantaneously to changes at the waterline. In many cases, the disturbance at the coastline is not present at the foreshore, which means that defining the foreshore orientation can have a large influence on the transformed nearshore wave. The orientation of the foreshore is fixed based on the original coastline position before nourishment.

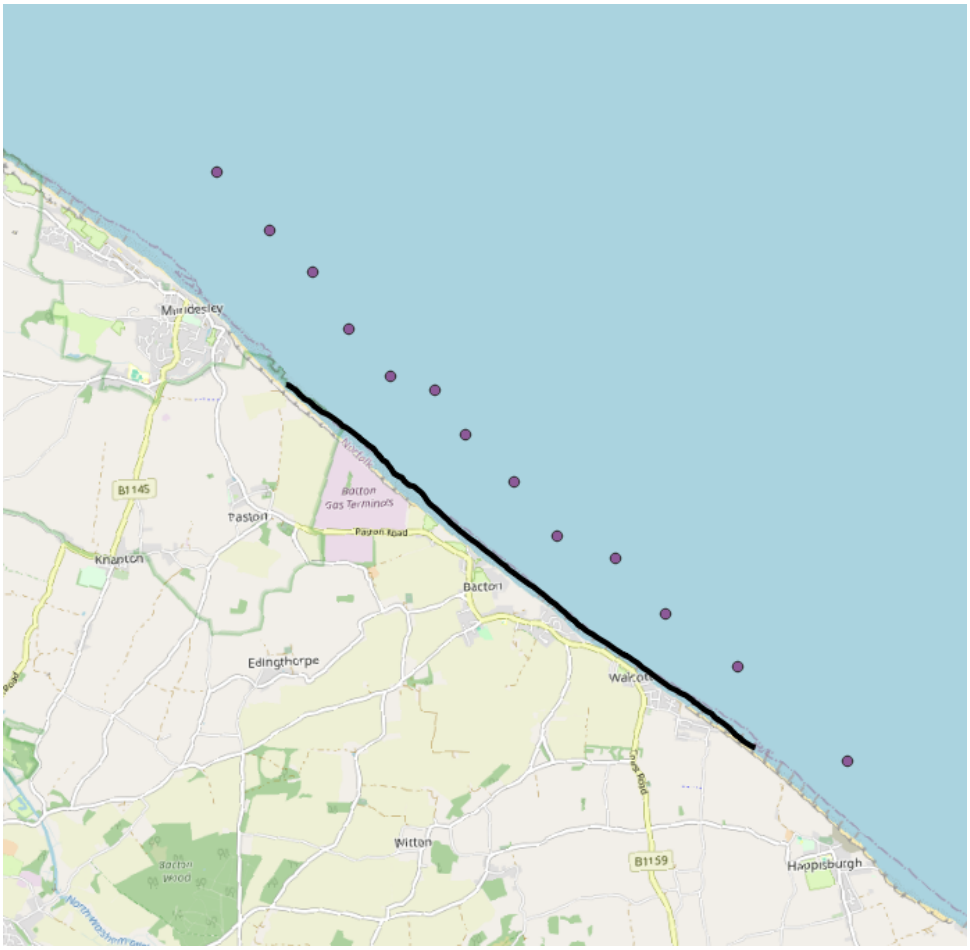

Figure 19: Location of the 13 nearshore wave data points and the initial coastline.

Profile parameters and wave definition

Next, ShorelineS also requires three profile parameters: $ddeep$, $dnearshore$ and d. The latter refers to the active profile height ranging from inner closure depth to the toe of the dunes. In the case of Bacton, the beach in front of the terminal was constructed at a level of +7m AOD. In all the monitoring reports RHDHV assumes the depth of closure to lie on a level of -8m AOD. However, as mentioned in paragraph 3.7, it follows that from measurement results, it can be concluded that the inner depth of closure lies deeper. Looking at the transects it is likely that beyond the -10m AOD point there is no change in bed level visible between measurements. Therefore, this is a sound assumption for the inner closure depth $dnearshore$. The final parameter is the deep water depth $ddeep$ and always corresponds to the point at which the wave data is derived. This wave data, as mentioned in subparagraph 2.5.2, can be defined in three ways:

- Using wave direction and a spreading sector. A uniform distribution is assumed between the mean wave direction and plus or minus half the spreading sector. For every time step a random wave direction will be chosen from this sector.
- Using a wave climate considering a number of wave conditions, where one condition will be selected at random.
- Using a time series of wave conditions

The performance of ShorelineS is assessed based on past measurements. A time series of wave conditions is used to closely mimic the forces that influenced the coast. For the time series a ERA5 dataset was downloaded from a location offshore and transformed to nearshore using a SWAN simulation. This SWAN simulation returned the wave data for 13 locations near the Bacton sandscaping. The location of these points is shown in figure 19. The water depth of this nearshore location is 12m ($ddeep$). The SWAN simulation also required water level data, and this was obtained from a measurement station at Cromer, approximately 14 km from Bacton.

ShorelineS defines the cross-shore profile as a constant, predefined slope. This slope is assumed for the entire coastline and is determined based on the average slope of an average transect located at the terminal. This resulted in a mean bed slope of 0.0594.

Transport equations

The next input parameter required is the selection of transport formulation and the different possibilities are listed in paragraph 2.5 and repeated here for readability: CERC1, CERC2, CERC3, Kamphuis, Mil-Homens and van Rijn. An explanation of all these individual transport formulations can be found in paragraph 2.5. The purpose of this research is to investigate if the inclusion of cross-shore redistribution improves the performance of ShorelineS in predicting the coastline evolution of a mega nourishment. For this, it is desirable if the equation is easy to interpret. CERC is the simplest longshore sediment transport equation as it contains the least amount of variables. CERC2 is a direct derivation from the official CERC equation, and therefore, this is the one selected for the simulation. This formulation implicitly refracts the offshore wave conditions supplied in the model. The formulation requires the following input parameters:

- porosity $p = 0.4$
- Depth induced breaker parameter gamma $\gamma = 0.78$
- water and sediment density $\rho_w = 1025$, $\rho_s = 2650$

Space and time step

The final parameters that need to be defined are the time and space step for the simulation. A typical grid cell size is of the order 50-100m. Coarse grid cells are suitable for large-scale problems, but smaller grid cells need to be accompanied by a small timestep. According to the user manual grid cell sizes around the 10 meters pose stability problems [27]. Since mega nourishment is of a large scale, a grid cell size of 100m was chosen. Two options are available for timesteps: variable timestep and fixed timestep. The variable timestep is automatically computed based on the transport rate. When this is used, the timestep will always be the minimum of this computed timestep and the timestep of the wave data. To ensure comprehensive analysis, a variable timestep is used, allowing for the inclusion of all input wave conditions. This approach is preferred over a fixed timestep to more accurately replicate coastline changes.

4.1.2 Evaluating current ShorelineS performance

To evaluate the performance of ShorelineS in predicting the evolution of the Bacton Sandscaping, a comparison is made with Shore measurements. The ShorelineS model returns coordinate positions of the MSL contour at a given predefined time interval. All these points together represent the modeled coastline. The measured coastline is obtained by extracting the MSL contour from the data using QGIS. If these coastlines are subtracted from a reference line or the cliff line it results in a beach width.

The comparison of both modeled and measured results is done in several ways. First, the general shape of the MSL contour is assessed qualitatively. Then performance is assessed qualitatively using the following three metrics: Absolute distance, Relative distance, and Planform area. These distances are calculated with the formulas below, where $dist$ is the distance the modeled or measured coastline has to the reference cliff line. The last metric, planform area, represents the total area of the beach. The next analysis compares the modeled coastline change to the coastline change that would follow from volume change. Since the model simulates coastline change based on a volume balance this analysis could provide valuable intel on the performance of the model. The final analysis is on the modeled coastline change for each period. In this analysis, the model gets re-initialized after each period. Where the measured MSL contour at that instant is used as the initial coastline to simulate the next period. For instance, the measured MSL contour at T2 is used as the initial coastline for the simulation running from T2 to T3. This analysis aims to provide more insight into where the errors are the largest.

$$|dist_{measured} - dist_{modeled}| \qquad \text{Absolute distance} \tag{33}$$

$$dist_{y,measured} - dist_{y,modeled} \qquad \text{Relative distance} \tag{34}$$

4.2 Integrating cross-shore redistribution in ShorelineS

This paragraph explains how the coastline redistribution is integrated into ShorelineS. To do so it first touches upon how cross-shore redistribution can be defined (4.2.1). Then it discussed how this redistribution can be derived from measurement data (4.2.2 and 4.2.3.).

4.2.1 Defining the redistribution of the sediment

Figure 20 shows a sketch of profile equilibration. The top profile change is typically one that would be a result of a 1D coastline model, like ShorelineS. Visible here is that the translation of the profile is uniform over the entire profile and how much the profile regresses is dependent on how much volume was lost during a certain period of time. The bottom figure represents results from measurements. In this case, it can be observed that the shift in coastline is not uniform over the profile. The top half retreats while the lower half extends. This is because of the redistribution of sediment within the profile. From this figure 20, it becomes clear that the measured coastline retreat around water level is bigger than the one resulting from the model, and this difference can be expressed as a factor.

$$\Delta y_{measured} > \Delta y_{modeled} \tag{35}$$

$$\Delta y_{measured} = R * \Delta y_{modeled}$$
$$R = \frac{\Delta y_{measured}}{\Delta y_{modeled}} \tag{36}$$

Here, R is the factor of equilibration and a function of time. This factor expresses the ratio between measured and modeled coastline change at a certain level. As time progresses, the equilibration will have fully taken place and the profile will have moved to an equilibrium profile. In this case, the translation of the profile becomes uniform and the regression of the coastline that comes from the model will be the same as the one measured. Hence, over time R will become equal to one. From the definition of the R-factor, it emerges that two metrics are required to calculate it, $\Delta y_{modeled}$ and $\Delta y_{measured}$. Both these metrics will be derived from measured data and the details of their calculation are presented in the following subparagraphs.

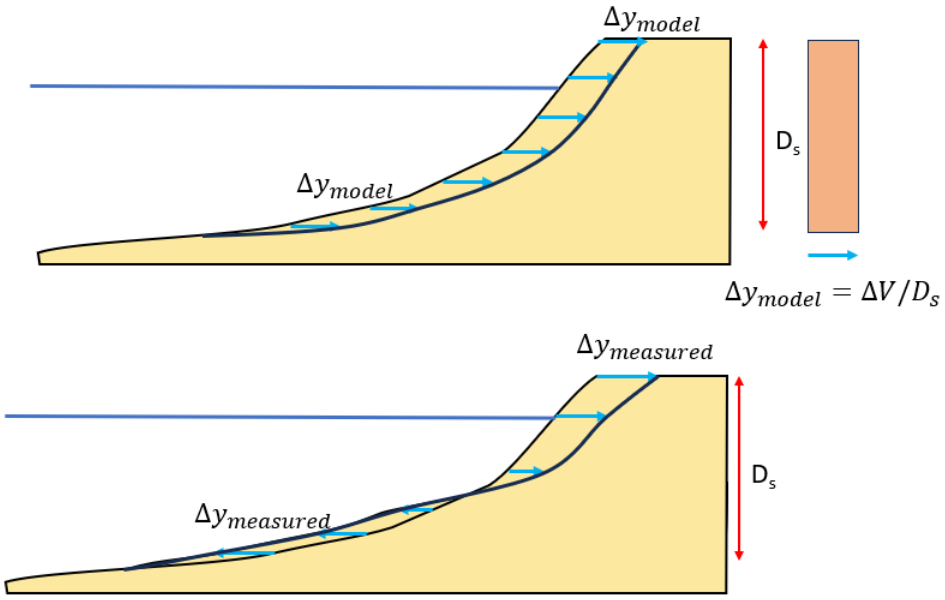

Figure 20: Sketch modeled profile translation (above) and measured profile translation (below).

4.2.2 Modeled coastline change $\Delta y_{modeled}$

Following the equilibrium profile theory of Dean [15] it can be said that the profile shape is only dependent on the fall velocity of the grain and therefore it is reasonable to assume that, in case of sediment gains or losses with a compatible grain, the profile form will remain the same and the profile will just shift land or seaward. Consequently, the coastline shift is only dependent on how much volume comes in or goes out. In 1D coastline models, it works the same as Dean described. The model predicts a volume change and this volume change is evenly distributed over the active cross-shore profile, resulting in a uniform translation of the profile. This fact together with the fact that the nourishment was done with compatible sediment makes it that it can be assumed that the calculated change in volume of a cross-shore profile between the measurements ($\Delta y_{calculated}$) can be used to represent the shift in coastline position that a 1D coastline model would predict ($\Delta y_{modeled}$). However, this only holds under the assumption that there is no sediment flux in or out of the active profile, so beyond the depth of closure. Because of this the volume change over a cross-shore transect between measurements is only calculated within the active profile. In conclusion, the calculated volume change of the active section

of the profile of a cross-shore transect can be used to mimic the shift in coastline position that would follow from a ShorelineS simulation and it is defined as follows:

$$\Delta y_{modeled} \approx \Delta y_{calculated}$$
$$\Delta y_{calculated} = \frac{\Delta V}{B + h_*} \tag{37}$$

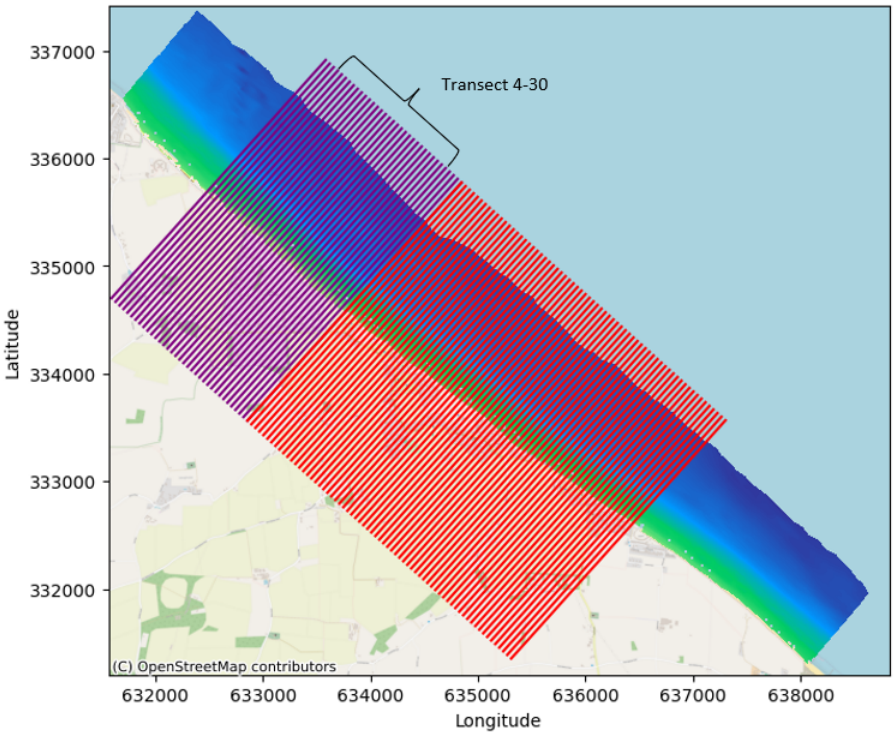

Figure 21: Transects located at the nourishment, purple ones indicate transects located at the terminal and red ones indicate transects located at the villages.

For the calculation of $\Delta y_{calculated}$ predefined transects are used. For the evaluation of the nourishment, RHDHV drew up 4000 transects with a spacing of 50m. One hundred of these transects are located at the nourishment itself. See figure 21. For each measurement, coastal elevation profiles were collected along each transect. In this way, it becomes possible to calculate the loss of volume ΔV in all these transects between measurements.

4.2.3 Measured coastline change $\Delta y_{measured}$

These same coastal elevation profiles from the measurements can be used to determine $\Delta y_{measured}$. By measuring the location of the coastline at a certain level between two measurements one can determine how much the coastline has shifted. Since the signal of coastline change can be disturbed by seasonal changes, it is desirable to measure coastline change at a level less affected by these. In paragraph 2.1, it is mentioned that the position of the coastline marks the location of the maximum storm level surge. Table 2 gives the extreme water level for different return periods. From this table, the +2.86m AOD 1/1 return period water level is

selected as this level is not influenced by seasonality .

The total nourishment project encompasses 100 transects. Not every transect is usable for the analysis described above. The two separate elements have different purposes, the terminal frontage is meant to feed the village frontage with sediment over time. The objective of this research is to investigate whether a 1D shoreline model can be improved for a mega nourishment by adding cross-shore redistribution. According to the literature, a mega nourishment is defined as a large, localized sand placement that creates a disturbance in the longshore direction, see paragraph 2.2. The purpose of a mega nourishment is to nourish neighboring coastal areas, and the terminal section meets this definition of a mega nourishment, but the village section does not. This is more of a classic beach nourishment. As a result, the transects located at the villages are excluded from the analysis. The transition zones are also not suitable for the analysis, since these transects are also very distorted in their signal. The remaining transects are transects 4 to 30.

The preceding established the time-dependency of the equilibration factor, but the exact nature of this relationship remains unclear. It is expected that sediment redistribution within the profile will be complete after a certain period, causing the factor to equal one. Two different relationships are tested: a linear relation and an exponential relation. Figure 22 shows how these would look like. The linear relationship demonstrates that, after a certain period, R will reach one and stay at that value. How long this will take is still unknown and will follow from the results. As will the required parameters of both relationships.

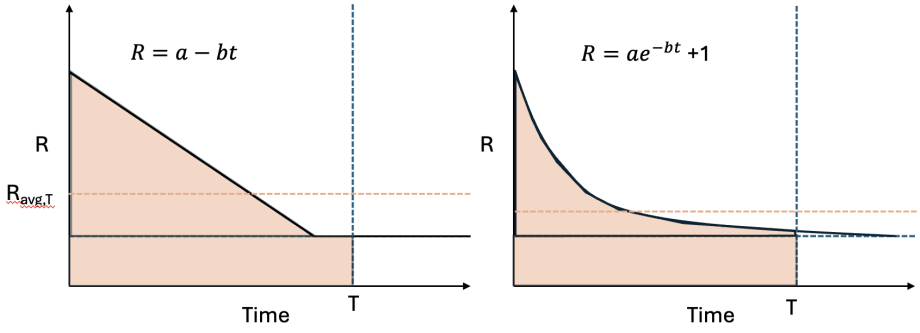

Figure 22: Relationship R with time, linear on the right and exponential on the left.

4.3 Adjusting modeled coastline positions for equilibration

This paragraph aims to explain how the predictive capability of the adjusted modeled coastline position for equilibration is evaluated. First, it elaborates on how cross-shore redistribution is integrated into ShorelineS results through the R-factor. Then, it is explained which metrics are used to quantify the performance of the adjusted ShorelineS model.

The simulations of the coastline in ShorelineS over time will be similar to the original simulations described earlier. There is one key difference: the added shift in the coastline due to profile redistribution. Imagine the simulation will run till a certain time T_N which corresponds to one of the measurement instances. ShorelineS will return a coastline that is shifted from the initial coastline, and the average modeled coastline change in this period is $\Delta y_{avg,modeled}$. To include cross-shore redistribution, the average modeled coastline change ($\Delta y_{avg,modeled}$) will be multiplied with the average equilibration factor $R_{avg,T}$ obtained from the data over the same period ($T_0 -> T_N$). To avoid double-counting the average coastline change predicted by the

model, it is subtracted from the total to arrive at the additional coastline change $\Delta y_{add,T_0T_N}$. It is this additional coastline change that is subtracted from the original model results to obtain the position of the coastline if cross-shore redistribution is included or, in other words, the adjusted coastline. See equation 38. An overview of all these steps is given in the flowchart.

$$\Delta y_{add,T_0T_N} = \Delta y_{avg,T_0T_N,modeled} * (R_{avg,T_0T_N} - 1) \tag{38}$$

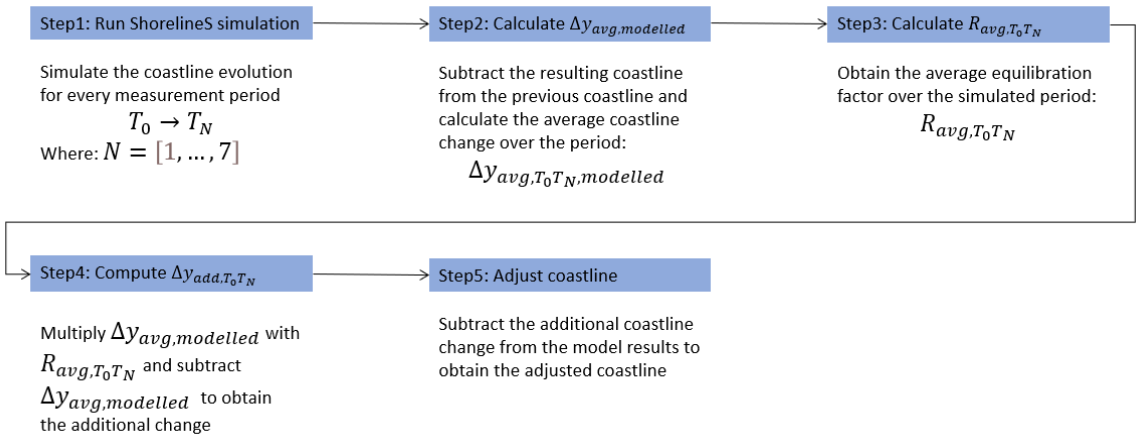

Figure 23: Methodology flowchart.

Given the distinct designs of the two elements, they will be examined individually and collectively. So, this sequence above will be executed for only the terminal section, the village section, and both sections combined. The impact of the R-factor on the simulated coastline will be assessed using the same performance metrics as described in subparagraph 4.1.2, using the metrics planform area, relative distance, and absolute distance.

5 Results

This chapter presents the findings from the various analyses conducted throughout this research. Building upon the methodologies outlined in Chapter 4, it first showcases the performance of the current ShorelineS model (5.1). Following this, the results of the equilibration factor calculations based on measurement data are presented in paragraph 5.2. In paragraph 5.3, the outcomes of the adjusted ShorelineS model runs are explored. In response to the obtained results, a new approach was developed and subsequently tested. An explanation of this approach and its results can be found in 5.4.

5.1 Current ShorelineS performance

This paragraph displays the results from the ShorelineS model as it is today, showing its predictive capabilities. First, a qualitative assessment is done (5.1.1). Then, in subparagraphs 5.1.2 and 5.1.3 the absolute and relative distance from the modeled and measured coastline are discussed respectively. The difference in planform area becomes apparent in 5.1.4. The results of an analysis done on modeled coastline change are presented in 5.1.5 and 5.1.6, where in 5.1.6 the simulation is re-initialized at every measurement instance. The paragraph finds its conclusion in 5.1.7.

5.1.1 Qualitative assessment

To give an overview of the general shape of the measured and modeled coast, Figure 24 presents the modeled and measured MSL contour and their distance to the cliff. In here the alongshore distance is displayed in chainages.

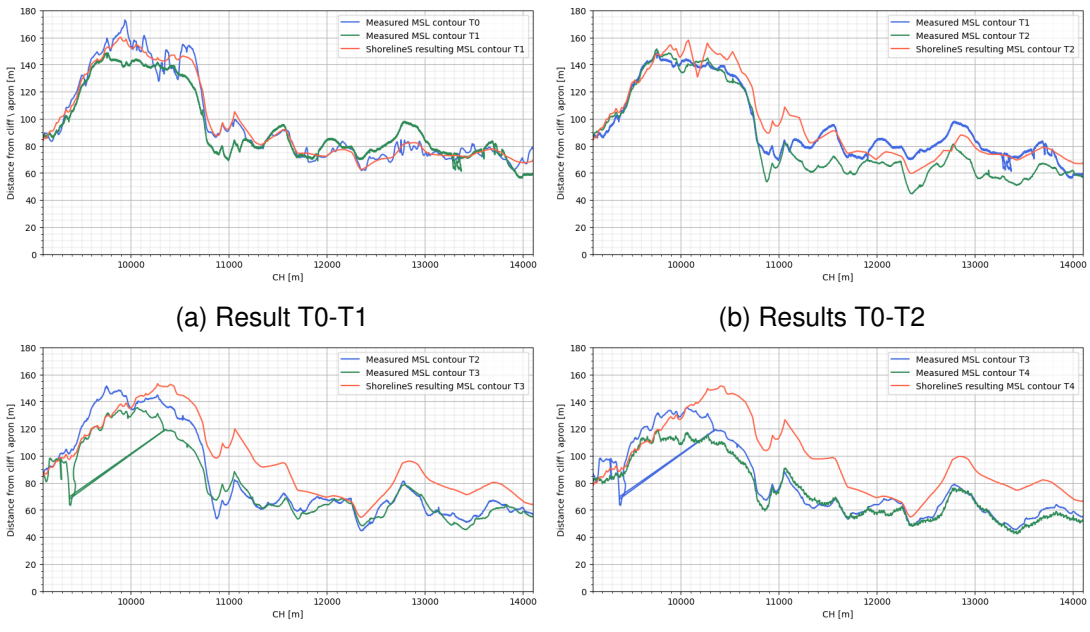

(a) Result T0-T1

(b) Results T0-T2

(c) Results T0-T3

(d) Results T0-T4

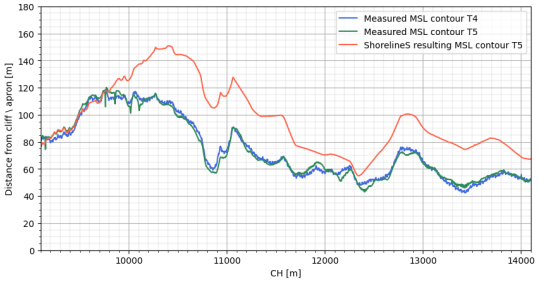

(e) Results T0-T5

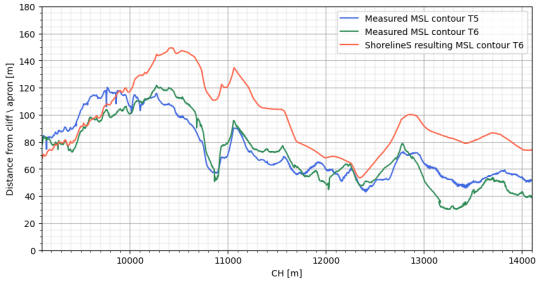

(f) Results T0-T6

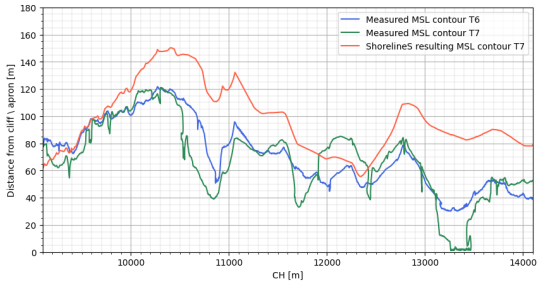

(g) Results T0-T7

Figure 24: ShorelineS results indicated in orange and Shore measurements indicated in green and blue, where the blue one presents the preceding measurement. All lines indicate a MSL contour.

In the beginning, the difference between measured and modeled is not very big, they seem to display roughly the same coastline. Only after a while one start to see a difference. What stands out is that the widest part of the nourishment, or the top, disperses to the right (southwest wards), but roughly maintains its width. Between CH9100 and CH9800, the model performs well, but around halfway to the terminal at CH10000, the lines separate. Around CH11000 and CH13000 there are two features in the model that continue to grow as time progresses. This development is not as expected but might be explained by background effects that are in the model. To check this a simulation is run with the same waves for the same period (T0-T7), but for a coast without the nourishment. The results of this are shown in figure 25 with the red line and display coastline change that is caused by background effects like the curvature of the original coast. Here, it becomes clear that around CH11000 and CH13000, the coastline is building out and this might explain the observed growth of the nourishment.

The plots may reveal irregularities in the measured MSL contour, particularly for T3. This is likely due to how QGIS interprets the contour data during import. Additionally, the sudden drop to zero in the T7 MSL contour is caused by gaps within the measurements. Please consider these limitations when interpreting the following results.

5.1.2 Absolute distance

Absolute distance shows how much the modeled coastline and measured MSL contour vary. It is an indication of the error the model makes. Table 12 shows the average absolute distance between the modeled and measured results per measurement instance. Notice how, over time, the error increases.

Survey	Terminal Avg. $[m]$	Village Avg.$[m]$	Combined Avg. $[m]$
T1	8.74	6.88	7.49
T2	7.98	15.42	12.9
T3	17.22	18.89	18.3
T4	20.63	24.01	22.9
T5	20.32	25.05	23.4
T6	17.38	30.52	26.1
T7	26.75	37.26	33.7

Table 12: Average absolute distance between modeled and measured results

5.1.3 Relative distance

Relative distance will show if the model is under or over-predicting the erosion of the coastline. If the relative distance is negative this means that the beach width measured at MSL is less than the one resulting from the model. Table 13 shows the average relative distance between measured and modeled coastlines. The table reveals that the model consistently underestimates the regression at MSL, and this underestimation becomes more pronounced over time.

Survey	Terminal $[m]$	Village $[m]$	Combined $[m]$
T1	-8.57	-0.01	-3.34
T2	-6.27	-15.30	-12.31
T3	-16.51	-18.79	-18.01
T4	-19.95	-23.91	-22.57
T5	-18.79	-24.89	-22.81
T6	-15.79	-30.30	-25.37
T7	-24.52	-34.35	-31.01

Table 13: Relative distance between modeled and measured results

5.1.4 Planform area

The planform area is the total area of the beach. Table 14 shows the planform area of both terminal and village sections and both sections combined, for every measurement instance. Measured results show a consistent decrease in the beach area for both the villages and the terminal sections with each following measurement, as already observed in the previous paragraph 3.6. The modeled planform area at the terminal is also decreasing, however at a much slower rate. In contrast, the planform area in the villages is gradually increasing. Again the background effects might be a possible explanation for the village area's growth. Consequently, the combined platform area remains relatively stable.

Measurement planform area	Terminal $[m^2]$	Villages $[m^2]$	Combined $[m^2]$	Modeled planform area	Terminal $[m^2]$	villages $[m^2]$	Combined $[m^2]$
T0	229,491	255,298	484,789	T0	-	-	-
T1	213,221	256,419	469,640	T1	227,797	256,458	484,225
T2	213,958	208,224	422,182	T2	224,621	258,737	483,358
T3	187,475	205,657	393,132	T3	215,536	267,669	483,205
T4	172,139	198,649	370,788	T4	206,058	277,562	483,620
T5	172,635	197,588	370,233	T5	204,572	279,734	484,306
T6	167,368	188,362	355,730	T6	194,213	288,364	482,577
T7	152,222	181,825	334,047	T7	193,907	295,180	489,087

Table 14: Measured and modeled planform area

5.1.5 Assessment of coastline change

This subparagraph assesses the modeled coastline change and compares it to the measured shift in MSL contour and the coastline change based on measured volume change. As previously mentioned in Chapter 2, the model assumes a volume balance and modulates a change in coastline position based on the change in volume. Therefore, it is useful to also compare the performance of ShorelineS with a calculated coastline change based on the measured change in volume. The modeled coastline change and the shift in MSL contour can directly be derived from the planform area as the change in planform area represents the total change of the coastline. The modeled coastline change together with the shift in MSL contour and the calculated coastline change based on volume change for the entire measured period (T0-T7) is plotted in figure 25. Also in this figure is the modeled coastline change for a coast without nourishment. For the plots presenting the coastline change between every survey see appendix B.

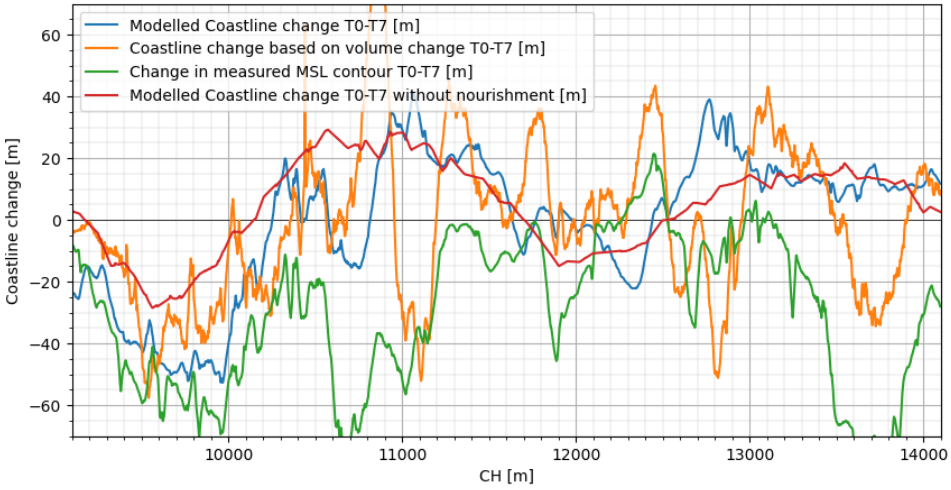

Figure 25: Coastline change modeled, measured and calculated based on volume change.

What can be observed from figure 25 is that over almost the entire nourishment the change in MSL contour is negative and larger than both the modeled change and the change calculated based on volume change. The first observation about the difference between MSL change and modeled change proves the hypothesis that the coastline change that one would measure around the waterline is larger than the one that would come from the model, $\Delta y_{measured} > \Delta y_{modeled}$. The second observation indicates that cross-shore redistribution is taking place as seen in Chapter 3. The retreat of the coastline around water level is bigger than what can be

expected based on volume change.

To better illustrate the difference between the modulated coastline change and the calculated coastline change, the sums of the coastline changes over each period over the entire nourishment are presented in a table 15, together with the daily change. What becomes clear from this table is that the model shifts between erosion and deposition. It begins with predicting erosion in the first three periods, then deposition in the next two. Noticeable is the large modeled deposition in the last period (T6-T7). Overall, the model simulates a net accretion. In contrast, the coastline change based on volume change begins with one period of accretion and then transitions to erosion, which is in line with the analysis conducted in paragraph 3.5. Generally, the coastline section loses sediment therefore the calculated change is negative. However, this decrease in coastal area is much smaller than the one following from the MSL contour. In summary, the model predicts slight accretion where volume loss is measured.

Survey period	Modeled coastline change $[m]$		Calculated coastline change $[m]$		Shift in MSL contour $[m]$	
T0-T1	-564	-10.4	10,232	189.5	-15,149	-280.5
T1-T2	-867	-6.9	-2798	-22.4	-47,458	-379.6
T2-T3	-153	-0.6	-5535	-22.0	-29,050	-111.3
T3-T4	415	1.9	-2705	-12.2	-22,344	-110.6
T4-T5	686	6.86	-3189	-31.9	-555	-5.6
T5-T6	-1729	-4.4	-7314	-18.8	-14,503	-37.2
T6-T7	6510	32.2	-2581	-12.8	-21,683	-107.3
T0-T7	4298	3.2	-13,890	-10.3	-150,742	-112.1

Table 15: Sum of Modeled, measured and calculated coastline change between surveys.

5.1.6 Analysis on ShorelineS performance per survey period

This analysis discusses the change in coastlines for each period. It aims to provide more insight into where the errors between the model and the measurements are the largest. The figures presenting the resulting MSL contours from this analysis together with the plots displaying the different coastline changes can be found in appendix C. The sum of the change in coastline between every survey is presented in table 16, together with the average wave power of that period. Wave power is a measure of the rate at which energy is carried by waves.

Survey period	Modeled coastline change $[m]$		Calculated coastline change $[m]$		Average wave power $[J/ms]$
T0-T1	-564	-10.4	10,232	189.5	951.6
T1-T2	-48	-0.4	-2798	-22.4	1153.5
T2-T3	827	3.3	-5535	-22.0	1159.3
T3-T4	8390	37.8	-2705	-12.2	795.6
T4-T5	2120	21.2	-3189	-31.9	1435.0
T5-T6	-19,478	-49.9	-7314	-18.8	1172.1
T6-T7	11,312	56.0	-2581	-12.8	1162.0
T0-T7	2558	1.9	-13,890	-10.3	1173.2

Table 16: Sum of modeled coastline change for re-initialized ShorelineS simulations

Again the model predicts a positive coastline change while there is a measured volume

loss. If the results in this table are compared to the results in table 15, it becomes clear that the changes the model simulates in the later periods are almost an order of magnitude larger in the re-initialized simulations. Similar to the results above, the modeled coastline change alternates in sign. It begins with two periods of slight erosion, followed by three periods of accretion, and then in T5-T6 a period with relatively high erosion followed by another period with relatively high accretion. This is unexpected. It was anticipated that, since the perturbation of the coastline in the alongshore direction would decrease over time as nature attempts to smooth out this perturbation, the coastline change would decrease over time. This behavior can be observed in the calculated coastline change. The analysis reveals that in period T2-T3, where the average wave power is approximately 1160 J/ms, a daily coastline change of 22.0 meters is found, while in period T6-T7 the average wave power is similar but the daily coastline change is only 12.8 meters. Period T4-T5 is an exception but can be explained by the relatively high average wave power. Something else that stands out is the difference in modeled erosion between periods T3-T4 and T4-T5 in both analyses, the daily coastline erosion during T3-T4 is larger than between T4-T5, while the average wave power during T4-T5 is almost twice the average wave power during T3-T4. This indicates that there is no clear relationship between the modeled coastline change and the average wave power in both analyses.

5.1.7 Conclusion

The model underpredicts the terminal's erosion and overestimates the feeding to the villages. Both the relative and absolute distance continuously grow, meaning that over time, the model's prediction on the MSL contour worsens. Also, the difference between the modeled and measured planform area becomes continuously larger. This growing mistake of the model is due to the model's imposed conservation of planform area. Looking at table 14, it can be observed that the modeled planform area stays relatively constant in comparison to the measured planform area. Indicating that the model conserves sediment in the system. If one looks at the sum of the modeled coastline change in table 15 it presents even a slight increase, meaning that the model predicts a small deposition of sediment in the area.

Results from the analyses in subparagraphs 5.1.5 and 5.1.6 indicate that the model generally does not perform well in predicting shoreline changes. For instance, no relationship can be found between average wave power and shoreline changes. Additionally, there is little agreement between the modeled shoreline change and the shoreline change calculated using volume change. From all these observations it can be concluded that the 1D coastline model ShorelineS does not do well in predicting the coastline evolution of the Bacton Sandscaping.

5.2 Equilibration factor

This paragraph presents the results from the calculations of the equilibration factor. The factor is defined as the measured coastline change divided by the calculated coastline change that is based on volume change in the active profile, see paragraph 4.2.1. The expression is given in 36 and repeated below for readability. Given that the measurements are not done continuously but on a random interval it is not possible to calculate the equilibration factor continuously over time. Therefore the result will give the calculated factor for every period between the measurements.

$$\Delta y_{measured} = R * \Delta y_{calculated}$$
$$R = \frac{\Delta y_{measured}}{\Delta y_{calculated}} \tag{39}$$

5.2.1 Results of Equilibration factor

Every line in figure 26 represents the calculation of the equilibration factor for every transect for all seven measurement periods. The color of the line shows the index of the transect plotted, starting with darker blue and ending with deep red. So the darkest blue line is the first transect number 4 and the deepest red line is the last transect number 30. A table with all the individual results is given in appendix D. The black line shows the median of all the transects and is given in the top row of table 17. The dashed blue line in the figure equals one.

If the equilibration factor is bigger than one, the measured coastline change is larger than the coastline change derived from volume loss. If the equilibration factor is equal to one, then that means that the measured coastline change is equal to the coastline change based on volume change. An equilibration factor smaller than one but still positive means the opposite and the measured coastline change is smaller than the coastline change based on volume change. These above-mentioned scenarios can be in either case where both values are positive or both values are negative. The last possibility is if the equilibrium factor is negative, this indicates opposite signs between measured and calculated coastline change. The latter case is undesirable for the purpose of this study since it focuses on how much larger the change in coastline positions should be due to equilibration of the profile, and an opposite sign between measured and modeled coastline change does not indicate anything about this.

Measurement period	T0-T1	T1-T2	T2-T3	T3-T4	T4-T5	T5-T6	T6-T7
Median Equilibration	5.77	7.17	1.29	1.47	0.47	1.80	0.06

Median Equilibration	4.79	6.02	1.29	1.47	0.47	1.80	0.06

Table 17: Median equilibrium factor

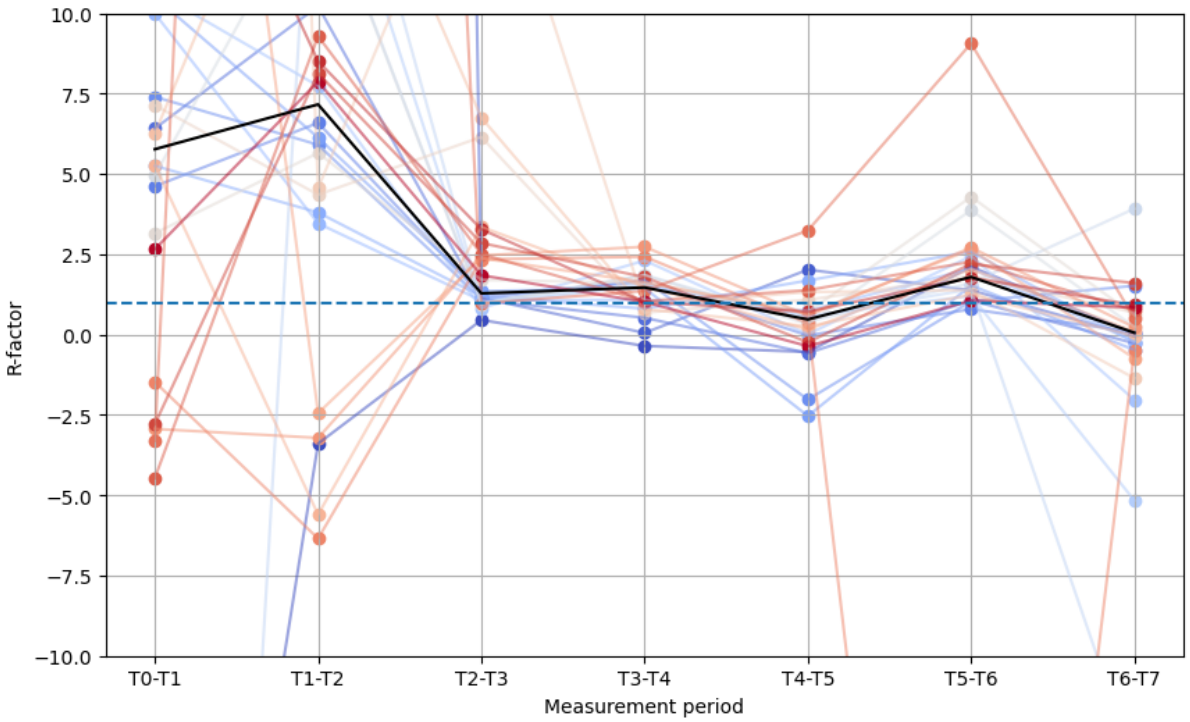

Figure 26: Calculated equilibrium factor per transect per period

The plot of figure 26 is cropped. This is done so because the equilibration factor shows a lot of large outliers. The presence of these outliers may be attributed to the division of one or two very small values during the calculation of these points. An example of such an outlier is in transect 5. The measured coastline retreat at +2.86m AOD over the period Oct 19 - Feb 20 was -14.5m and the one that would follow from the volume change is -0.045m. Hence the factor that would be calculated for this period is +300. Limiting the R-factor to positive and setting an upper bound slightly changes the median value, as is shown in the bottom row of table 17. In measurement period 2, between Feb 20 and Nov 20, the equilibration factor becomes close to one for the first time. Afterward, the line of the median sort of wiggles up and down around this value one. The deviation in the data remains quite large though.

The methodology proposes testing two different relationships between the equilibration factor R and time, each containing two parameters, a and b. To obtain these parameters and the associated relationship a curve fit is applied to the median regression factor. This curve fitting resulted in the following relations, where t is in days.

$$R(t)_{linear} = 7.74 - 0.014t \tag{40}$$

$$R(t)_{exponential} = 7.14exp(-0.0036t) + 1 \tag{41}$$

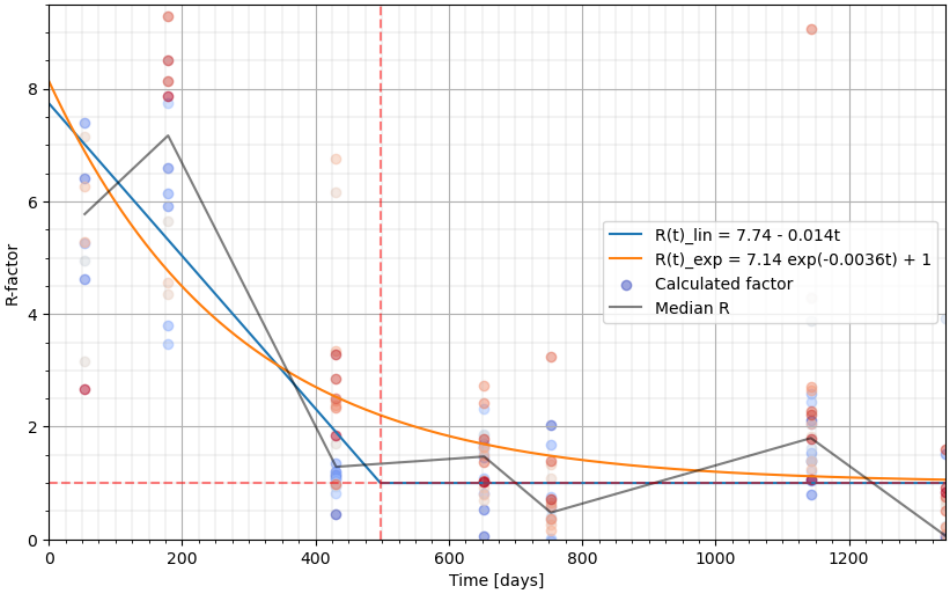

Figure 27: Relations equilibration factor and time

Figure 27 shows the two relationships of R over time, together with the calculated R-factor from the data and the median. All calculated R-factors are reported on the day the measurement is completed. The R-factor begins with a high mean of 7-8 and a broad distribution. Subsequently, it converges towards 1, with a decreasing range. Both relations seem to follow this same behavior. Note that the figure is cropped and the outliers fall out of the plot. From the formulation, it becomes clear that for the linear relationship, the equilibration factor becomes equal to one after 498 days, indicated by the vertical dashed red line. After day 498 the equilibration factor will remain equal to one for the linear approximation. In case of the exponential relation the R-factor will never really equal one since it is an exponential relation. However, after 1193 days the R-factor equals 1.1. The average R-factor over every simulated period is listed below in table 18. Table 19 shows the absolute error the curve fitted relations make to the median equilibration factor. The RMSE of the linear relationship is 0.919, and for the exponential relationship, this is 1.094.

Relationship	T0-T1	T0-T2	T0-T3	T0-T4	T0-T5	T0-T6	T0-T7
Linear	7.385	6.537	4.829	3.574	3.232	2.470	2.250
Exponential	7.505	6.282	4.646	3.765	3.475	2.720	2.474

Table 18: Average equilibration factor for different relations

Relationship	T0-T1	T1-T2	T2-T3	T3-T4	T4-T5	T5-T6	T6-T7	Average
Median R-factor	5.774	7.169	1.287	1.470	0.474	1.797	0.062	-
Linear error	-1.237	1.852	-0.614	0.470	-0.525	0.797	-0.938	-0.028
Exponential error	-1.111	2.406	-1.240	-0.220	-1.008	0.677	-0.996	-0.213

Table 19: Error between curve fitted relations and median R-factor

5.2.2 Conclusion

Both the linear and exponential relationships seem to follow the decreasing trend of the measured equilibration factors, ultimately converging towards one. Linear and exponential models

demonstrate similar RMSE and total error when compared to the median R-factor. However, the linear model exhibits slightly better performance in both metrics. Looking at the average equilibration factor over the modeled period, both relations give similar values. Because of this similarity and the slightly better performance in RMSE and absolute error, only the linear relation is further considered in this study. Consequently, this also means that equilibration of the profile will take about 500 days or around 1 year and 4 months.

5.3 Performance of the adjusted ShorelineS results

This paragraph presents the results of the adjusted ShorelineS simulations. Following the methodology outlined in Chapter 4, each section will be analyzed separately before combining them, starting with the terminal section (5.3.1), followed by the villages (5.3.2). In 5.3.3, both sections are combined. Again, the metrics used to evaluate the performance of the model are absolute distance, relative distance and resulting planform area.

5.3.1 Terminal only

This subparagraph shows the results of the adjusted ShorelineS results for the terminal area. By comparing the planform area of the terminal section between the initial post-construction measurement and subsequent model results, the average shift of the coastline along the terminal can be determined. The results are listed below and presented in meters. They are all negative, meaning that the beach width decreased during that period. In the second period (T0-T2), on average, over the entire length of the terminal section, the coastline shifted landward with $-2.865m$. When this average modeled coastline change is multiplied by the average equilibration factor over the same period and subsequently subtracted with itself, following equation 38. One arrives at an additional coastline retreat of $-15.863m$. So over the entire period T0-T2 the model predicted a coastline retreat of $-2.865m$ but according to the adjusted model results including profile equilibration, it should have been $-18.728m$.

Period	T0-T1	T0-T2	T0-T3	T0-T4	T0-T5	T0-T6	T0-T7
$\Delta y_{avg}\ [m]$	-0.998	-2.865	-8.209	-13.784	-14.658	-20.751	-20.931
R_{linear}	7.385	6.537	4.829	3.574	3.232	2.470	2.250
$\Delta y_{add}\ [m]$	-6.372	-15.863	-31.432	-35.480	-32.717	-30.504	-26.163

Table 20: Modeled average coastline change over the terminal

The shape of the adjusted coastline remained the same as the modeled one but shifted landward with the extra coastline retreat. This means that in terms of the general shape of the coastline nothing changes to previous model results. Therefore the results again display a dispersion of the top of the nourishment. One difference is that, while the original modeled coastline closely follows the measurements for the northern part (left part) of the nourishment, the adjusted coastline now lies below it. In contrast, the adjusted coastline follows the southern part of the measured MSL contour better than the original modeled coastline. What can also be observed from the results is that for the earlier measurements, the adjusted and original modeled coastlines lie quite close to each other, but when time progresses this distance increases due to the increasing average modeled coastline change (Δy_{avg}). Also interesting to see is that after the model simulation T0-T4 the distance between the two coastline decreases again. This aligns with the expectations and can be explained by a decreasing average equilibration factor over time. Besides, the average change in coastline over the terminal between

measurements becomes less. As one can see in table 20 the average coastline change modeled between the simulation that ran from T0-T6 and T0-T7 is approximately the same.

Period	Planform area $[m^2]$	Relative distance $[m]$	Absolute distance $[m]$
T0	-	-	-
T1	217,133	-2.30	4.72
T2	198,114	9.32	10.27
T3	162,581	14.64	18.57
T4	146,282	15.21	20.34
T5	149,431	13.65	21.86
T6	142,771	14.45	18.34
T7	149,786	1.14	20.76

Table 21: Results adjusted model runs terminal only

Table 21 presents the results for the adjusted model run focusing solely on the terminal section. It details the resulting platform area (m²), the average relative distance (m) between the adjusted and measured MSL contour, and the average absolute distance (m) between them, all calculated along the entire terminal length. When looking at the relative distance one can see that the adjusted model results begin with a slight under-prediction. The planform area resulting from the adjusted model results is larger than reality. Afterward, the adjusted model results are over-predicting the coastline retreat and the planform area resulting from the adjusted coastline is increasingly smaller than measured. From T3 to T6 the relative distance is quite constant. Interestingly the measured and adjusted planform area at instance T7 are almost equal. The absolute distance showing the error between the adjusted coastline and the measured coastline shows an increase from T1-T3. Afterward, it remains relatively constant at around 20 m of average distance between one another.

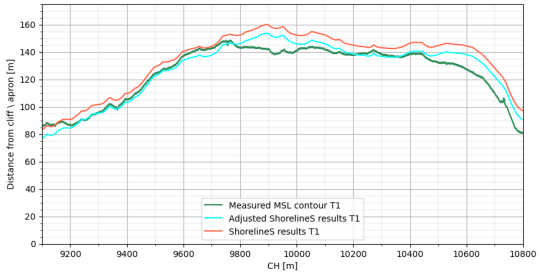

(a) Adjusted model results terminal T1

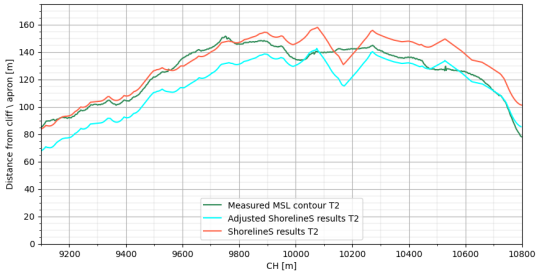

(b) Adjusted model results terminal T2

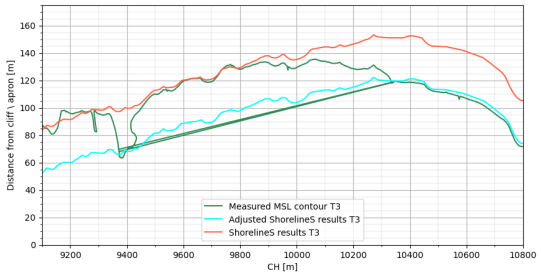

(c) Adjusted model results terminal T3

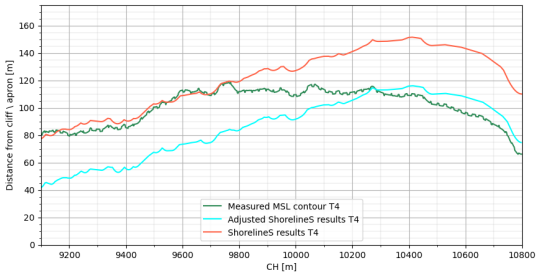

(d) Adjusted model results terminal T4

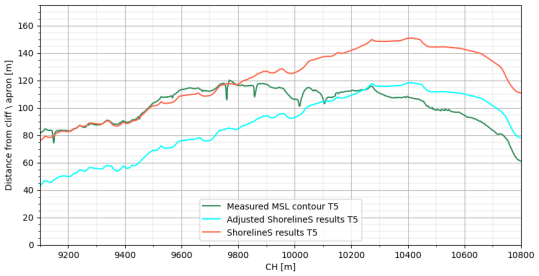

(e) Adjusted model results terminal T5

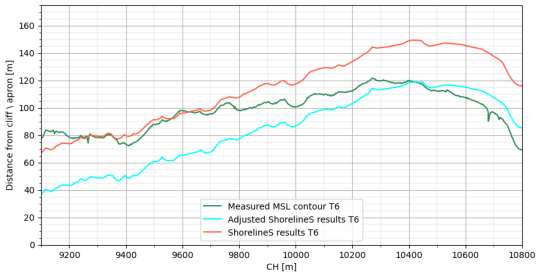

(f) Adjusted model results terminal T6

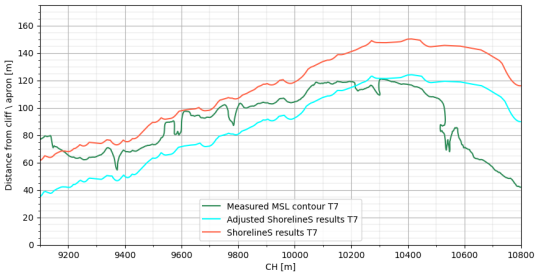

(g) Adjusted model results terminal T7

Figure 28: ShorelineS results vs Adjusted model runs terminal only

5.3.2 Village only & Whole nourishment

This subparagraph shows the results of the adjusted ShorelineS simulations for the village section and both sections combined.

Village only: The average modeled coastline change over the village section for every measurement period together with the additional coastline change are listed in table 22. The unusual finding of these results is that, on average, the coastline expands seaward. This same behavior is already observed in paragraph 5.1 and it is thought to be caused by background effects. Therefore, when the coastline is adjusted with an equilibration factor R, it will only expand seaward even further. The plots of the measured, modeled and adjusted coastline of the village section and entire nourishment can be found in appendix E. The plots clearly indicate that the measured MSL contour lies below the modeled coastline, and the adjusted coastline lies even further seaward. Similar to the results of only the terminal section after T4, the extra coastline change decreases a bit due to the decreasing R-factor. However, it is not as much.

Period	T0-T1	T0-T2	T0-T3	T0-T4	T0-T5	T0-T6	T0-T7
$\Delta y_{avg}\ [m]$	0.351	1.042	3.749	6.746	7.404	10.020	12.085
R_{linear}	7.385	6.537	4.829	3.574	3.232	2.470	2.250
$\Delta y_{add}\ [m]$	2.211	5.769	14.355	17.364	16.526	14.729	15.106

Table 22: Modeled average coastline change over the village

Considering this expanding coast, it is logical to see that the planform area resulting from the adjusted coastline is also continuously increasing, and so is the average relative and average absolute distance. As can be seen in table 23.

Period	Planform area $[m^2]$	Relative distance $[m]$	Absolute distance $[m]$
T0	-	-	-
T1	263,858	-2.625	6.89
T2	277,749	-21.07	21.14
T3	314,895	-33.10	33.25
T4	334,712	-41.23	41.38
T5	334,132	-41.38	41.58
T6	336,844	-44.99	45.25
T7	344,892	-49.41	49.22

Table 23: Results adjusted model runs village only

Entire nourishment: Previously observed in paragraph 5.1, the modeled planform area of the entire nourishment does not change over time. What the terminal section loses in area, the village section gains. Hence the average coastline change over the entire length of the nourishment is almost nil. Therefore the extra coastline change coming from the equilibration factor is also very small, as illustrated in table 24. Note how the extra coastline change slowly becomes smaller and smaller and then changes sign.

Period	T0-T1	T0-T2	T0-T3	T0-T4	T0-T5	T0-T6	T0-T7
$\Delta y_{avg}\ [m]$	-0.490	-0.626	-0.707	-0.616	-0.479	-0.818	0.485
R_{linear}	7.385	6.537	4.829	3.574	3.232	2.470	2.250
$\Delta y_{add}\ [m]$	-3.129	-3.466	-2.707	-1.586	-1.069	-1.202	0.606

Table 24: Modeled average coastline change over the entire nourishment

Ultimately one can see that the relative and absolute distance from the measurements to the adjusted coastlines increases with time. This is because the model simulates an approximately constant planform area, while in reality, this is not true. The adjusted planform area seems to increase over time, this is not due to an increase in the modeled planform area but caused by the decreasing extra coastline change Δy_{extra}.

Period	Planform area $[m^2]$	Relative distance $[m]$	Absolute distance $[m]$
T0	-	-	-
T1	468,589	-0.24	7.15
T2	466,215	-8.86	10.24
T3	469,642	-14.06	16.00
T4	475,669	-21.02	21.44
T5	478,926	-21.47	22.62
T6	476,554	-24.28	25.02
T7	492,084	-31.68	34.19

Table 25: Results adjusted model runs whole nourishment

5.3.3 Conclusion

When the equilibration factor is only applied to the terminal section, the model results go from under-predicting to overpredicting the retreat of the MSL contour, especially the northern top part of the nourishment, where the current ShorelineS simulation nicely follows this section of the nourishment. On the contrary, the bottom or south part, is better followed by the adjusted ShorelineS results.

The absolute error between current ShorelineS simulations and adjusted ShorenlineS simulations are similar. However, the adjusted ShorelineS results outperform the non-adjusted ShorelineS results in terms of metric relative distance. Consequently, the planform area resulting from the adjusted ShorelineS results comes closer to reality than the one resulting from the non-adjusted ShorelineS results. For these reasons, it can be concluded that the corrected coastlines perform slightly better than the original ShorelineS runs that do not incorporate cross-shore redistribution. But solely if the adjustment is applied to the terminal section only. Because when looking at the effect of the equilibration factor on the entire nourishment, the story changes. In this case, the change induced by the R-factor is almost negligible and the inclusion of the R-factor does not improve the model performance. This is caused by the fact that the average modeled coastline change (Δy_{avg}) between measurement instances is very little. Consequently, the R-factor is multiplied by a small number, and automatically, the correction is also small. The results change again when the R-factor is applied only to the village section. The R-factor increases the model's error, as the model predicts coastline expansion in this section and the R-factor increases this. Thus, in this case, the incorporation of the equilibrium factor only worsened the results.

The difference in results between both sections can be explained by the model's imposed conservation. In the model, the sediment lost from the terminal section moves to the village section. Because of this, the village section continuously grows, and the R-factor amplifies this. Looking at the entire nourishment, the change in coastline is almost zero, due to this conservation. Therefore, the R-factor has almost no effect.

The results indicate that including cross-shore redistribution slightly improves the model performance on the terminal section, but on the contrary, it only worsens the performance of the village section. The effect of the R factor on both sections combined is almost nil. Because of these findings a new approach is suggested. One that would only apply the R-factor to the terminal section and leave the village unchanged. This new approach will be discussed in the following paragraph.

5.4 New approach

In response to the obtained results, a new approach was set up and tested. In this paragraph, this approach is explained (5.4.1) and its results are presented (5.4.2). In 5.4.3 a conclusion is drawn.

5.4.1 Methodology new approach

This new approach differs from the earlier approach in two ways. The R-factor is only applied to the terminal section, and the adjusted ShorelineS results are reintroduced back into ShorelineS. In comparison to earlier, the simulation is done until a certain moment T_N, where $N = [0, ..., 6]$. After this, the coastline is adjusted with the R-factor, and these adjusted ShorelineS results are inserted into ShorelineS to simulate the next period. In this way, the coastline is corrected during the simulation. More on how new coastline adjustment works is given below. The updated flowchart is shown below in figure 29.

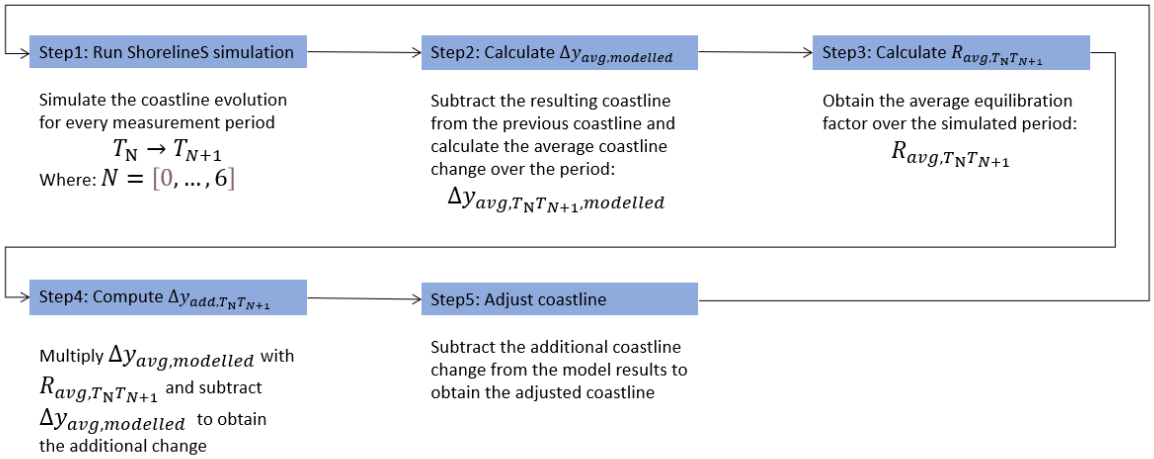

Figure 29: Updated flowchart

In the previous approach, incorporating the equilibrium factor in the village section led to unsatisfactory results. Namely, the model predicted coastline expansion and the R-factor amplified this. Hence, with this new approach, the coastline adjustment is done differently. At the terminal, the adjustment will happen the same as last time, but for the villages, no adjustment will take place. To avoid jumps in the coast, interpolation is applied to a transition region. A visualization of this is given in figure 30. Here, the black line is a classical result that would follow from a ShorelineS simulation, and the blue line is the adjusted coastline. The dashed red line indicates the border between the terminal section and the village section. As said the terminal coastline will be adjusted with the additional coastline change just as before. Just right from the dashed line, one can see the transition zone. In this zone, the adjustment linearly decreases to zero over a length of 300 m. The blue line will be reintroduced back into ShorelineS as input coastline. An important detail is that the average coastline change over the period is only calculated for the terminal section since only this section is adjusted.

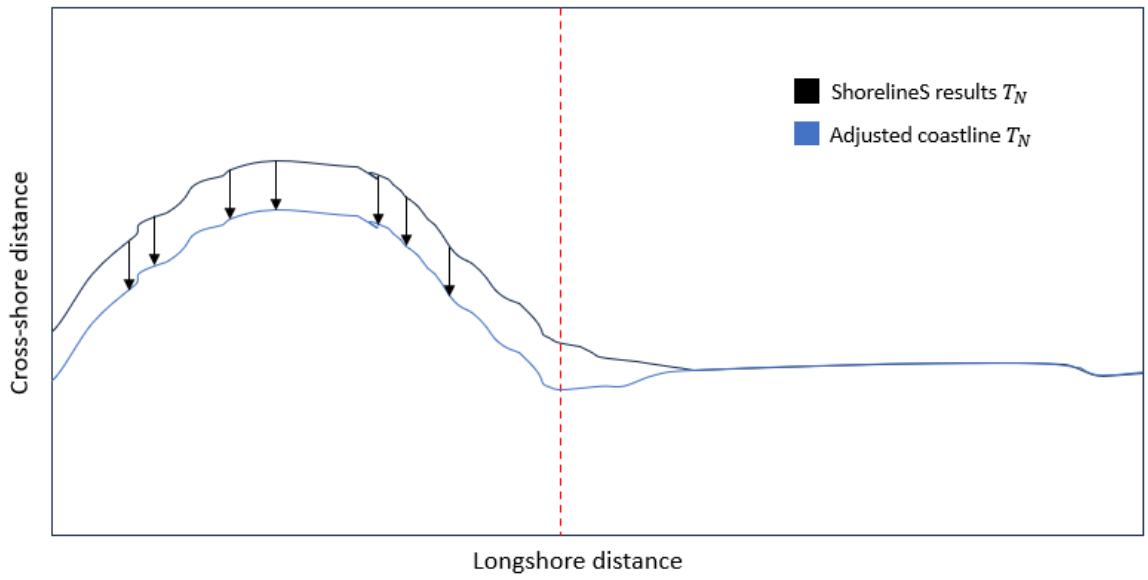

Figure 30: Coastline adjustment

5.4.2 Results new approach

This subparagraph presents the results of the new approach. The new method requires recalculating the average equilibration factor per period, as the periods now run from T0-T1, T1-T2, T2-T3, etc. The results are given in table 26. It can be observed that for the linear relationship after period T2-T3 the correction almost becomes zero as the R-factor is one or close to one. For the exponential relation holds the same, the R-factor becomes close to one. However, this point is reached later on. Again only the linear relationship is further considered. The resulting additional coastline change for every modeled period are presented in table 27. In total, the coastline at the terminal is shifted 27.3 m.

Relationship	T0-T1	T1-T2	T2-T3	T3-T4	T4-T5	T5-T6	T6-T7
Linear	7.385	6.171	3.616	1.137	1.000	1.000	1.000
Exponential	7.505	5.754	3.484	2.055	1.581	1.260	1.085

Table 26: Average equilibration factor for different relations, new approach

Period	T0-T1	T1-T2	T2-T3	T3-T4	T4-T5	T5-T6	T6-T7
$\Delta y_{avg}\ [m]$	-0.998	-1.756	-4.307	-4.063	-0.625	-4.91	0.877
R_{linear}	7.385	6.171	3.616	1.137	1.000	1.000	1.000
$\Delta y_{extra}\ [m]$	-6.372	-9.080	-11.267	-0.557	0	0	0

Table 27: Modeled average coastline change, new approach

Plots of the resulting coastlines are presented in appendix F. These figures present the measured, modeled, and adjusted coastlines for all seven measurement periods. The coastline extension around chainages 11000 and 13500 is clear in these plots, which is likely due to the underlying background factors. Note that the adjusted coastline lies landward of the actual coastline to the left of chainage 10300, while it generally lies seaward of the actual coastline to the right of this point. Comparing the average relative distance and absolute distance in table 28 with the ones from table 25, it can be said that the new approach performs slightly better, in the sense that it scores better in both metrics. Also, the calculated total planform area comes closer to reality but is still far off.

Period	Planform area $[m^2]$	Relative distance $[m]$	Absolute distance $[m]$
T0	-	-	-
T1	472,484	-1.01	5.98
T2	456,013	-6.82	13.17
T3	439,952	-8.12	18.30
T4	444,628	-14.81	22.77
T5	446,321	-14.95	24.46
T6	449,400	-18.85	27.18
T7	459,059	-25.07	33.87

Table 28: Results adjusted model runs new approach

Figure 31 shows the resulting coastline at instance T7 for both methods. The resulting shape of the coastline looks similar only two key differences between the new and old approaches are apparent. Firstly, the nourishment along the terminal is displaced approximately 25 meters landward. Which compares to the total adjustment applied. Because of this correction, the top of the nourishment is closer to the actual top of the nourishment in comparison

to the earlier results, and the ShorelineS results without correction. Secondly, the coastline extension around chainage 14000 is more pronounced in the new approach compared to the previous. Part of this volume probably originates from the area between CH11000 and CH12300. This part has not been corrected by the R-factor but has experienced more erosion than before. Nevertheless, this is not enough volume to explain the total expansion. Figure 31 also shows the measured coastline at T7. The figure illustrates that the adjusted model over-predicts coastline retreat between chainages 9100 and 9800. Where the original ShorelineS lies close to reality.

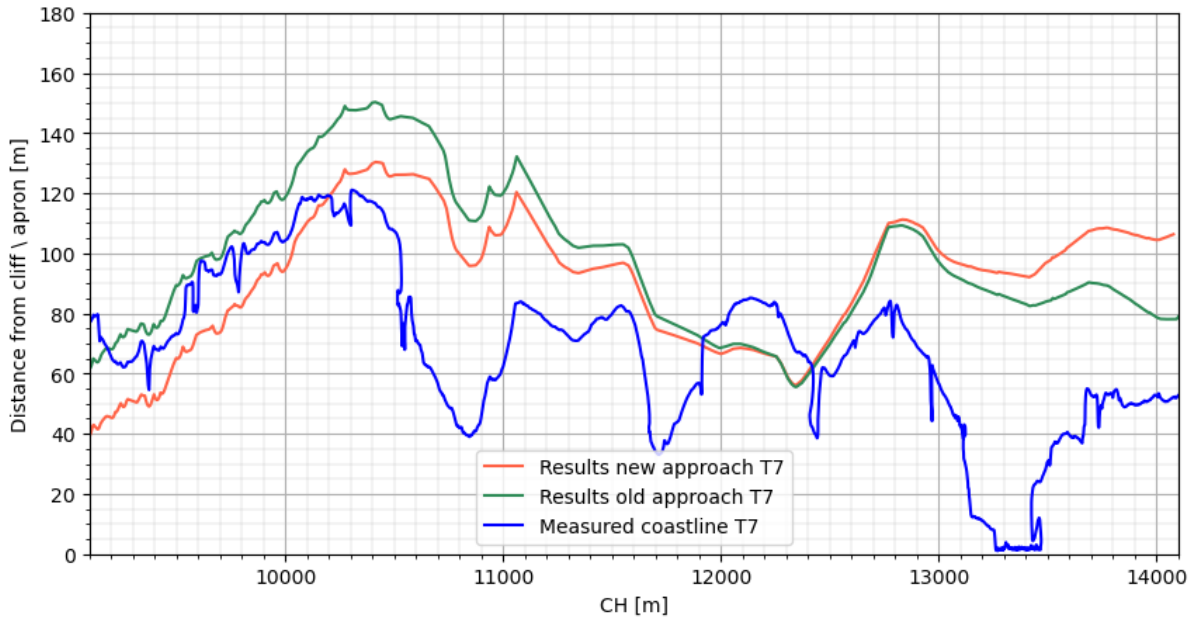

Figure 31: Comparison old and new approach

The coastline transformation between T0 and T7 is depicted in Figure 32. The orange line displays the coastline change without nourishment and is similar to the one in figure **??**. The green line indicates the measured coastline change, while red and blue indicate the modeled coastline change. Red is the result from the old approach, which is almost identical to the non-adjusted ShorelineS result, and blue is the new adjusted coastline result. Here again, it can be observed that the newly adjusted coastline generally follows the measured coastline more closely, except to the south of chainage 12300. This graph also shows that the peaks and troughs in the coastline changes for both the simulations with nourishment coincide with those of the simulation without nourishment. Especially, around the villages section (CH10800-CH14100). In this section, it can also be observed that these so-called background effects govern the coastline changes of the model run with nourishment. For the reason that the inclusion of the nourishment in the model does not alter the change in coastline much. The areas where the simulated coastline differs most from the measured coastline correspond to areas where the model would predict coastline accretion in the case of no nourishment. So between CH10200-CH11700 and CH12600-CH14100 the distance between measured and modeled coastline is largest. Please keep in mind that between CH13500 and CH13900 there is an error in the measurement.

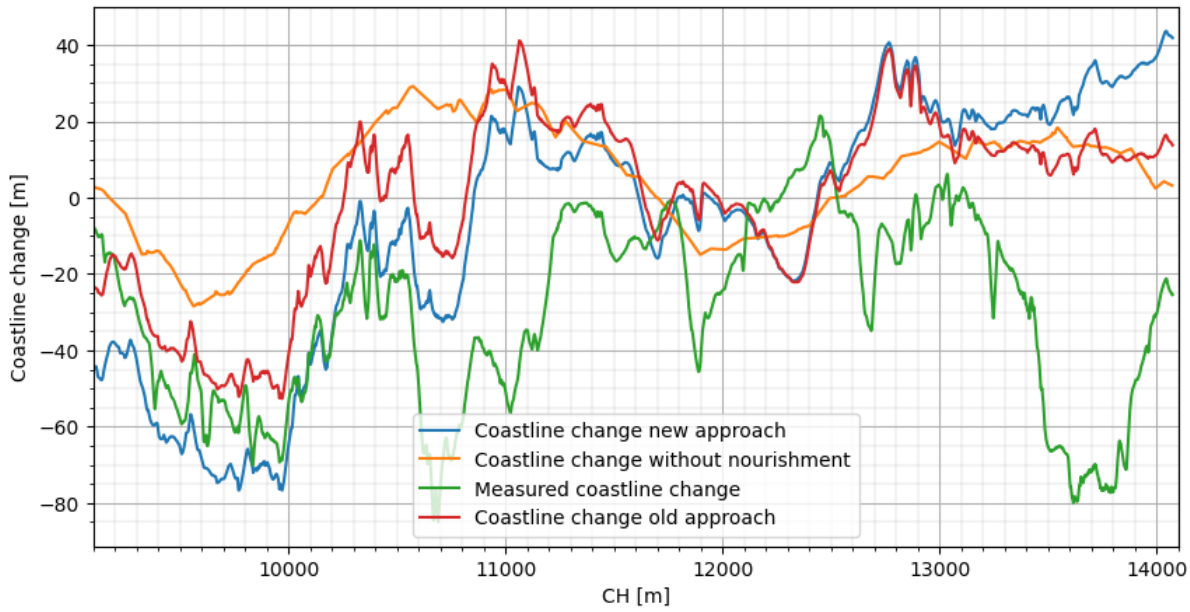

Figure 32: Coastline change between T0-T7

5.4.3 Conclusion

The model imposes a conservation of planform area across the entire domain, contrary to reality. Planform area loss within the model is solely determined by the R-factor. As can be seen in the results of ShorelineS simulations without the addition of the R-factor in table 14, there is only a 1% change in planform area over the entire measured period, while in reality 31% is lost. Therefore it can be concluded that the error made by the model is not only due to the neglect of cross-shore redistribution but also caused by the conservation of sediment in the model. This has a significant impact on the resulting outcomes. When looking at the orange line in figure 32, which represents the coastline change in the case without nourishment, it can be seen that there are areas of accretion between CH10200-CH11700 and CH12600-CH14100. However, when looking at the measured coastline change, there is erosion over the entire nourished area. Logically, these two areas are also exactly the locations where the model has the largest error relative to reality. In other words, the resulting coastline from ShorelineS has the greatest cross-shore distance from the actual coastline in these areas. This is also easily explained because, in this area, there is not only a neglect of cross-shore redistribution but also modeled accretion. In the terminal section, where the model is corrected for cross-shore redistribution, the measured and modeled coastlines are already much closer together. Consequently, drawing conclusions based on these results is challenging due to the significant model errors.

As concluded in paragraph 5.3, the adjusted coastline (according to the old approach) and the original non-adjusted ShorelineS results are almost identical. Consequently, these can be considered equal when assessing the new approach's performance against the old approach. The difference observed between the old approach and the new approach around the terminal section is due to the adjustment applied in this section. It can be said that, generally speaking, between CH9800 and CH12100, the new approach performs better than the old method. But outside this region, the previously obtained coastline lies closer to the measurements. When looking at the metrics: Absolute distance, relative distance and planform area. The new approach scores better in comparison to no adjustment or the old approach, and this improvement comes from including cross-shore redistribution. Although the improvement is little, it does indicate that there is potential to include cross-shore redistribution to enhance the

predictive performance of 1D coastline models.

To conclude, despite the model's inherent conservation of planform area, the inclusion of cross-shore redistribution with the R-factor in ShorelineS slightly enhances the model's predictive capabilities. This indicates that there is potential for the inclusion of cross-shore redistribution in 1D coastline models, but it still needs a lot of research.

6 Discussion

The aim of this thesis is to investigate whether the inclusion of cross-shore redistribution could improve the predictive capabilities of the ShorelineS model on the Bacton Sandscaping study case. This chapter entails the discussion. In 6.1, the general research findings are discussed. In 6.2, limitations are identified. Some attention is paid in 6.3 to the limitations of the model used. Suggestions for future research are made in 6.4.

6.1 General findings

Observations from the Bacton monitoring data, discussed in Chapter 3, indicate that the redistribution of sediment within the profile significantly influences the coastline change of Bacton. Dean [15] also mentions the importance of this cross-shore sediment redistribution in coastline evolution, highlighting that the timescale of such redistribution is crucial as broader beaches offer greater storm protection. De Schipper et al. [16] and Kroon et al. [21] did research on the evolution of two other mega nourishments, the Sand Engine and the Hondsbossche dunes respectively. De Schipper found that it took 18 months for the constructed profile with a 1:32 slope to move to a 1:53 natural slope that was present before construction. So it took the cross-shore profile of the Sand Engine approximately 550 days to move to an equilibrium. For the timescale of redistribution on the Hondsbossche dunes, Kroon found that it took two winters for the steeper constructed profile to transform into a naturally occurring profile slope found in adjacent coastal sections. It is estimated from the found linear equation in paragraph 5.2 that the profile will reach equilibrium in approximately 500 days. This is fairly consistent with the findings of Kroon and de Schipper for the Sand Engine and the Hondsbossche dunes, but it is somewhat faster. This difference may be related to the difference in size between the Bacton Sandscaping and the other two mega nourishments. The Bacton Sandscaping is an order of magnitude smaller in volume than the other two nourishments.

The results presented in paragraph 5.1 reveal that the 1D coastline model falls short in accurately predicting coastline change. As suggested in the introduction 1 this limitation comes from the model's neglect of cross-shore sediment redistribution. Results from including cross-shore redistribution with the R-factor indicate a slight improvement in the prediction of ShorelineS. Nevertheless, the model still makes a large error with the measurements and the inherent conservation of planform area causes this. Therefore, the results challenge the assumption that ShorelineS's inaccuracies are primarily caused by the exclusion of cross-shore redistribution. While cross-shore sediment redistribution undoubtedly plays a role in coastline evolution, its impact on ShorelineS's performance in this particular case is not as pronounced as initially expected. Other limitations of the model, which will be explained in paragraph 6.2, might have a bigger effect on its performance. Still, the results show that there is potential for the inclusion of cross-shore redistribution to improve 1D coastline models.

6.2 Model limitation

The model likely contains multiple limitations that contribute to its deviation from reality. Therefore, it may have been premature to assume that the model's error is solely due to the neglect of redistribution. As the results clearly show, ShorelineS modulates volume conservation over the nourishment, causing significant differences between the modeled coastline and the actual coastline. It is this conservation of sediment that has a large influence on the obtained results.

For the simulation in ShorelineS, the CERC2 was selected to estimate longshore sediment transport. This is a direct derivation of the official CERC equation. The CERC formula is relatively simple, which makes it easy to interpret, and that is why it is still widely applied. What makes the formula so simple is the exclusion of various parameters such as grain size, bed slope, and wind- or tide-driven currents. Consequently, CERC is a significant simplification of reality. In contrast, other transport equations do include these parameters, thus offering a more complete representation.

A final limitation of the study is the limited amount of updating done on the coastline. Fully integrating the R-factor into ShorelineS was difficult as ShorelineS is a very extensive Matlab code. Therefore, it was decided to apply its effects to the results subsequently. This updating is done only seven times, corresponding to the measurements. However, it might have been better to update the profile more frequently and on a set interval. In this way there will be more interaction with the model.

6.3 Limitations and implications of the R-factor

One limitation of the R-factor is that the +2.83 m AOD contour is used for calculating the R-factor, while the +0.11 m AOD MSL contour is used as the input coastline for ShorelineS. This decision was made because the equilibrium factor must be calculated using the measured coastline change, and since the coastline is located at +2.83 m AOD, this was the contour selected. Meanwhile, ShorelineS assumes the coastline is located around MSL. In essence, two different locations are compared, which leads to an overestimation of the position change around MSL. To illustrate this, take a look at figure 33. In this figure, the black line represents a post-nourishment initial profile, and the blue line shows a profile translation typical for a 1D coastline model. Orange represents a profile that would naturally arise. As outlined in the methodology, the R-factor is determined by dividing the measured coastline change at level +2.86 m AOD by the calculated coastline change based on volume loss. These two coastline changes are indicated by the two black arrows in the figure. The figure clearly illustrates how the result differs when the R-factor is calculated around Mean Sea Level (+0.11m AOD), indicated by the two green arrows. In this case, it is significantly smaller. This is entirely due to the redistribution of sediment within the profile. From higher up in the profile, more sediment is transported downwards compared to lower sections. To resolve this issue and accurately compare locations, the following approach is necessary. Initially, the model should be run as is to obtain coastline position 1, as indicated in Figure 33. Subsequently, the vertical distance between the +0.11m AOD contour and the +2.86m AOD contour should be subtracted from coastline position 1. This results in coastline position 2. The final step involves subtracting the additional coastline change from coastline position 2 to arrive at the adjusted coastline at +2.86 m AOD.

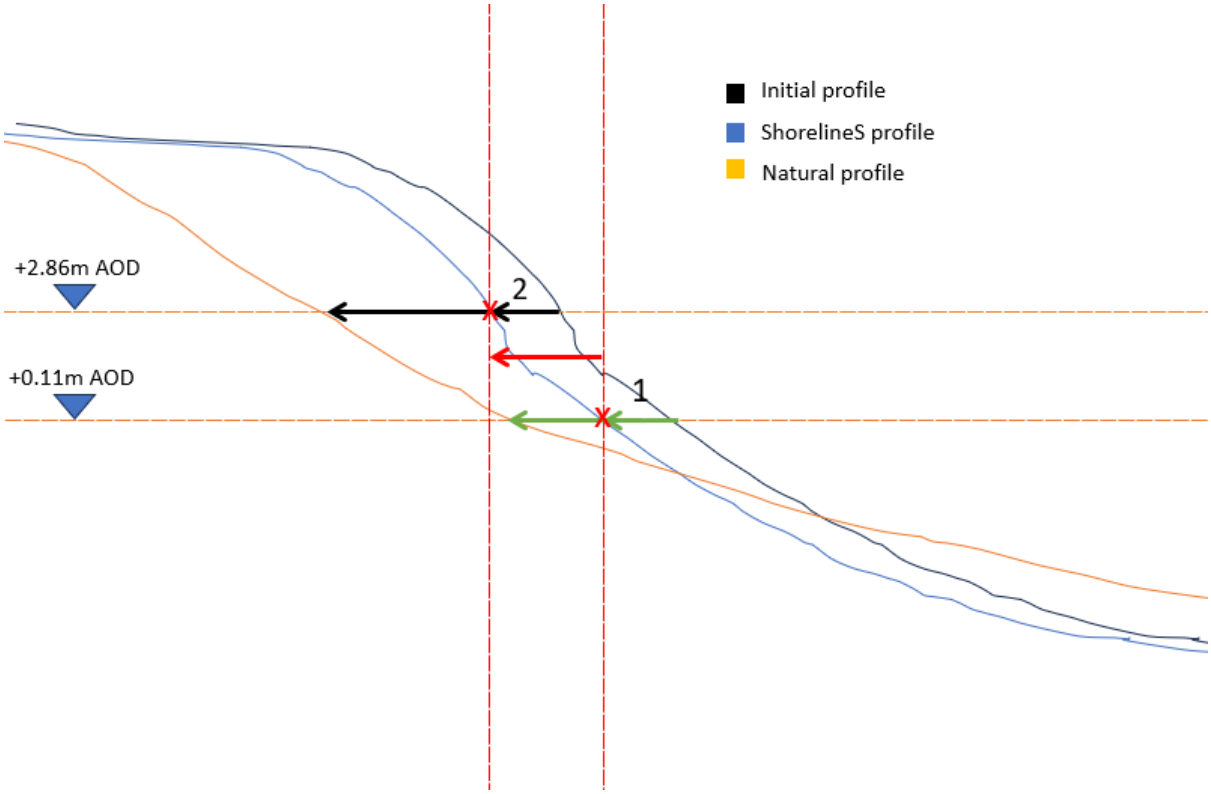

Figure 33: Discussion equilibration factor

Another limitation is that this research chose to include cross-shore redistribution with a factor. The results show that this factor is highly sensitive to small values, which could dramatically increase it, leading to significant outliers in the data. To overcome this problem in the future an addition could be tried:

$$y_{actual} = y_{modeled} + y_{additional} \tag{42}$$

The proposed addition, represented by $y_{additional}$, offers an interesting potential solution to the sensitivity issue with cross-shore redistribution. This addition, which is possibly influenced by factors such as initial profile, equilibrium profile, median grain size, wave climate, and time, is significantly less sensitive to small numbers. If implemented, this addition could potentially provide a more suitable and robust method for including cross-shore redistribution in a 1D coastline model, opening up new possibilities for research and development in the field.

The final limitation was the restricted data availability for calculating the R-factor. Only seven measurements, taken at irregular intervals, were accessible, hindering the identification of temporal trends. Moreover, due to differing design objectives between the village and terminal sections, with the latter intended for accretion, data from the village section could not be utilized in the R-factor calculation.

6.4 Future research

Based on the model's limitations, it can be advised to execute more model calibration on Bacton Sandscaping to ensure that the model will perform better in predicting the nourishment's evolution. Testing the different available longshore sediment transport formulas could be part

of this calibration to see which transport formula works best in this case. Additionally, the impact of more frequent coastline updates using the R-factor could be explored. Currently, the coastline is adjusted only seven times, coinciding with the measurement points. It would be interesting to investigate the consequences of monthly or weekly coastline updates.

The limitations of the R-factor have revealed an underlying issue with the assumption that it is a multiplicative factor. It suggests that it could also be an addition. Nevertheless, alternative approaches for incorporating cross-shore redistribution within a 1D shoreline model might exist. These possibilities could be analyzed further.

More research is required on cross-shore redistribution to overcome the limitations of the R-factor in the future. Conducting measurements on multiple mega nourishments will give a broader picture of how the constructed profile will form into an equilibrium profile. Doing these measurements at fixed intervals will also make it possible to detect time trends. It might also be useful to conduct some physical testing to find which parameters influence the equilibration of the profile. This method allows for a clearer visualization of the relationships between cross-shore profile redistribution and the forces acting upon it. All this will enable a better understanding of cross-shore redistribution and the effect it has on the coastline evolution of mega nourishments. All these suggestions will collectively enhance the incorporation of cross-shore redistribution within a 1D shoreline mode.

In addition, a sensitivity study can be done on cross-shore redistribution to see how much of an effect it has on the evolution of the Bacton Sandscaping.

7 Conclusion

The Bacton Sandscaping was designed to protect the gas terminal against flooding and prevent the buried infrastructure of the gas terminal from being exposed. Simultaneously, the design also required not to increase erosion to the neighboring villages as these were already under serious threat of coastal erosion. Approximately four years have passed since its completion, and several severe storms have occurred, but none have caused overtopping at the villages or damaged the buried pipelines. This success of the Bacton Sandscaping gives confidence that this type of solution works, and it raises the question of whether it is not widely applicable in other coastal areas in the UK.

For the design, Royal HaskoningDHV developed a conceptual model based on the 1D LITLINE model and the 2D TELEMAC-MASCARET area model. In this conceptual model, LITLINE was the central design engine. LINTLINE only includes longshore sediment transport, but it was thought there would be a lot of offshore sediment loss, and to account for this, the cross-shore sediment movement resulting from the 2D area model was added as sink and sources into the LITLINE model. Analyses following construction revealed that cross-shore sediment redistribution significantly influences the evolution of nourishment. Despite including cross-shore transport through sinks and sources, LITLINE still did not produce satisfactory results as it did not account for this redistribution. This is why this thesis researched how the predictive capabilities of a 1D coastline model, like LITLINE, on the evolution of mega nourishments can be improved by including cross-shore redistribution. The Bacton Sandscaping case study was selected for this research, and the ShorelineS model was utilized as the 1D coastline model as it was readily available.

This research first touches upon cross-shore redistribution and then delves into how 1D coastline models generally predict coastline evolution. Followed by an analysis of the current performance of ShorelineS in predicting the evolution of the Bacton Sandscaping. After this, the thesis introduces the new equilibration factor or R-factor that adjusts ShorelineS results to a coastline that includes cross-shore redistribution. Finally, these newly adjusted coastlines are compared to measurements to see how the prediction of ShorelineS is altered after the inclusion of cross-shore redistribution.

7.1 Key findings

Following the result of the simulations done in ShorelineS in its current state, it can be concluded that it falls short in predicting the coastline evolution of the Bacton Sandscaping. ShorelineS underestimates the erosion of the terminal section, as one expects, due to the exclusion of cross-shore redistribution. A notable finding was that the model retained sediment over the entire nourished area. Over the entire measured period, the model simulates almost no change in planform area while, in reality, the nourishment lost 31%. According to the model, almost all the sediment that is eroded from the terminal is deposited in front of the villages. Hereby overestimating the feeding of the terminal to the villages. Another notable finding was that the model struggles to accurately predict shoreline changes. Specifically, there's no correlation between wave power and shoreline changes, and the modeled shoreline change often differs significantly from the volume-based calculation.

A new R-factor was introduced to include cross-shore redistribution. This factor is defined as a factor that is multiplied with the modeled coastline change to obtain the coastline change that includes cross-shore redistribution. Data from the Bacton Sandscaping was used to ap-

proximate the R-factor. Here, volume change between measurements of the active profile was used to simulate the coastline change a model would predict. These same measurements were used to obtain the actual coastline change. Then, dividing the actual coastline change with the one based on volume change in the profile would result in the R-factor of that profile during this time period.

$$R = \frac{\Delta y_{measured}}{\Delta y_{modeled}} \tag{43}$$

Over time, it is expected that redistribution will have fully taken place, and therefore, the R-factor should go to one. Two different relationships for the R-factor were tested: a linear relationship and an exponential relationship. A curve fit is applied to both relationships using the median of the resulting data point. This gave the formulas 44 and 45. Both seem to follow the decreasing median R-factor, ultimately converging towards one. The linear relation takes approximately 500 days to converge to one and this is in line with found literature. Additionally, the linear relationship has a smaller RMSE and total error to the median R-factor and is further considered in the study.

$$R(t)_{linear} = 7.74 - 0.014t \tag{44}$$

$$R(t)_{exponential} = 7.14exp(-0.0036t) + 1 \tag{45}$$

The analysis of the adjusted ShorelineS results is done as follows. Since the nourishment consists of two distinct elements, the terminal section and the village section, both differ in design requirements. Therefore, the inclusion of cross-shore redistribution is analyzed separately for both sections and combined. The results showed that including the R-factor in ShorelineS improved the prediction for the terminal section but worsened the results for the village section. This difference in results between both sections can be explained by the model's imposed conservation of sediment. Sediment eroded in front of the terminal gets deposited in front of the villages. Because of this, the village section continuously grows, and the R-factor amplifies this. Looking at the entire nourishment, the change in coastline is almost zero due to this conservation. Therefore, the R-factor has almost no effect. These results provide a reason to try a new approach. This approach differs from the earlier approach in two ways. The R-factor is only applied to the terminal section, and the adjusted coastline is reintroduced back into ShorelineS. These new results indicate that the inclusion of cross-shore redistribution slightly improves the performance of ShorelineS, especially in front of the terminal. However, the conservation of sediment from the model still largely influences the results.

To conclude, measurement of Bacton Sandscaping revealed that cross-shore redistribution has a big effect on the evolution of mega nourishment. However, the assumption that the error in ShorelineS is solely due to the neglect of cross-shore redistribution might be premature. Given that the model results show sediment retention, the model likely contains additional limitations that contribute to its inaccuracy in representing reality. Nonetheless, despite the retention of sediment by the model, the results do indicate that a slight improvement can be made when including cross-shore redistribution using the R-factor.

7.2 Recommendations

The following recommendations can be made based on the key findings from the research.

1. To better understand what drives cross-shore redistribution, one could conduct more research. Investigating multiple nourishments with different profiles could contribute to finding a good relationship between forcing and equilibration. It is advised that should one take measurements of nourishment on redistribution, to do this on a set interval. So, it becomes possible to discover trends.

2. One could also conduct some physical testing to find which parameters influence the equilibration of the profile. This will all contribute to a wider understanding of the equilibration of a cross-shore profile.

3. Future research should focus on alternative formulations of including cross-shore redistribution into 1D coastline models. The discussion already mentions an additive relationship, but more relationships could be possible

4. A big limitation in this research was the inherent sediment retention of ShorelineS. To overcome this problem, one could conduct more calibration of the model on the Bacton sandscaping.

5. Future research can be done on the effect of including cross-shore redistribution on the results of ShorelineS or other 1D coastline models. As concluded, the assumption that the error ShorelineS made with reality was due to the exclusion of cross-shore redistribution was premature. Therefore, it is interesting to see how big of an effect this inclusion has on ShorelineS's results.

References

AECOM. (2010). *Kelling to lowestoft ness shoreline management plan* (Tech. Rep.). Author.

Andrew Ashton, A. B. M., & Arnoult, O. (2001). Formation of coastline features by large-scale instabilities induced by high-angle waves. *Nature*.

Bagnold, R. (1963). Beach and nearshore processes part 1: Mechanics of marine sedimentation. *The earth beneath the sea: history*.

Bayram, A. (2007). A new formula for the total longshore sediment transport rate. *Coastal Engineering*.

Borsje, R., & Flikweert, J. (2020). *Short term morphological analysis* (Tech. Rep.). Royal HaskoningDHV UK LTD.

Borsje, R., & Flikweert, J. (2021a). *Morphological analysis period 3: Nov 2020 - sep 2021* (Tech. Rep.). Royal HaskoningDHV UK LTD.

Borsje, R., & Flikweert, J. (2021b). *Short term morphological analysis period2: Feb - nov 2020* (Tech. Rep.). Royal HaskoningDHV UK LTD.

Borsje, R., Flikweert, J., Goodliffe, R., & Hesk, P. (2023). Bacton sandscaping - initial performance of a mega nourishment. *ice Publishing*.

Bruun, P. (1954). *Coastal erosion and the development of beach profiles (technical memorandum n0. 44)*. Beach Erosion Board, US Army Corps of Engineers.

Clipsham, V. (2016). *Bacton gas terminal coastal protection stage 2.1* (Tech. Rep.). Royal HaskoningDHV UK LTD.

Clipsham, V. (2018). *Bacton- walcott design report stage 2.2* (Tech. Rep.). Royal HaskoningDHV UK LTD.

Clipsham, V., Flikweert, J. J., Goodliffe, R., Courtnell, E., Fletcher, A., & Hesk, P. (2021). Bacton to walcott sandscaping, uk: a softer approach to coastal management. *ice Publishing*.

Dano Roelvink, A. E. M. G., Bas Huisman, & Reyns, J. (2022). Efficient modeling of complex sandy evolution at monthly to century time scales. *Frontiers in marine science*.

Dean, R. (1977). Equilibrium beach profiles: Us atlantic and gulf coast (ocean engineering report no. 12). *Department of Civil Engineering and College of Marine Studies*.

Dean, R. G. (2003). *Beach nourishment: theory and practice*. World Science.

de Schipper, M. A., de Vries, S., Ruessink, G., de Zeeuw, R. C., Rutten, J., van Gelder-Maas, C., & Stive, M. J. (2016). Initial spreading of a mega feeder nourishment: Observation of the sand engine pilot project. *Coastal Engineering*.

Engineers, U. A. C. O. (2002). *Coastal engineering manual: Chapter1 coastal terminology and geological environments* (Tech. Rep.). U.S. Army Corps of Engineers.

Hallermeier, R. J. (1978). Uses for a calculated limit depth to beach erosion. *Coastal Engineering*.

Hanson, H., & Kraus, N. (2011). Long-term evolution of a long-term evolution model. *Journal of Coastal Research*.

Kamphuis, J. (1991). Alongshore sediment transport rate. *Journal of waterway, port, coastal and ocean engineering*.

Kroon, A., de Schipper, M., de Vries, S., & Aarninkhof, S. (2022). Subaqueous and subaerial beach changes after implementation of a mega nourishment in front of a sea dike. *Marine Science and Engineering*.

Mil-Homens, J. (2013). Re-evaluation and improvement of three commonly used bulk longshore sediment transport formulas. *Coastal Engineering*.

Morelle, R. (2021). Norfolk sand: Has a colossal experiment worked? *BBC News*.

Pelnard-Considère. (1956). *Essai de theorie de l'évolution des formes de rivage en plage de sable et de galets* (Tech. Rep.). Énergie mecaniqeu de la houle.

Rostaing, B., Guthrie, G., Adnitt, C., & Flikweert, J. (2015). *Bacton gas terminal coastal protection stage 1 report - option appraisal* (Tech. Rep.). Royal HaskoningDHV Uk LTD.

Shorelines technical reference [Computer software manual]. (n.d.).

Shorelines technical reference [Computer software manual]. (n.d.).

Soulsby, R., & Damgaard, J. (2005). Bedload sediment transport in coastal waters. *Coastal Engineering*.

van Rijn, L. (2014). A simple general expression for longshore transport of sand, gravel and shingle. *Coastal engineering*.

A Appendix: Hydrodynamic conditions

Hydrodynamic conditions between every measurement period.

Period 0

From 26 August 2019 (T0) to 19 October 2019 (T1).

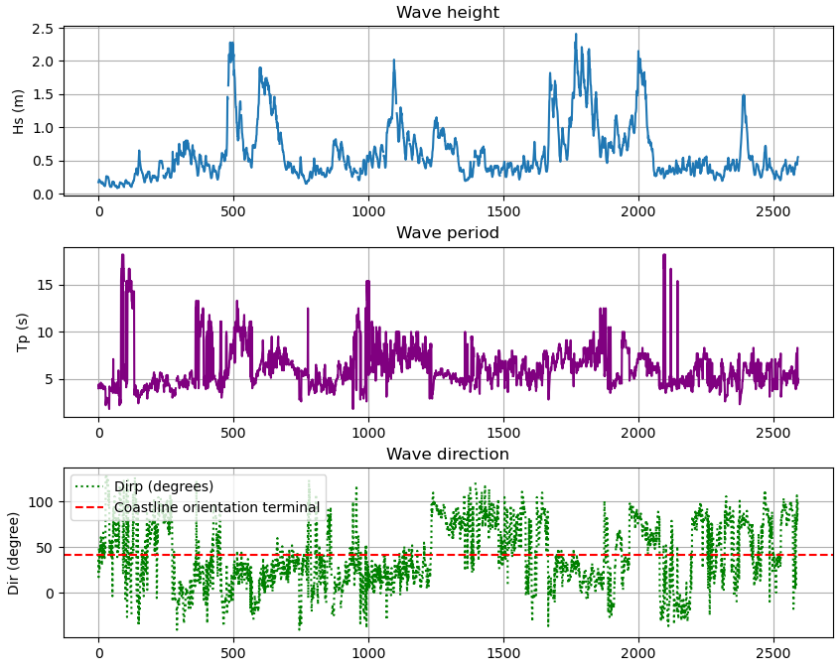

Figure 34: Time series of the hydrodynamic conditions Aug19-Oct19

Period 1

From 19 October 2019 (T1) to 21 February 2020 (T2).

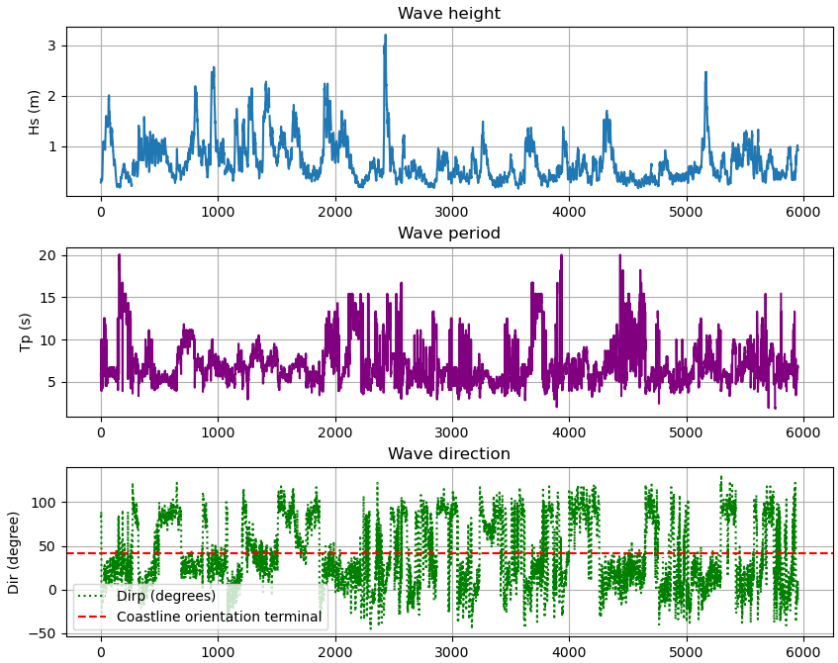

Figure 35: Time series of the hydrodynamic conditions Oct10-Feb20

Period 2

From 21 February 2020 (T2) to 30 October 2020 (T3).

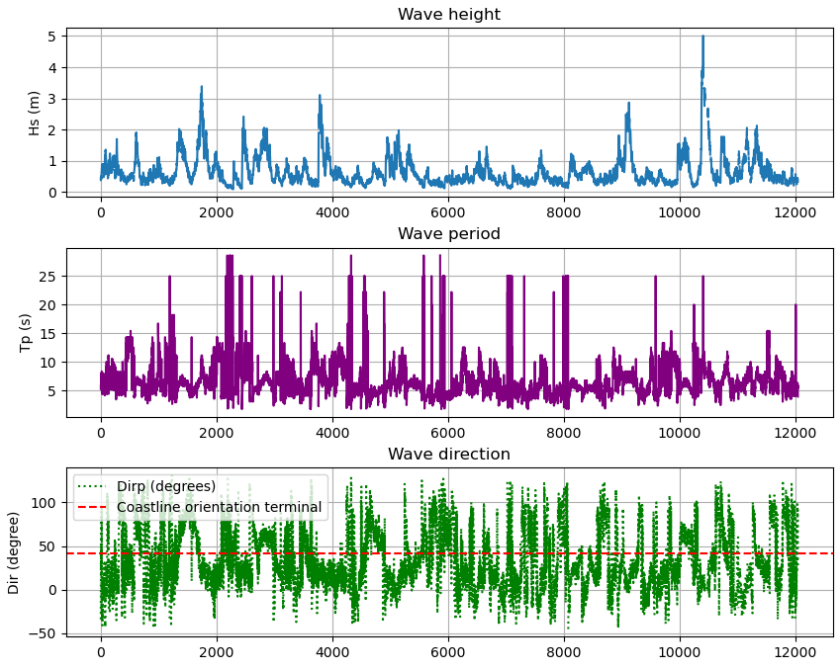

Figure 36: Time series of the hydrodynamic conditions Feb20-Oct20

Period 3

From 30 October 2020 (T3) to 9 June 2021 (T4).

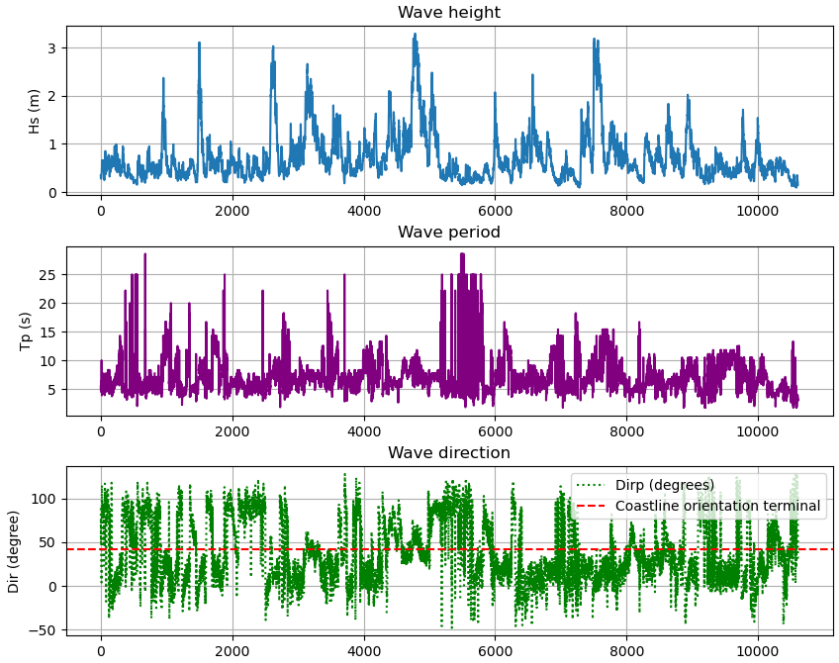

Figure 37: Time series of the hydrodynamic conditions Oct20-Jun21

Period 4

From 9 June 2021 to 17 (T4) 17 September 2021 (T5).

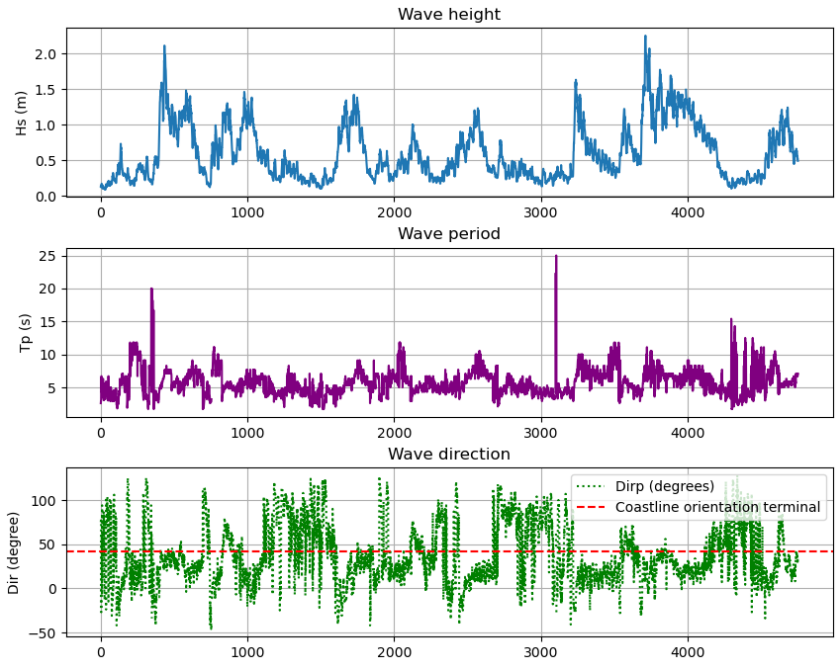

Figure 38: Time series of the hydrodynamic conditions Jun21-Sep21

Period 5

From 17 September 2021 (T5) to 12 October 2022 (T6).

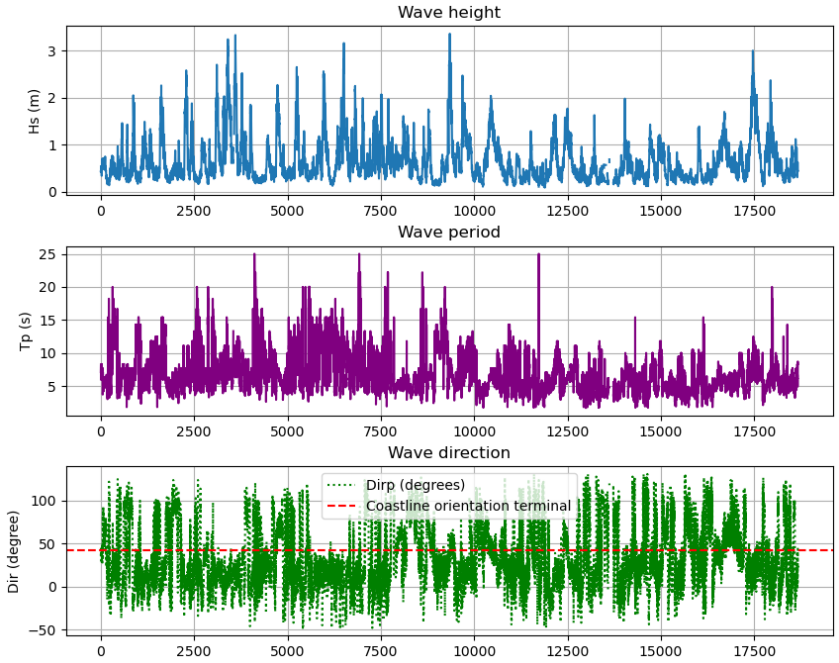

Figure 39: Time series of the hydrodynamic conditions Sep21-Oct22

Period 6

From 12 October 2022 (T6) to 2 May 2023 (T7).

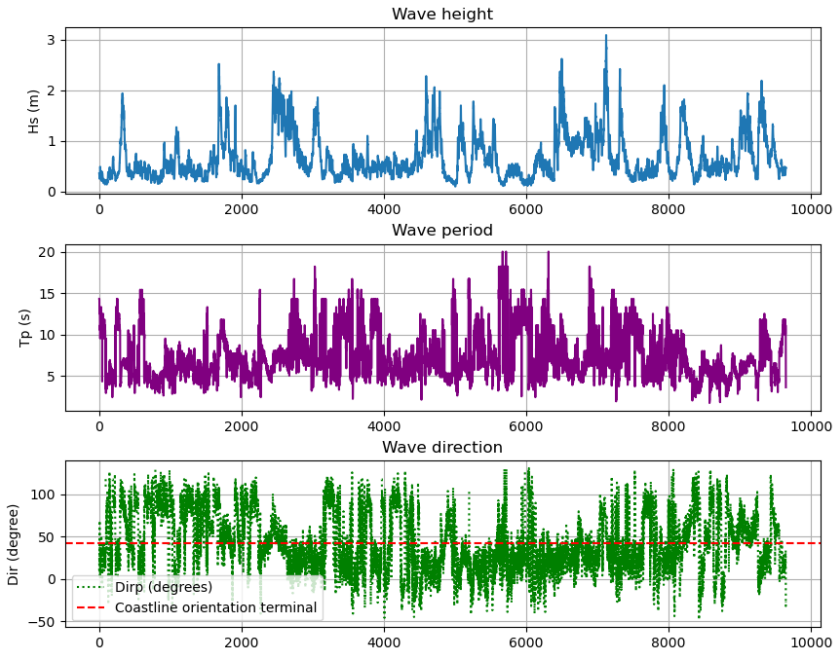

Figure 40: Time series of the hydrodynamic conditions Oct22-May23

Entire measurement period

From 26 August (T0) to 2 May 2023 (T7).

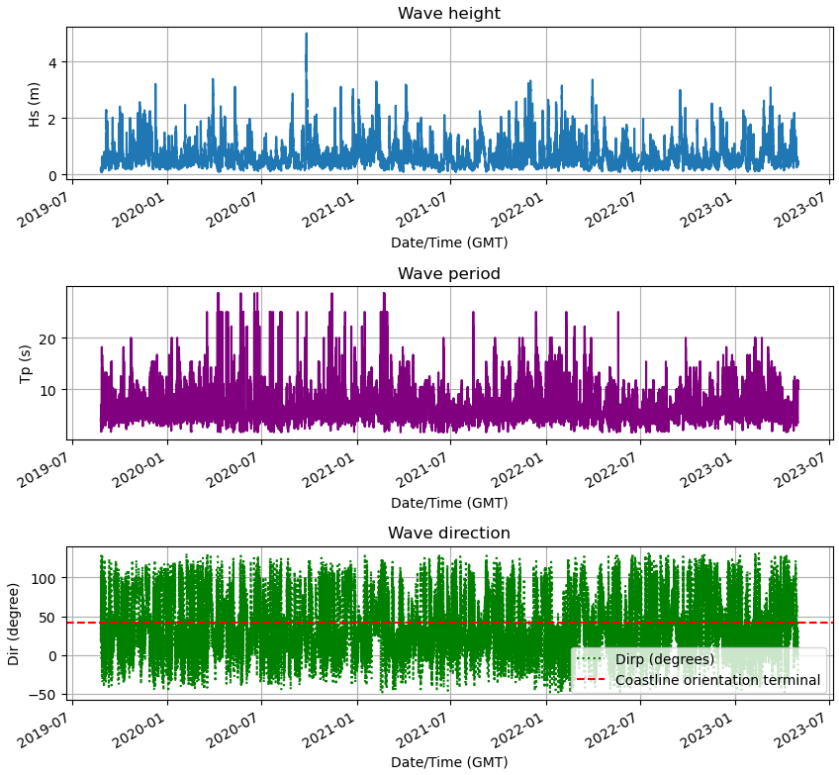

Figure 41: Time series of the hydrodynamic conditions from Aug19-May23

For the study of the morphological response of nourishment, RHDHV created wave roses to visualize the wave climate in between survey periods. Not every period is present here since this study did not cover the last two surveys. The wave roses are displaced in figure 42. In a wave rose diagram, the solid black line depicts the coastline, while the dashed black line represents a line perpendicular to the coast. Consequently, waves arriving at the coast at a 45-degree angle come almost directly from the north. The figure shows six wave roses, and the first wave rose in the top left corner shows the wave climate between the period just after construction and the first Shore survey (T0-T1). The last rose in the bottom right corner covers the whole period between the completion and the fifth Shore survey (T0-T5).

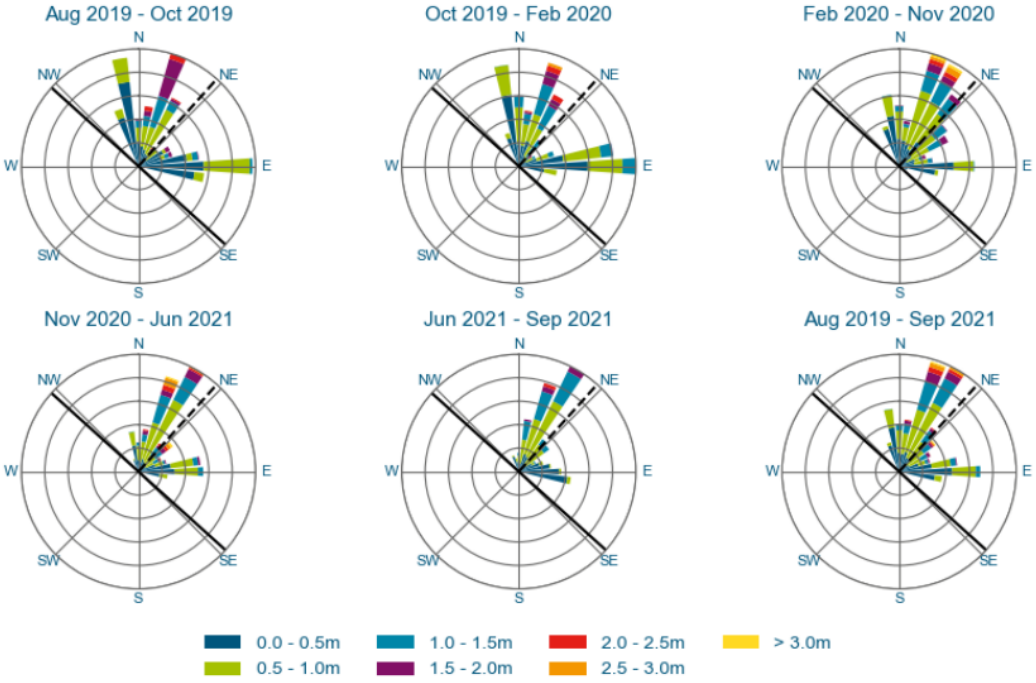

Figure 42: Wave climate in the periods between surveys T0-T5 displayed as wave rose, from [6]

Wave rose of visualizing the wave climate in the last two survey periods.

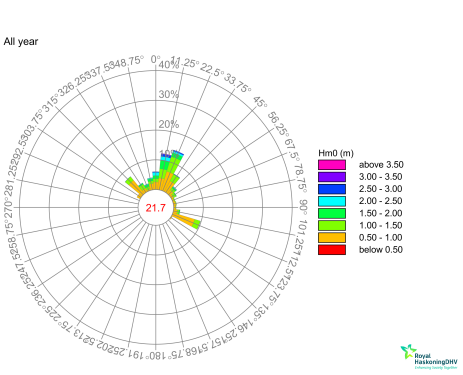

(a) Wave rose Sep 2021 - Oct 2022

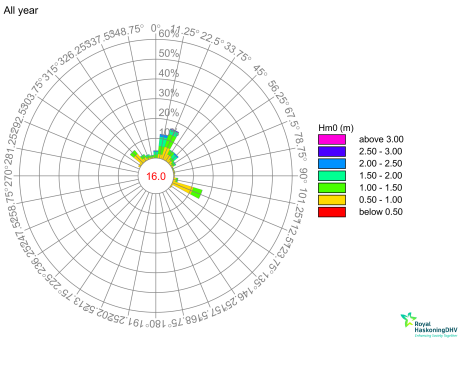

(b) Wave climate in the periods between Oct 2022 - May 2023 displayed as wave rose

Figure 43: Wave rose period 5 and 6

B Appendix: Assessment of the coastline change

Plots showing the modeled coastline change (blue) together with the coastline change calculated based on volume change (orange) and change in the MSL contour measured (green).

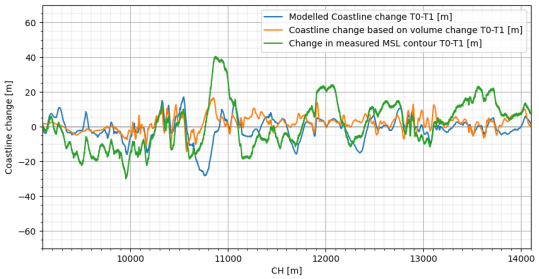

(a) Coastline change T0-T1

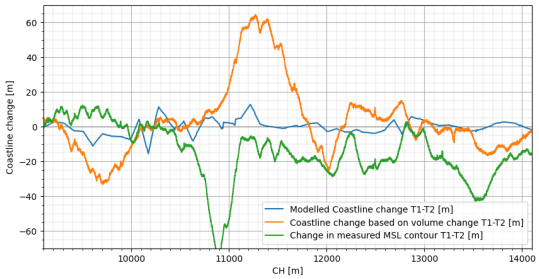

(b) Coastline change T1-T2

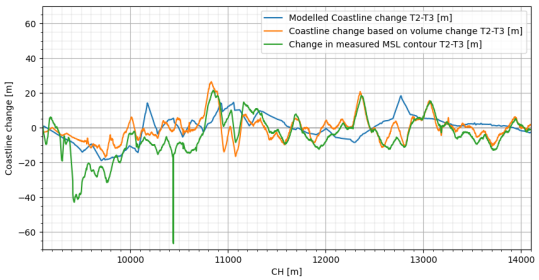

(c) Coastline change T2-T3

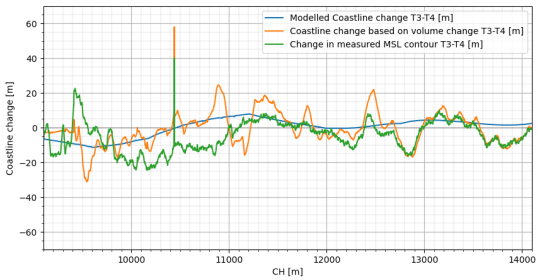

(d) Coastline change T3-T4

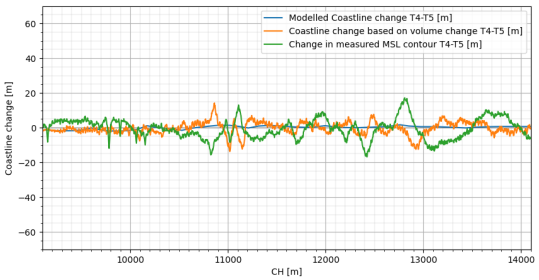

(e) Coastline change T4-T5

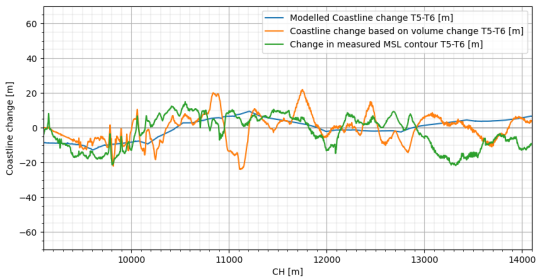

(f) Coastline change T5-T6

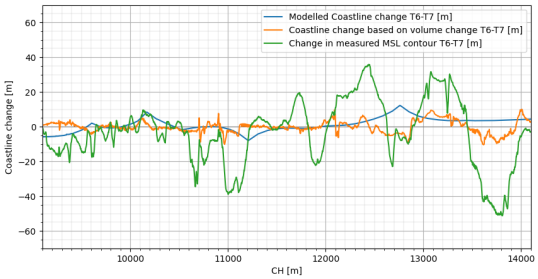

(g) Coastline change T6-T7

Figure 44: Modeled, Calculated and measured coastline change for every period

C Appendix: ShorelineS simulations per survey period

This appendix presents the resulting MSL contours and simulated coastline changes from ShorelineS runs where the model has been re-initialized at every survey instant, which means that after the measurement instant, the measured MSL contour is used as initial coastline input for the next simulated period. The first figure presents the resulting MSL contours from every simulation, it visualizes what the starting point of the model is and how it is changed over this period. Simultaneously, is present how the MSL contour changed according to measurements. The second figure depicts the modeled coastline change, observed MSL contour shifts, and calculated coastline change derived from volume variations across each period.

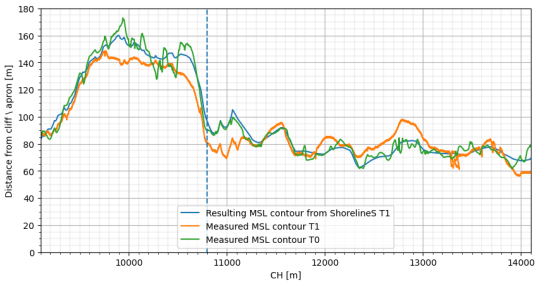

(a) MSL contour T0-T1

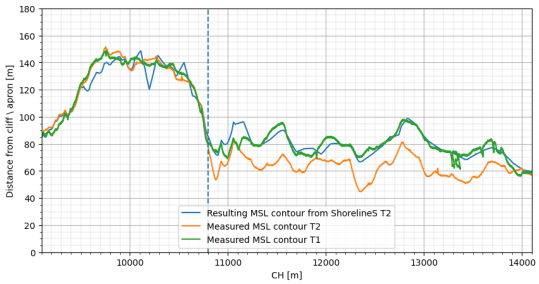

(b) MSL contour T1-T2

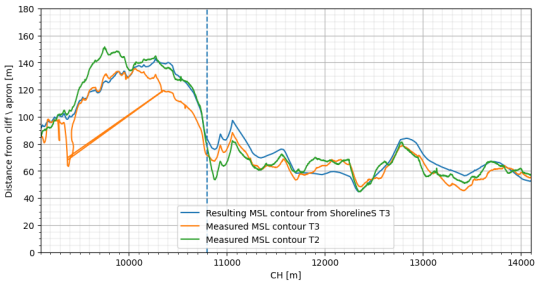

(c) MSL contour T2-T3

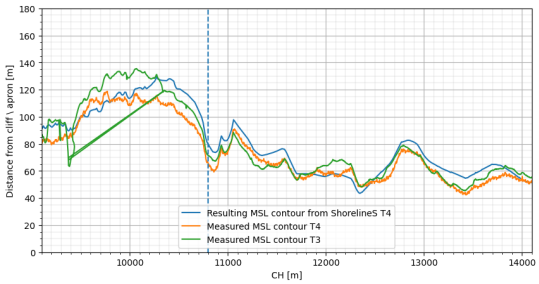

(d) MSL contour T3-T4

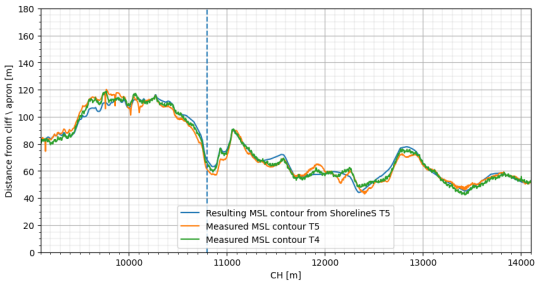

(e) MSL contour T4-T5

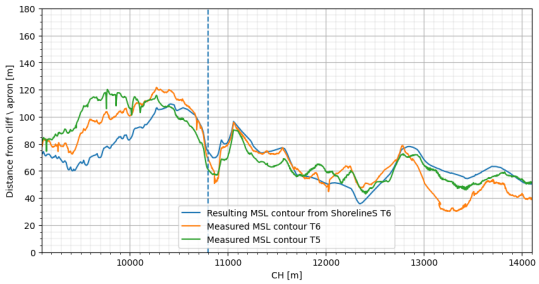

(f) MSL contour T5-T6

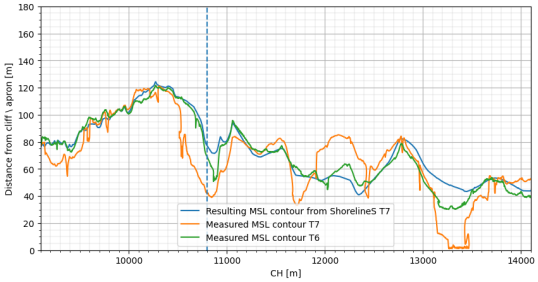

(a) MSL contour T6-T7

Figure 46: Resulting MSL contours from the re-initialized ShorelineS simulations

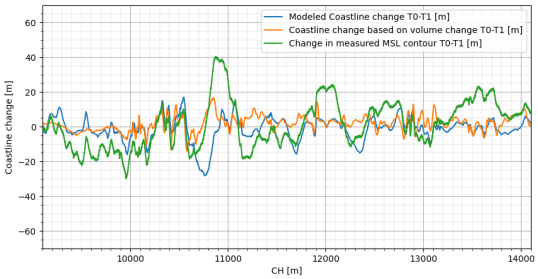

(a) Coastline change T0-T1

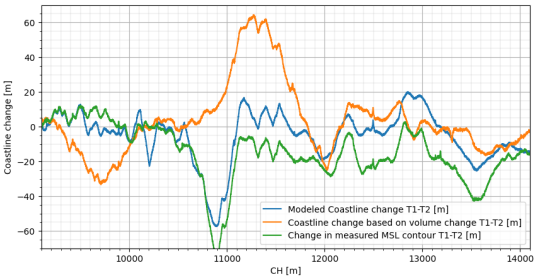

(b) Coastline change T1-T2

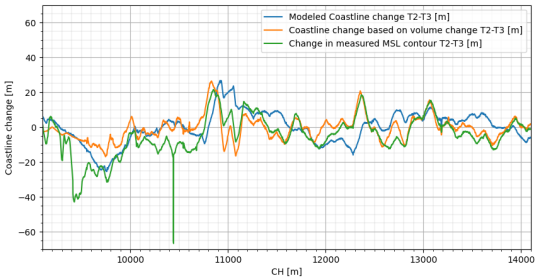

(c) Coastline change T2-T3

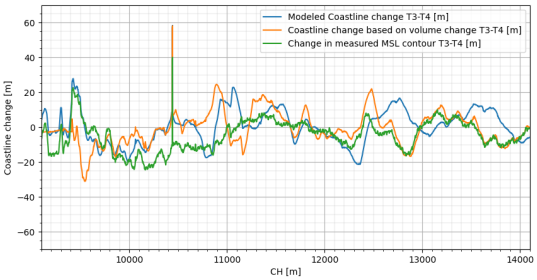

(d) Coastline change T3-T4

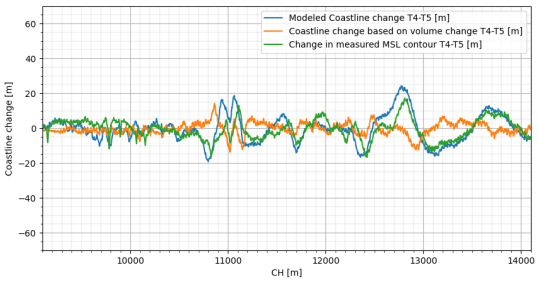

(e) Coastline change T4-T5

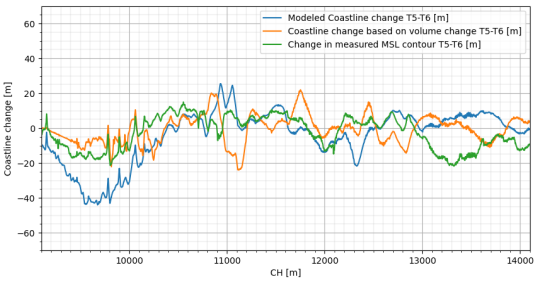

(f) Coastline change T5-T6

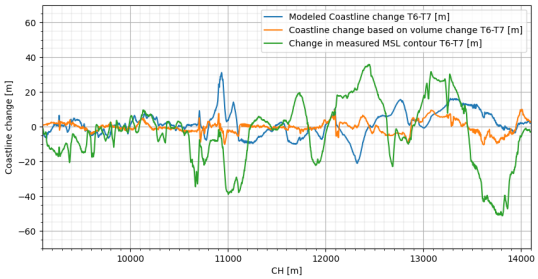

(a) Coastline change T6-T7

Figure 48: Resulting Modeled, Calculated and measured coastline change for every period for the re-initialized ShorelineS simulations

D Appendix: Calculation results equilibrium factor

These tables present the results for the calculations of the R-factor.

	Period 0			Period 1			Period 2		
Transect	Δy_m	Δy_c	R	Δy_m	Δy_c	R	Δy_m	Δy_c	R
4	-21.0843	0.5977	-35.2740	-9.8584	2.9071	-3.3910	-2.6871	-5.8929	0.4559
5	-22.4814	-2.0107	11.1807	-14.5299	-0.0449	323.2866	-4.9267	-4.3062	1.1440
6	-28.5537	-4.4489	6.4180	-18.0579	-1.7653	10.2292	-7.5069	-6.9576	1.0789
7	-31.2119	-6.7534	4.6216	-18.3451	-2.7820	6.5942	-10.5655	-8.7029	1.2140
8	-27.0565	-3.6540	7.4044	-15.7753	-2.6683	5.9120	-11.0837	-9.9265	1.1165
9	-20.3508	-1.9360	10.5114	-14.1232	-2.3020	6.1350	-13.8491	-10.1844	1.3598
10	-22.4046	-4.2617	5.2571	-15.6760	-4.1207	3.8042	-11.7566	-9.8517	1.1932
11	-27.2269	-2.7231	9.9983	-11.3241	-3.2680	3.4651	-14.4426	-13.5772	1.0636
12	-27.7755	-2.5991	10.6862	-13.1829	-1.7024	7.7436	-12.8113	-15.5041	0.8262
13	-22.9265	-0.6321	36.2667	-12.0866	-0.7285	16.5907	-13.8357	-14.6538	0.9441
14	-19.5204	0.2921	-66.8078	-11.3365	-0.5834	19.4297	-13.1517	-13.1161	1.0026
15	-25.6436	-1.8828	13.6199	-11.2413	-0.7899	14.2306	-11.8599	-12.2792	0.9657
16	-31.5492	-6.3605	4.9601	-14.5627	-1.0282	14.1627	-7.2829	-7.5919	0.9593
17	-35.3733	-11.2098	3.1555	-13.7099	-2.4233	5.6574	-8.6784	-5.0864	1.7062
18	-29.2460	-4.0949	7.1419	-14.3165	-3.2845	4.3587	-10.6658	-1.7328	6.1550
19	-20.2039	-0.1466	137.7920	-15.1985	-3.3315	4.5619	-7.8832	-0.4732	16.6568
20	-21.6404	-3.4519	6.2689	-10.7314	-0.5826	18.4177	-11.2235	-1.6613	6.7555
21	-24.8894	-4.7149	5.2788	-9.1262	1.6299	-5.5990	-11.9264	-3.5555	3.3541
22	-23.8527	-0.6444	37.0147	-8.5586	3.5064	-2.4408	-11.3305	-4.7519	2.3843
23	-17.5156	5.9711	-2.9333	-8.7716	2.7307	-3.2121	-10.5205	-4.2642	2.4671
25	-9.16220	6.2298	-1.4707	-10.4871	1.6524	-6.3462	-4.0581	-1.7322	2.3430
26	-10.3406	3.1294	-3.3042	-15.1123	-0.1474	102.4877	-3.0193	-3.1031	0.9729
27	-13.1343	2.9434	-4.4622	-13.2508	-1.4259	9.2927	-8.0412	-3.2072	2.5072
28	-12.2081	4.3825	-2.7856	-13.7012	-1.6834	8.1389	-8.0305	-2.8133	2.8544
29	-11.9371	-0.6123	19.4928	-13.2778	-1.5595	8.5137	-9.3271	-2.8426	3.2811
30	-20.4892	-7.6971	2.6619	-13.6462	-1.7319	7.8790	-10.8156	-5.8490	1.8491

	Period 3			Period 4			Period 5			Period 6		
Transect	Δy_m	Δy_c	R	Δy_m	Δy_c	R	Δy_m	Δy_c	R	Δy_m	Δy_c	R
4	0.5319	-1.5205	-0.3494	1.2566	-2.3456	-0.5353	-13.1459	-6.2186	2.1137	0.1038	2.7311	0.0380
5	-0.2675	-4.8230	0.0554	0.3012	0.1487	2.0251	-11.0158	-7.9676	1.3825	-0.0971	2.2521	-0.0436
6	-1.9494	-3.7070	0.5258	0.2733	-0.4770	-0.5723	-10.4454	-9.8015	1.0656	-0.5697	2.1371	-0.2667
7	-2.9936	-1.8262	1.6390	0.0726	-2.9997	-0.0245	-8.1068	-10.2153	0.7932	0.1397	1.6411	0.0851
8	-6.7679	-3.9722	1.7037	2.6897	-1.3312	-2.0192	-13.7355	-13.2189	1.0396	-0.1873	-0.1239	1.5231
9	-7.7466	-5.3451	1.4493	3.3482	-1.3235	-2.5295	-14.0101	-9.1300	1.5344	1.2094	-2.5551	-0.4731
10	-6.9797	-8.6063	0.8109	-1.3807	-0.8188	1.6870	-16.4382	-6.3453	2.5904	1.2041	-4.9159	-0.2448
11	-6.1722	-5.6689	1.0888	-2.4632	-3.2966	0.7474	-20.0593	-9.7353	2.0603	0.5407	-2.6100	-0.2079
12	-12.1608	-5.2692	2.3081	-0.0094	-0.6968	0.0131	-18.8464	-7.7066	2.4454	-2.9908	1.4733	-2.0290
13	-11.7726	-7.6737	1.5348	-1.2529	-2.1534	0.5815	-17.0211	-14.0806	1.2085	-4.7858	0.9272	-5.1609
14	-10.7410	-6.7448	1.5935	-1.7428	-3.1777	0.5482	-16.6238	-11.7363	1.4162	-4.6003	0.3436	-13.3877
15	-11.2133	-6.0346	1.8592	-1.4742	-3.6811	0.4004	-18.9233	-11.7602	1.6086	-0.6740	-0.1711	3.9229
16	-14.9695	-8.1345	1.8400	-0.5070	-1.5128	0.3354	-18.2457	-4.7049	3.8782	-0.2948	-1.2253	0.2403
17	-12.2409	-7.5965	1.6113	-1.7916	-2.5387	0.7056	-17.0098	-3.9621	4.2920	-1.0112	-1.6681	0.6061
18	-8.0005	-11.6344	0.6876	-2.8669	-2.6395	1.0861	-15.7129	-8.6396	1.8186	-1.4034	-2.0365	0.6891
19	-7.2174	-7.8658	0.9175	-3.8026	-2.8674	1.3263	-14.8035	-10.6354	1.3915	-2.2773	1.6826	-1.3532
20	-6.6641	-8.3334	0.7996	-0.7379	-2.8669	0.2572	-16.1215	-12.9853	1.2419	-0.2405	6.2303	-0.0381
21	-8.8346	-5.9292	1.4899	-0.5116	-3.0971	0.1652	-13.9045	-6.8112	2.0413	0.2781	2.8534	0.0974
22	-9.0878	-5.5740	1.6303	-0.7975	-1.2416	0.6427	-11.0904	-4.1801	2.6526	0.8297	-1.1243	-0.7386
23	-7.1537	-2.6130	2.7377	-2.3834	-4.0450	0.5891	-8.8630	-3.2673	2.7125	-0.2107	-0.9223	0.2283
25	-11.6117	-4.7874	2.4269	-1.3838	-3.8869	0.3560	-6.8018	0.1583	-42.9683	0.4586	-0.9807	-0.4679
26	-7.7319	-5.6637	1.3651	-2.8973	-0.8934	3.2442	-6.3132	-0.6962	9.0670	-0.4315	-0.8561	0.5041
27	-4.9003	-4.6864	1.0456	-2.1614	-1.5607	1.3855	-5.7328	-2.5224	2.2723	-1.1267	-1.4931	0.7542
28	-7.3825	-4.1176	1.7928	0.7542	-3.1520	-0.2399	-6.0699	-2.7512	2.2057	-2.5478	-1.5878	1.6043
29	-4.6898	-4.5915	1.0214	-2.0943	-2.9155	0.7185	-3.2856	-1.8501	1.7753	-2.6624	-2.8950	0.9195
30	-5.6548	-5.5503	1.0187	0.3436	-0.9596	-0.3587	-2.6869	-2.5240	1.0644	-3.5770	-4.2286	0.8460

E Appendix: Results for the adjusted coastline

This appendix displays the measured, modeled and adjusted coastlines in front of the village and the entire nourishment for all seven instances.

Villages only

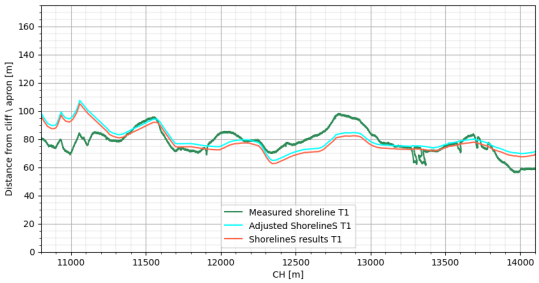

(a) Adjusted model results village T1

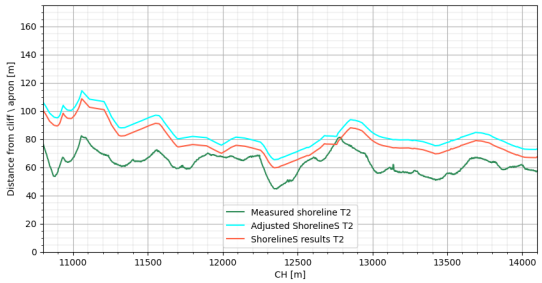

(b) Adjusted model results village T2

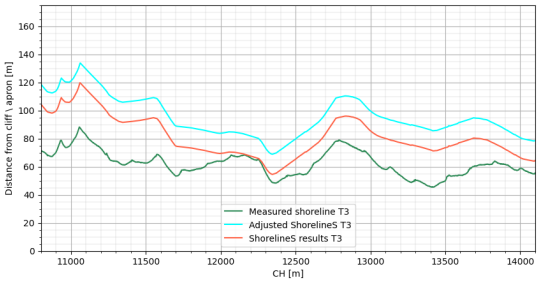

(c) Adjusted model results village T3

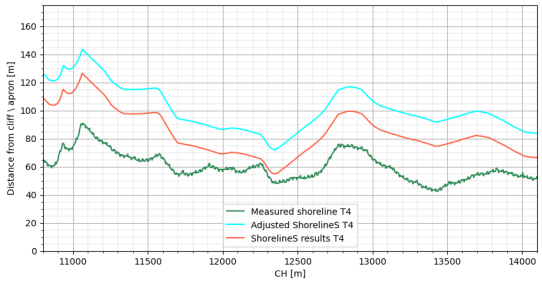

(d) Adjusted model results village T4

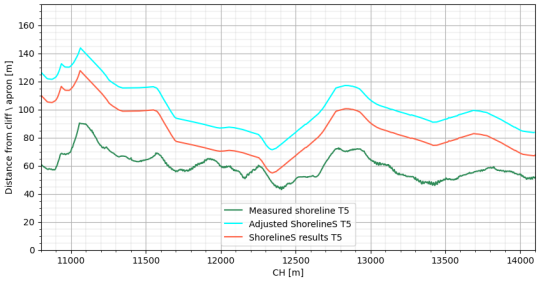

(e) Adjusted model results village T5

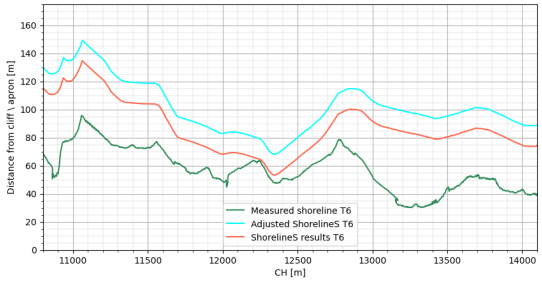

(f) Adjusted model results village T6

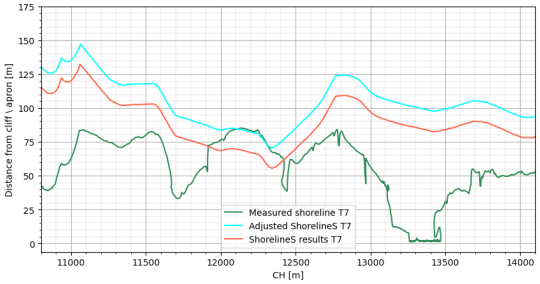

(g) Adjusted model results village T7

Figure 49: ShorelineS results vs Adjusted model runs village only

Entire nourishment

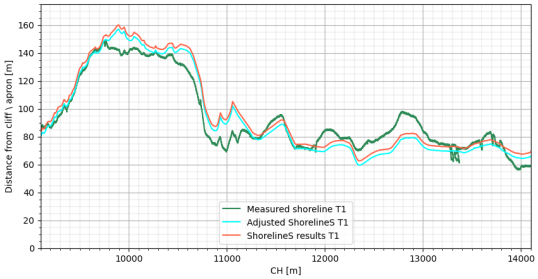

(a) Adjusted model results T1

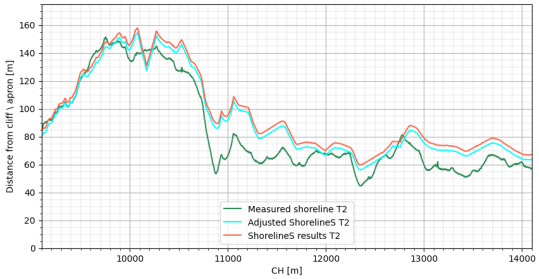

(b) Adjusted model results T2

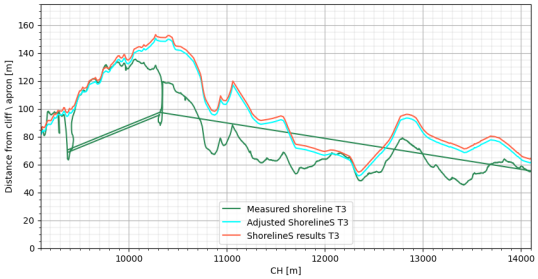

(c) Adjusted model results T3

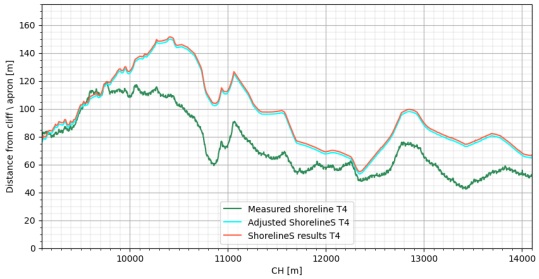

(d) Adjusted model results T4

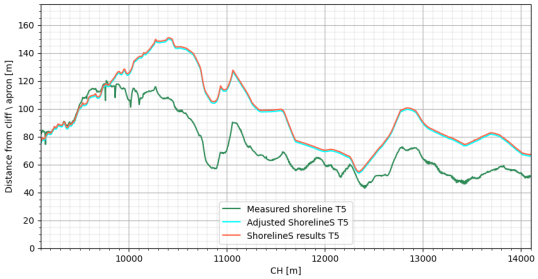

(e) Adjusted model results T5

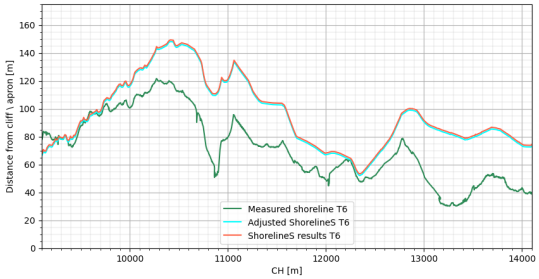

(f) Adjusted model results T6

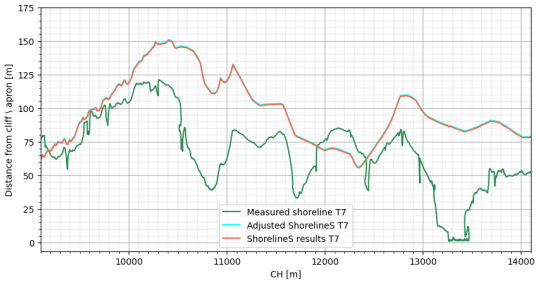

(g) Adjusted model results T7

Figure 50: ShorelineS results vs Adjusted model runs village only

F Appendix: Resulting coastline new approach

This appendix displays the measured, modeled and adjusted coastlines for the entire nourishment for all seven instances according to the new approach.

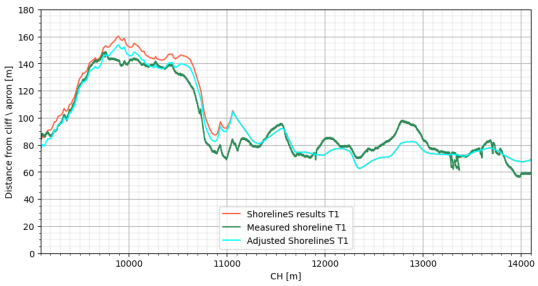

(a) Adjusted model results T1

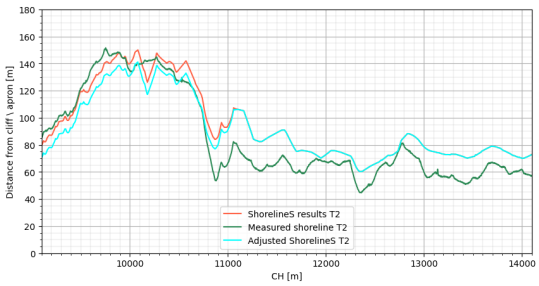

(b) Adjusted model results T2

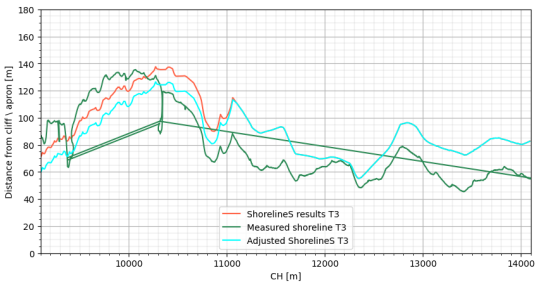

(c) Adjusted model results T3

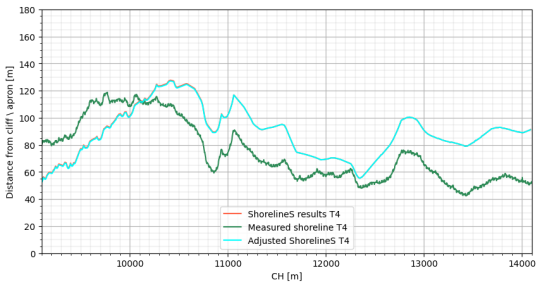

(d) Adjusted model results T4

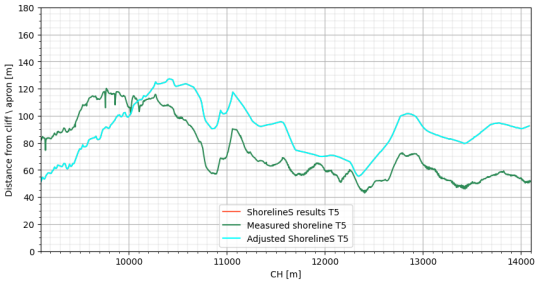

(e) Adjusted model results T5

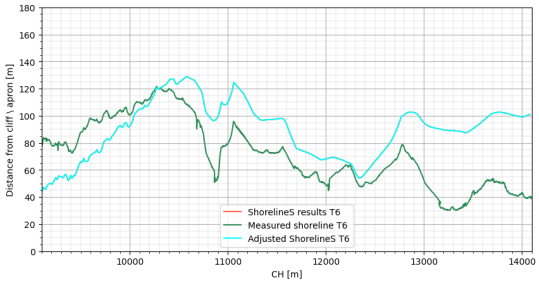

(f) Adjusted model results T6

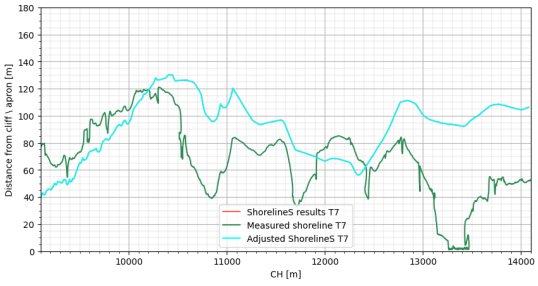

(g) Adjusted model results T7

Figure 51: ShorelineS results of new approach